0008-7114

Caryologia

International Journal of Cytology, Cytosystematics and Cytogenetics

2025
Vol. 78 - n. 3

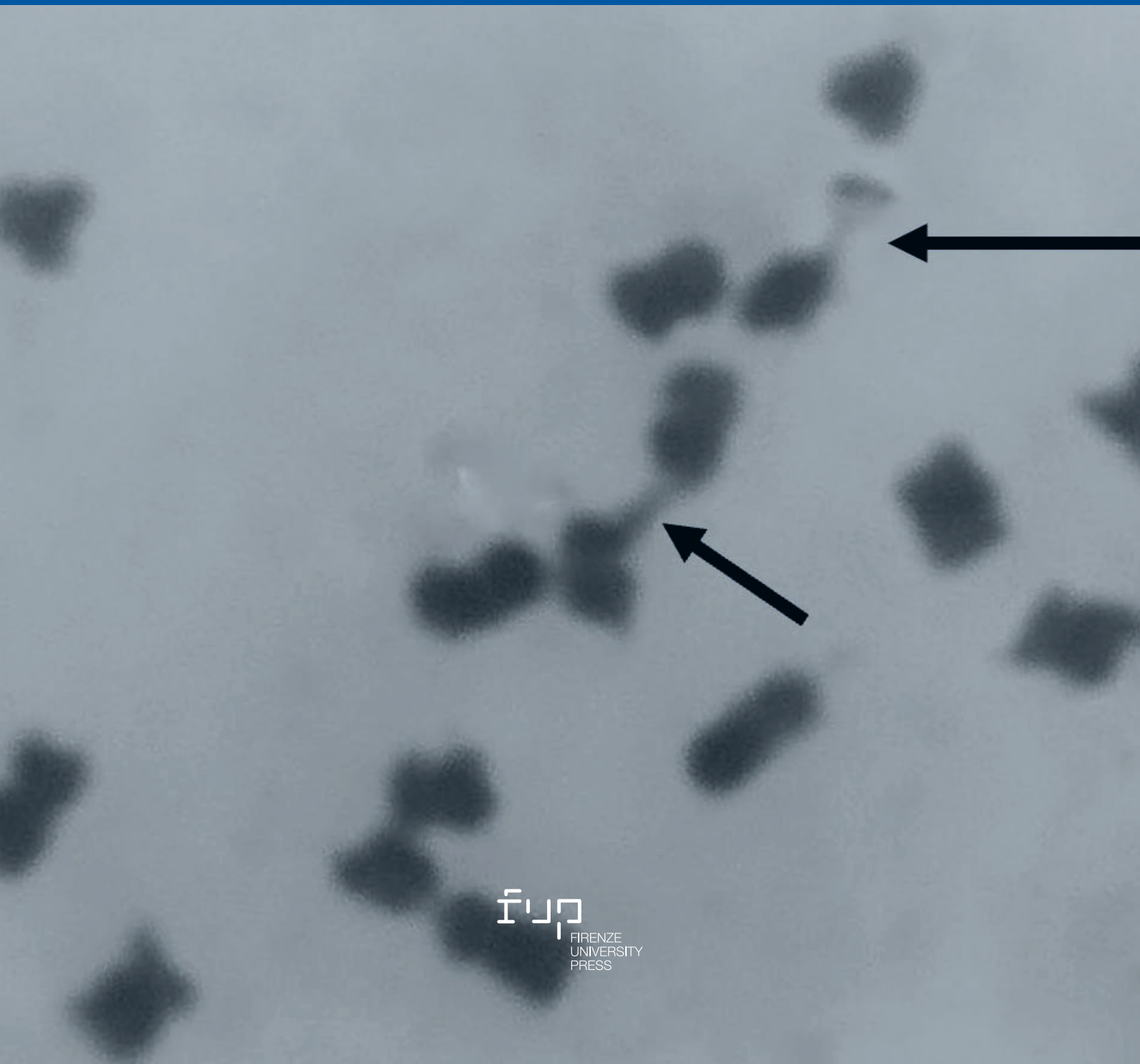

FIRENZE UNIVERSITY PRESS

Caryologia. International Journal of Cytology, Cytosystematics and Cytogenetics
Caryologia is devoted to the publication of original papers, and occasionally of reviews, about plant, animal and human karyological, cytological, cytogenetic, embryological and ultrastructural studies. Articles about the structure, the organization and the biological events relating to DNA and chromatin organization in eukaryotic cells are considered. *Caryologia* has a strong tradition in plant and animal cytosystematics and in cytotoxicology. Bioinformatics articles may be considered, but only if they have an emphasis on the relationship between the nucleus and cytoplasm and/or the structural organization of the eukaryotic cell.

Cover: figure from the article inside by da Silva Frade, L. F. et al. "Divergence in the chromosomal distribution of repetitive sequences in Neotropical cichlid species of the genus *Lugubria*", showing double FISH with telomeric sequence probes and 18S rDNA sequence probes in the karyotype of *L. cincta*, *L. strigata*, and *L. lugubris*.

Caryologia

International Journal of Cytology, Cytosystematics and Cytogenetics

Volume 78, Issue 3 - 2025

Firenze University Press

***Caryologia*. International Journal of Cytology, Cytosystematics and Cytogenetics**
https://riviste.fupress.net/index.php/caryologia
ISSN 0008-7114 (print) | ISSN 2165-5391 (online)

Direttore Responsabile: **Alessio Papini**

Published by Firenze University Press

Firenze University Press
Università degli Studi di Firenze
via Cittadella, 7, 50144 Firenze, Italy
www.fupress.com

Caryologia
International Journal of Cytology, Cytosystematics and Cytogenetics

Firenze University Press
https://riviste.fupress.net/index.php/caryologia

OPEN ACCESS

Citation: Okomoda, V. T., Olufeagba, S. O., Tarbee, M. F., Mverga, S. T., Akwaji, D. A., Dauda, A. B., Ricketts, O. A., Yossa, R., & Ikwanuddin, M. (2025). Delayed fertilization and short-term storage methods affects the viability of stripped eggs of African catfish *Clarias gariepinus*. *Caryologia* 78(3): 3-13. doi: 10.36253/caryologia-3424

Received: March 22, 2025

Accepted: November 11, 2025

Published: December 24, 2025

Data Availability Statement: All relevant data are within the paper and its Supporting Information files.

Competing Interests: The Author(s) declare(s) no conflict of interest.

Delayed fertilization and short-term storage methods affects the viability of stripped eggs of African catfish *Clarias gariepinus*

Victor Tosin Okomoda[1,2,3,*], Samuel Olabode Olufeagba[2], Mfanega Frank Tarbee[2], Samuel Tordue Mverga[2], Daniel Ajor Akwaji[2], Akeem Babatunde Dauda[4], Oluwapelumi Ricketts Amighty[1], Yossa Rodrigue[5], Mhd Ikwanuddin[3,6]

[1] *WorldFish, Ibadan, Nigeria*
[2] *Department of Fisheries and Aquaculture, College of Forestry and Fisheries, Joseph Sarwuan Tarka University (formerly Federal University of Agriculture Makurdi), Makurdi P.M.B. 2373 Makurdi, Nigeria*
[3] *Institute of Tropical Aquaculture and Fisheries, Universiti Malaysia Terengganu, 21030 Kuala Nerus, Terengganu, Malaysia*
[4] *Department of Fisheries and Aquaculture, Federal University Dutsin-Ma, PMB 5001, Dutsin-Ma, Katsina state, Nigeria*
[5] *WorldFish, Penang, Malaysia*
[6] *STU-UMT Joint Shellfish Research Laboratory, Shantou University, Shantou 515063, Guangdong, China*
*Corresponding author. Email: okomodavictor@yahoo.com

Abstract. The fertilization of eggs may be delayed during induced fish breeding due to unforeseen circumstances. It is, therefore, necessary to know the optimal delay period and explore short-term storage options that can extend the viability of the eggs in such instances. In two studies, African catfish *Clarias gariepinus* eggs were obtained from broodstocks induced using ovaprim® hormone at 0.5ml/kg. A batch of the stripped eggs was then exposed in triplicate to atmospheric oxygen for 0, 1, 2, 3, 4, 8 and 12 hours post-stripping (HPS). In contrast, another batch was stored for 8 hours using sole and combined methods of "refrigeration", "addition of extender" and "aeration". The eggs were then fertilized using fresh sperm in all instances. In both experiments, egg characteristics, breeding parameters, and biometric parameters of hatched fry were recorded. Results showed a size reduction in the eggs as the time of exposure to atmospheric oxygen increased. Also, the fertilization and hatchability of eggs were similar to 4HPS; beyond this threshold, the value declined significantly to zero. However, the hatched fry's biometric parameters showed no significant difference among treatments ($P<0.05$). The second study showed a poor breeding performance of eggs stored in all the different storage methods tested. Meanwhile, egg sizes and biometric parameters of the few hatched fry show no significant difference among the treatments ($P<0.05$). It was therefore concluded that the fertilization of stripped *C. gariepinus* eggs should not be later than 4HPS to optimize the breeding performance of the fish.

Keywords: African catfish, Egg storage, Breeding parameters, Saline water, Refrigeration.

INTRODUCTION

Aquaculture has grown to the point of being acknowledged as the fastest-growing food-producing sector in the world (Megbowon *et al.,* 2013; Tacon, 2020). This is because of its essential role in providing high-quality, cheap proteins to over 7 billion people worldwide (FAO 2020). The rapid growth of the sector in both inland and marine environments affects the livelihood and socioeconomic characteristics of many through the broad aquaculture value chain (Kalinina *et al.,* 2020). Fish seed availability is an essential component of fish culture, as it largely determines the success of the aquaculture sector. Over the past few years, scientific advancement has introduced new technologies that have improved the artificial propagation of fish in captivity. Innovations such as sperm storage, hormone administration, novel spawning methods and rearing systems have shaped the development of aquaculture, thereby contributing to its rapid growth (Yue and Shen, 2021). Despite the breakthrough in artificial propagation, egg quality and oocyte viability loss after ovulation still limit the mass production of many species (Furuita *et al.,* 2003; Rizzo *et al.,* 2003).

In fish breeding, the viability of eggs is determined by the broodstock quality and the eggs' handling after stripping (Okomoda et al., 2018). Under normal conditions, ovulated eggs are fertilized immediately with high-quality sperm to ensure good breeding performance and fry hatchability (Olufeagba and Okomoda 2016). However, conditions such as unavailability or death of quality male broodstock may lead to delayed fertilization of the stripped eggs. At this point, the options available for fish breeder are limited, one of which is to expose the stripped eggs to prevailing atmospheric conditions or attempt short-term storage to preserve the oocytes from losing their viability until alternative quality male broodstocks are gotten. The success and efficiency of different gamete storage methods in fish culture have been well-documented in several studies. Unfortunately, attention has been focused chiefly on sperm than ova preservation (Withler and Lim 1982; Nguenga *et al.,* 2004; Idahor *et al.,* 2018). One of the viable methods of short-term storage is refrigeration; however, the nature of power supply in most remote areas has made it imperative to look for alternative non-power-dependent storage methods (Dettlaff *et al*., 1993).

Of all the notable fish species of interest in West Africa, *Clarias gariepinus* has found a pride of place in terms of overall aquaculture production and value chain (Dauda *et al.,* 2018). The fish, native to Africa, is widely cultivated in ponds, cages, and pens (Khedkar and Khedkar, 2003; Okomoda et al., 2018). *C. gariepinus* is well known to tolerate harsh environmental conditions, making it a choice species for culture in many environments (Adebayo *et al.,* 2015; Omoniyi *et al.,* 2018). Noteworthy is that many researchers have reported different possible methods and means of storing *C. gariepinus* milts (Adeyemo et al., 2007; Idahor *et al.,* 2018; Tilahun and Yalew, 2024). However, there has been almost no report on the short-term storage of its eggs to date. Short-time storage of ova has been somewhat successful in other fish species such as *Cyprinus carpio* (Rothbard *et al.,* 1996), *Sarotherodon mossambicus* (Harvey and Kelley 1984), *Oncorhynchus keta* (Jensen and Alderdice 1984), and *Heterobranchus longifilis* (Nguenga *et al.,* 2004). Against this backdrop, this research was designed to examine the appropriate method of short-term ova storage of the African catfish fish *C. gariepinus* and determine the optimum time of its delayed fertilization.

MATERIALS AND METHODS

This study was conducted at the hatchery unit and laboratory of the Department of Fisheries and Aquaculture, Joseph Sarwuan Tarka University Makurdi (JOSTUM), Benue State, Nigeria (latitude 7° to 8° North and longitude 8° to 9° East). Fifty-four broodstocks of African Catfish *C. gariepinus* (39 females and 15 males of average 1500g) with similar breeding history were obtained from a reliable source in Makurdi and taken to the Fish Hatchery unit of JOSTUM. Using a 1000-litre tank, the broodfish were acclimatized and stabilized for seven days before they were used for the experiment. During the period, they were fed a commercial diet (Coppens 45%CP) to satiation, and the water quality was maintained at optimum. Generally, for the two studies conducted, the female broodstocks were weighted and injected with Ovaprim® using a 10 ml syringe intramuscularly at an angle of 30-45° below the dorsal fin using the manufacturer's recommendation of 0.5 ml/kg of the broodstock. They were then kept in separate tanks throughout the latency period, depending on the nature of the experimental design before stripping was done. Fresh milt was also obtained at different time intervals based on the experimental needs by sacrificing the male brooder and surgically removing the visceral organs to get the testes sac. The testes were then cut into small pieces so the milt could ooze out and used to fertilize the eggs as appropriate for the different treatments in the two studies designed.

Experiment One: Viability of *Clarias gariepinus* eggs stripped and exposed to atmospheric oxygen for varying periods.

Four gravid females of the experimental fish were injected and conditioned in different bowls for a latency period of 10 hours. Thereafter, the eggs in them were stripped out by gently pressing the abdomen of the females with a thumb from the pectoral fin towards the genital papilla. The ovulated eggs were released quickly in a thick jet from the genital vent and were collected into clean, dried bowls. After stripping, the eggs were exposed to atmospheric oxygen conditions at the following time intervals: 0, 1, 2, 3, 4, 8, and 12 hours post stripping (HPS), denoted as 0HPS, 1HPS, 2HPS, 3HPS, 4HPS, 8HPS and 12HPS respectively. Each treatment was done in three replicates, and each set was fertilized with fresh milt obtained from the same male. This process was done by releasing drops of the milt on the designated eggs at the appropriate time post-striping. The egg and milt were mixed thoroughly in the plastic bowl, and freshwater was added to activate the sperm. Fertilized eggs in each treatment were accordingly spread in an already prepared hatching bowl (10 litres) with a hatching net (mesh size of 2 mm) already suspended. The eggs were incubated in this condition till hatching.

Experiment Two: Viability of *Clarias gariepinus* eggs stored for a short duration using different methods.

Upon determining the threshold delayed time post stripping that is lethal to the egg's viability, the second study was done to improve the shelf-life of the eggs by storing them using different methods under the lethal duration earlier determined. These storage methods include using an extender (physiological saline) and aeration at room temperature or refrigeration. Like the previous experiment, four gravid females were injected and conditioned in different bowls for a latency period of 10 hours, followed by stripping. The gentle press on the abdomen of the females releases the eggs from the genital papilla. The ovulated eggs collected were then distributed in three replicates into seven treatment groups.

Trt 0 = Eggs stripped and fertilized immediately (+ve Control)

Trt 1 = Egg exposed to room temperature without an extender (-ve Control)

Trt 2 = Egg exposed to room temperature with the addition of extender

Trt 3 = Egg exposed to room temperature with the addition of an extender and aeration.

Trt 4 = Egg kept in the fridge without the extender.

Trt 5 = Egg kept in the fridge with the addition of extender.

Trt 6 = Egg kept in the fridge with the addition of extender and aeration.

The extender used was physiological saline (i.e., 5% saline solution), and aeration was achieved using mechanical air pumps fitted with air stones. Treatment zero, the positive control, was fertilized immediately after stripping. In contrast, treatment one to six were stored for 8 hours, after which the differently stored egg samples were artificially fertilized using freshly collected milt from similar males per replicate batch. This process was done by releasing drops of the milt on the designated stored eggs, and the egg/milt mixture was then mixed thoroughly in the plastic bowl. A freshwater was added thereafter to activate the sperm and initiate fertilization. The fertilized eggs in each treatment were then incubated in the prepared bowls (10 litres) with a hatching net (mesh size of 2 mm) suspended in them. The eggs were incubated in this condition till hatching.

Embryogenesis observation of eggs during incubation

During the incubation of the different treatments, the embryogenesis of the fertilized egg was monitored closely. In brief, 50 fertilized eggs were collected at regular intervals from each treatment and observed under a Nikon dissecting microscope fitted with a camera to take pictures. Observations of the eggs were initially done every 10 minutes until the morula stage. Thereafter, it was done hourly until hatching was observed following the previous methods adopted by Olufeagba et al. (2016) and Okomoda et al. (2018) for the same species. A new batch of eggs was collected at each observation, and pictorial evidence of the different developmental stages and observable abnormalities was captured *in situ*. Deviation from normal developmental embryogenesis patterns was noted as abnormal and recorded.

Determination of performance and larvae characteristics

Using the techniques of fertilization estimation developed by Okomoda *et al.* (2018), the percentage of eggs fertilized was estimated at the early stage of the egg division using the equation shown below:

$$\% \text{ Fertilization} = \frac{\text{Fertilized eggs in the sub}-\text{sample}}{\text{Total number of eggs in the sub}-\text{sample}} \times 100$$

The hatching rate of each cross was evaluated by expressing the value of hatch fry as a percentage of the total number of eggs incubated.

$$\%\text{Hatchability} = \frac{\text{Number of hatched larvae}}{\text{Total number of spawned eggs}} \times 100$$

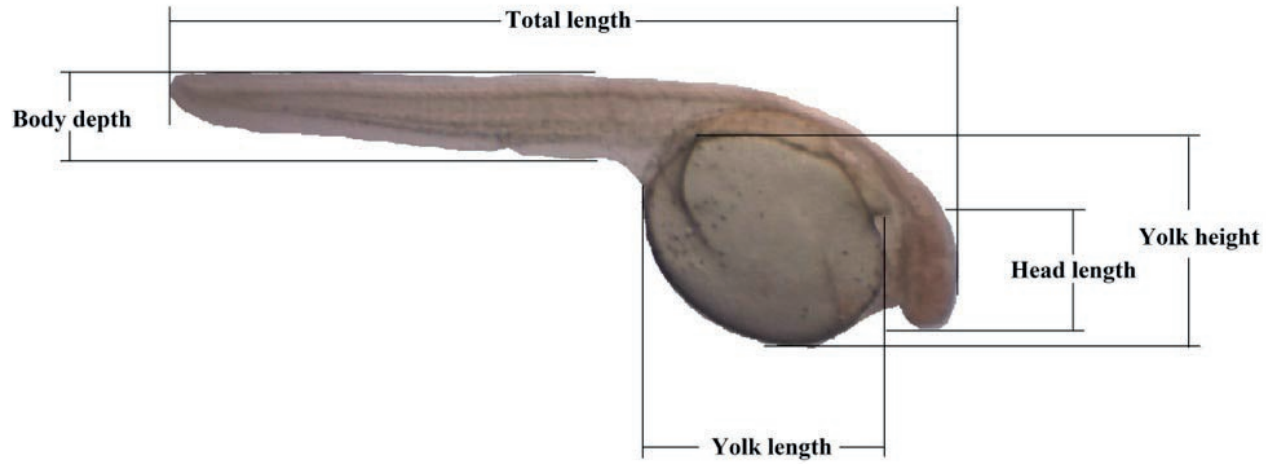

Figure 1. Biometric parameters of hatchling. (Source: Okomoda *et al.* 2017).

Biometric characteristics of the eggs and the newly hatched larvae (Figure 1) were also recorded using the scaled picture from the microscope. The morphological characteristics measured include the larvae's total length, head length, yolk height, yolk length, body depth and yolk volume. The Yolk volume was also calculated according to the formula given by Blaxter and Hampel (1963):

$V = (\pi/6)\ LH^2$

V is the yolk size volume, L is the yolk size length, and H is the yolk size height.

Water quality parameters such as pH, dissolved oxygen, total dissolved solids, electric conductivity, and temperature were monitored every three hours throughout the incubation period for the treatments and their replicates in the two experiments. This was done using Hanna's digital multi-parameter water checker (Model HL 98126). The water quality was maintained at optimum: pH=7.00±0.22; Dissolved Oxygen = 5.00±0.11 mgL^{-1}; TDS = 220±0.15 mgL-1; Cond. = 605±0.44 µS/cm; T°C = 29.0±0.05°C. Descriptive statistics of the breeding parameters, egg, and larvae characteristics were analyzed using the Minitab 14 computer software. Data were initially tested for normality and homogeneity of variance before Analysis of Variance (ANOVA) was done. Where significant differences occurred, means were separated using Fisher's least significant difference at a significance level of $p \leq 0.05$. However, when the assumptions of normality and homogeneity did not hold, data were analyzed using the Kruskal-Wallis non-parametric test.

RESULTS

Viability of stripped African catfish eggs exposed at room temperature for varying period

The characteristics of stripped eggs exposed to prevailing atmospheric conditions at varying times are stated in Table 1. Results revealed that the minor axis before fertilization was not different between the control and treatment groups 1HPS, 2HPS and 3HPS. However, it significantly reduced at higher exposure times (i.e., 4HPS, 8HPS and 12HPS). Hence, the minor axis before fertilization was higher at the 2HPS (1.40µm) and lowest at the 12HPS (0.57µm). The major axis, the egg volume, and the egg area before fertilization were also not significantly different between the control and treatment groups 1HPS and 2HPS. Similarly, the values significantly reduced for the three variables as the exposure to atmospheric oxygen increased, with the least observed in the 12HPS. A similar trend was also observed after fertilization in the minor axis, major axis, egg volume, and egg area.

In most cases, the highest value was observed in the control, while the lowest was at 12HPS. The fertilization and hatchability percentage of the stripped eggs shown in Table 2 reveal a significant decrease in value with delayed fertilization time. The severity was observed in the 8HPS (13.87% and 0.78%, respectively) and 12HPS (0.4% and 0.00%, respectively) for the fertilization and hatchability rates. However, The abnormal egg development percentage was higher at 8HPS (92.74%) and lowest in the control (0.56%).

Table 3 shows the characteristics of hatched larvae from the delayed fertilized eggs. Results revealed no

Table 1. Egg characteristics of stripped African catfish *Clarias gariepinus* eggs following delayed fertilization with sperm.

	Control	1HPS	2HPS	3HPS	4HPS	8HPS	12HPS	P-value
Minor Axis before fertilization (μm)	1.27±0.22^{ab}	1.23±0.20^{ab}	1.40±0.32^{a}	0.87±0.09^{abc}	0.60±0.12^{c}	0.77±0.09^{bc}	0.57±0.09^{c}	0.024
Major Axis before fertilization (μm)	1.53±0.15^{a}	1.57±0.20^{a}	1.53±0.33^{a}	0.97±0.15^{b}	0.73±0.09^{b}	0.87±0.09^{b}	0.67±0.03^{b}	0.004
Egg Volume before fertilization (μm^3)	1.44±0.64^{ab}	1.42±0.60^{ab}	2.03±1.00^{a}	0.41±0.13^{b}	0.16±0.74^{b}	0.29±0.08^{b}	0.12±0.04^{b}	0.002
Egg Area before fertilization (μm^2)	6.27±1.67^{ab}	6.32±1.78^{ab}	7.40±2.81^{a}	2.71±0.64^{bc}	1.44±0.44^{c}	2.14±0.44^{bc}	1.20±0.23c	0.031
Minor Axis After fertilization (μm)	1.63±0.19^{a}	1.50±0.23^{a}	1.57±0.27^{a}	1.13±0.19^{ab}	0.83±0.12^{b}	1.10±0.27^{ab}	0.80±0.10^{b}	0.049
Major Axis After fertilization (μm)	1.93±0.09^{a}	1.77±0.15^{ab}	1.93±0.12^{a}	1.40±0.15^{bc}	1.07±0.12^{c}	1.40±0.25^{bc}	0.97±0.03^{c}	0.001
Egg Volume After Fertilization (μm^3)	2.83±0.79^{a}	2.28±0.82^{ab}	2.73±1.08^{a}	1.03±0.15^{ab}	0.43±0.15^{b}	1.11±0.50^{ab}	0.34±0.08^{b}	0.001
Egg Area After Fertilization (μm^2)	10.02±1.61^{a}	8.53±1.95^{ab}	9.68±2.19^{ab}	5.08±1.25^{bc}	2.88±0.69^{c}	5.21±1.79^{bc}	2.45±0.38^{c}	0.013

The mean in the same column with different superscripts differ significantly ($p<0.05$). Note HPS = Hours Post Stripping.

Table 2. Breeding parameters of stripped African Catfish *Clarias gariepinus* eggs following delayed fertilization with sperm.

	Control	1HPS	2HPS	3HPS	4HPS	8HPS	12HPS	P-value
%Fertilization	95.36±2.41^{a}	78.00±2.48^{b}	70.62±0.20^{c}	61.87±2.77^{d}	62.44±2.29^{d}	13.87±2.40^{e}	0.4±0.23^{f}	0.001
% Abnormal egg development	0.56±0.36^{b}	1.70±0.50^{b}	1.78±0.64^{b}	3.28±0.18^{b}	7.05±3.13^{b}	92.74±4.30^{a}	66.70±33.3^{a}	0.001
% Hatchability	87.01±5.62^{a}	71.75±0.96^{b}	61.90±3.28^{bc}	52.34±4.58^{cd}	44.71±8.37^{d}	0.78±0.24^{e}	0.00±0.00^{e}	0.001

The mean in the same column with different superscripts differ significantly ($p<0.05$). Note HPS = Hours Post Stripping.

Table 3. Hatched larvae characteristics of stripped African Catfish *Clarias gariepinus* eggs after delayed fertilization with sperm.

	Control	1HPS	2HPS	3HPS	4HPS	8HPS	P-value
Total Length (mm)	3.07±0.29	3.03±0.09	2.98±0.03	2.97±0.03	2.90±0.21	2.07±0.15	0.686
Head Length (mm)	0.59±0.10	0.55±0.00	0.57±0.07	0.57±0.07	0.57±0.03	0.63±0.03	0.310
Yolk Height (mm)	1.53±0.09	1.53±0.33	1.53±0.33	1.53±0.33	1.53±0.33	1.53±0.33	1.000
Yolk Length (mm)	1.73±0.12	1.97±0.03	2.00±0.10	2.00±0.08	1.93±0.03	1.87±0.09	0.082
Body Depth (mm)	0.60±0.06	0.63±0.07	0.57±0.07	0.57±0.07	0.67±0.03	0.60±0.06	0.818
Yolk Area (mm^2)	8.40±1.02	9.47±0.32	9.63±0.21	9.63±0.21	9.31±0.18	8.97±2.54	0.450
Yolk Volume (mm^3)	2.18±0.39	2.43±0.13	2.48±0.11	2.48±0.11	2.38±0.09	2.29±0.04	0.842

The mean in the same column with different superscripts differ significantly ($p<0.05$).
Note HPS = Hours Post Stripping.

significant difference between the control and the treatment groups in terms of the Total length, Head length, Yolk Height, Yolk length, Body depth, Yolk area and Yolk volume.

The pictorial evidence of the normal embryogenetic development of the delayed fertilized eggs of African Catfish (*C. gariepinus)* is shown in Figure 2. The different embryogenetic stages were completed within 24hrs 19minutes and includes the following: Fertilized egg (0min); One-cell stage (32mins); Two-cell stage (57mins); Four-cell stage (1hr 2mins); Eight-cell stage (1hr 43mins); Sixteen-cell stage (1hr 51mins); Thirty-two cell stage (2hrs 3mins); Sixty-four cell stage (3hrs 19mins); Morula (4hrs 47mins); Blastula (6hrs 2mins); Gastrula (10hrs 14mins); 95% Epiboly (12hrs 7mins); Somite begins (16hrs 18mins); Advance somite (18hrs 39mins); Prime (22hrs 58mins); Hatchling (24hrs 19mins).

Viability of Stripped African Catfish Eggs stored for a short duration using different methods

The characteristics of *C. gariepinus* eggs stored for 8 hours using different methods are shown in Table 4. The result revealed no significant difference in the major (1.60 to 1.95μm and 1.55 to 1.95μm) and minor axis (1.10 to 1.60μm and 1.43 to 1.60μm) of the eggs before and after fertilization, respectively for the treatment and control groups. While there was no significant difference in the Egg volume (1.01 to 3.30μm^3) and area (5.53 to 10.93μm^2) before fertilization, it significantly increased

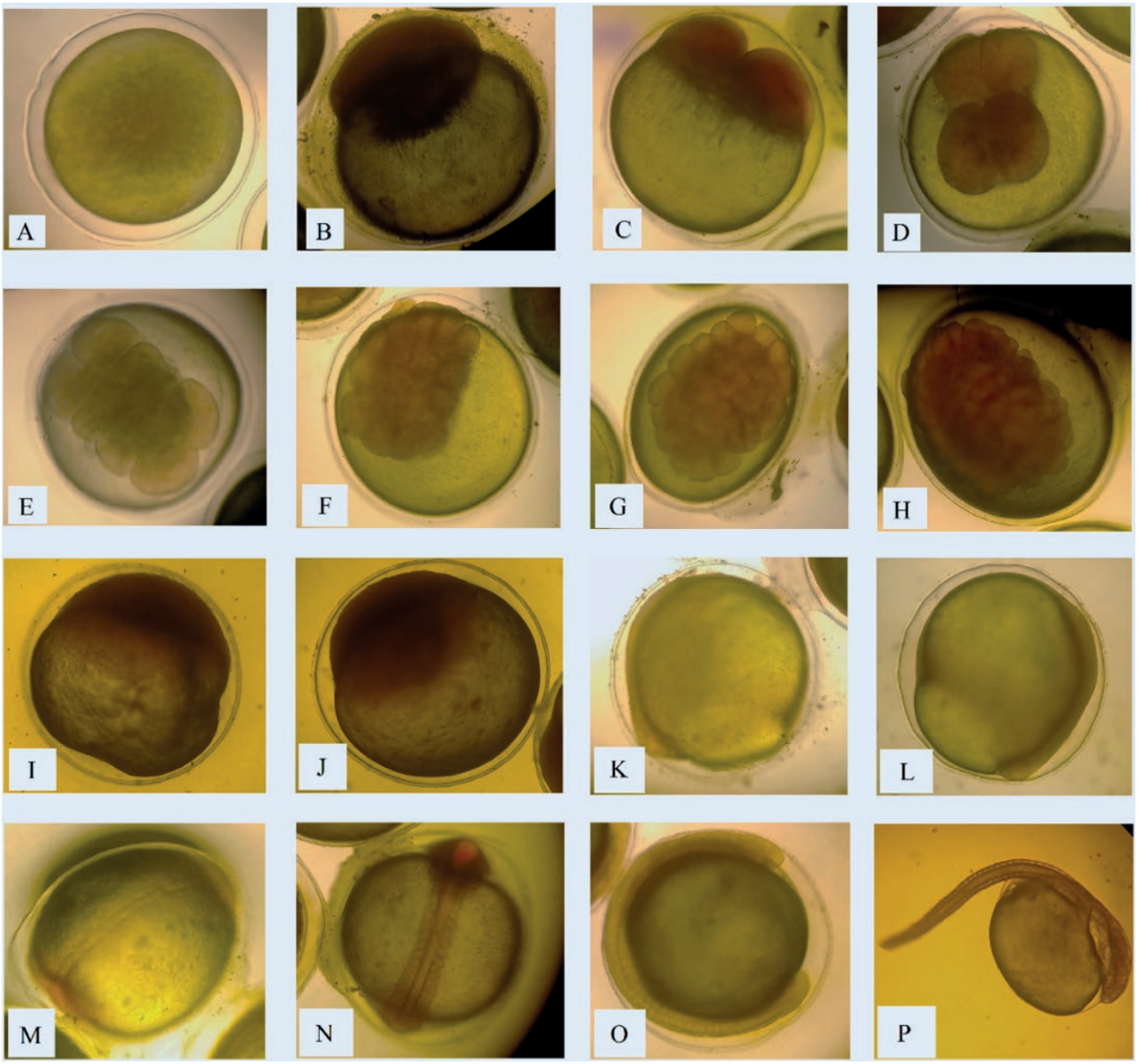

Figure 2. Normal embryogenesis stages as observed in African Catfish *Clarias gariepinus* under laboratory conditions: (A) Fertilized egg; (B) One-cell stage; (C) Two-cell stage; (D) Four-cell stage; (E) Eight-cell stage; (F) Sixteen-cell stage; (G) Thirty-two cell stage; (H) Sixty-four cell stage; (I) Morula; (J) Blastula; (K) Gastrula; (L) 95% Epiboly; (M) Somite begins; (N) Advance somite; (O) Prime; (P) Hatchling.

after fertilization with the lowest observed in the negative control TRT1 (1.97μm^3 and 6.67μm^2) and the highest in TRT2 (3.55μm^3 and 11.37μm^2) respectively.

The breeding performance of the eggs is also shown in Table 5. The result reveals a significant reduction in the fertilization rate of the eggs stored using the different methods (8.23 to 15.23%) compared with the positive control group (83.69%). Abnormality percentages of the treatment groups of the different storage methods were also above 90% and above, resulting in zero hatched fry in most treatments (except TRT1 with 0.78% hatchability).

Figure 3 also shows the embryogenetic development of the eggs of *C. gariepinus* stored using different methods before fertilization with fresh sperm. The various stages of development were completed within 24 hours, with the hatch larva emerging normally. The abnormality observed during the embryogenesis ranges from partial aggregation/and uneven division of the cell cytoplasm to abnormal epiboly development (Figure 4).

Table 4. Egg Characteristics of African catfish *Clarias gariepinus* eggs stored using different methods for 8 hours.

	Control	TRT 1	TRT 2	TRT 3	TRT 4	TRT 5	TRT 6	P-value
Minor Axis before fertilization (μm)	1.10±0.11	1.38±0.16	1.60±0.14	1.50±0.15	1.58±0.08	1.78±0.13	1.60±0.07	0.097
Major Axis before fertilization (μm)	1.60±0.30	1.63±0.09	1.85±0.12	1.78±0.13	1.85±0.05	1.95±0.05	1.88±0.05	0.259
Egg Volume before fertilization (μm^3)	1.01±0.19	1.74±0.52	2.61±0.51	2.21±0.52	2.43±0.27	3.30±0.51	2.53±0.24	0.112
Egg Area before fertilization (μm^2)	5.53±1.03	7.15±1.26	9.44±1.29	8.49±1.29	9.16±0.57	10.93±1.04	9.42±0.48	0.096
Minor Axis After fertilization (μm)	1.60±0.20	1.33±0.14	1.85±0.09	1.65±0.16	1.63±0.11	1.57±0.09	1.43±0.05	0.088
Major Axis After fertilization (μm)	1.75±0.15	1.55±0.17	1.95±0.05	1.88±0.05	1.95±0.05	1.83±0.05	1.73±0.10	0.069
Egg Volume After fertilization (μm^3)	2.43 ± 0.79^{ab}	1.97 ± 0.44^{c}	3.55 ± 0.42^{a}	2.77 ± 0.52^{ab}	2.74 ± 0.36^{ab}	2.69 ± 0.28^{ab}	1.84 ± 0.15^{c}	0.043
Egg Area After Fertilization (μm^2)	8.88 ± 1.86^{abc}	6.67 ± 1.34^{c}	11.37 ± 0.83^{a}	9.77 ± 1.10^{ab}	9.96 ± 0.77^{ab}	9.03 ± 0.57^{abc}	7.71 ± 0.46^{bc}	0.042

The mean in the same column with different superscripts differ significantly ($p<0.05$).

Table 5. Breeding parameters of African catfish *Clarias gariepinus* eggs stored using different methods for 8 hours.

	Control	TRT 1	TRT 2	TRT 3	TRT 4	TRT 5	TRT 6	P-value
%Fertilization	83.69 ± 2.98^{a}	15.23 ± 3.42^{b}	8.85 ± 1.43^{b}	8.23 ± 0.79^{b}	8.52 ± 1.49^{b}	13.35 ± 3.64^{b}	11.10 ± 0.24^{b}	0.001
% Abnormal egg development	0.76 ± 0.38^{c}	89.43 ± 4.32^{b}	100.00 ± 0.00^{a}	100.00 ± 0.00^{a}	100.00 ± 0.00^{a}	100.00 ± 0.00^{a}	100.00 ± 0.00^{a}	0.001
%Hatchability	72.44 ± 3.44^{a}	0.78 ± 0.41^{b}	0.00 ± 0.00^{b}	0.00 ± 0.00^{b}	0.00 ± 0.00^{b}	0.00 ± 0.00^{b}	0.00 ± 0.00^{b}	0.001

The mean in the same column with different superscripts differ significantly ($p<0.05$).
Keys:
Control = Eggs stripped and fertilized immediately (+ve Control)
TRT 1 = Egg exposed to room temperature without an extender (-ve Control)
TRT 2 = Egg exposed to room temperature with the addition of extender
TRT 3 = Egg exposed to room temperature with the addition of extender and aeration.
TRT 4 = Egg kept in the fridge without the extender.
TRT 5 = Egg kept in the fridge with the addition of extender.
TRT 6 = Egg kept in the fridge with the addition of extender and aeration.

DISCUSSION

Differences in the sizes of the eggs have been previously linked to broodstock quality and broodstock size (Bromage and Roberts, 1995; Ataguba *et al.,* 2013). The egg size range of *C. gariepinus,* as reported by Hassan *et al.* (2018), is larger than those reported for this study and could, therefore, be linked to the different broodstocks used. It is also noteworthy that because of the prolonged exposure of the egg to the atmosphere oxygen, the egg sizes were observed to shrink before fertilization with sperm. This may be because of dehydration under prolonged delayed fertilization and exposure to atmospheric oxygen. The top layer of the egg mass was observed to dry up, making the eggs of treatments 1HPS to 12HPS appear smaller. For the second experiment, however, there was no significant difference in the egg size when stored using the different methods. Although no concrete scientific explanation could be made for this observation, it is interesting to note that exposure of the freshwater fish eggs to 5% saline treatment for 8 hours did not cause significant size reduction anticipated from dehydration possible due to the hypertonic environment in which the eggs were placed. Like the finding of Olufeagba *et al.* (2016), an increase in the size of the eggs was observed after fertilization with sperm in both experiments. This observation of egg size increase after fertilization may be due to the entry of sperm into the micropyle of the fertilized egg or the hydration of the non-fertilized eggs (Okomoda et al., 2018).

Once eggs are stripped, they are expected to be fertilized immediately so the embryogenic development of the egg can begin. The findings of this first study show that delayed fertilization affected the viability of eggs, and detrimental effects were observed at a time threshold beyond 4 hours. According to Samarin *et al.* (2015), the significant loss in viability due to the delay of fertilization could result from egg ageing. The finding of this first study is, therefore, in consonant with the report by many previous authors, which suggests that egg viability is inversely proportional to post-ovulation time (Bobe and Labbe, 2010; Suquet *et al.,* 2000 and Urbanyi *et al.,* 1999). In an attempt to improve the viability of the eggs further, different methods which involved the sole and combined administration of refrigeration, aeration and extender

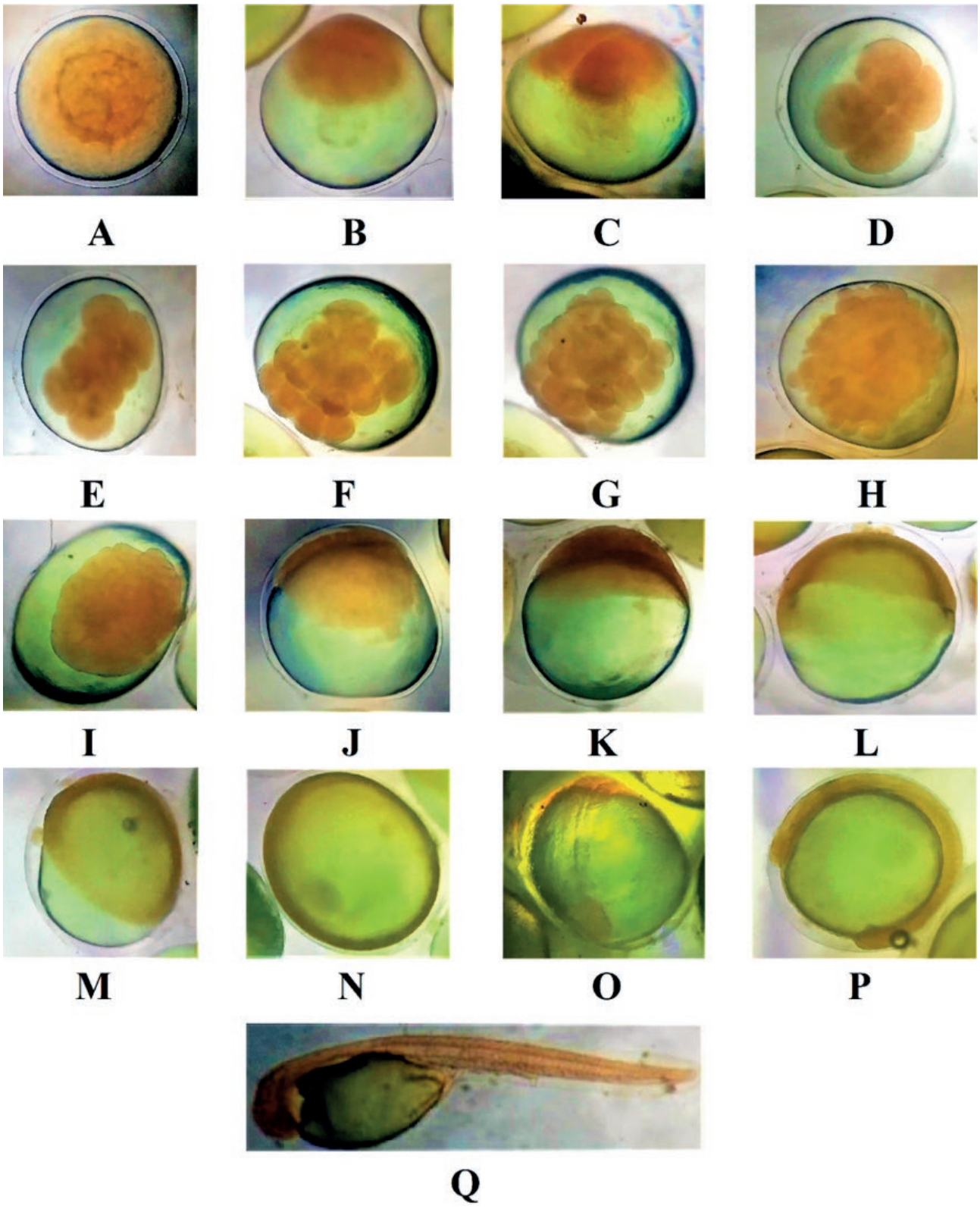

Figure 3. Normal embryogenesis stages of African Catfish *Clarias gariepinus* under laboratory conditions of storage: (A) Fertilized egg; (B) One-cell stage; (C) Two-cell stage; (D) Four-cell stage; (E) Eight-cell stage; (F) Sixteen-cell stage; (G) Thirty-two cell stage; (H) Sixty-four cell stage; (I) Morula; (J) Blastula; (K) Gastrula; (L) 75% Epiboly; (M) 90% Epiboly; (N) 95% Epiboly; (O) Somite begins; (P) Prime; (Q) Hatchling.

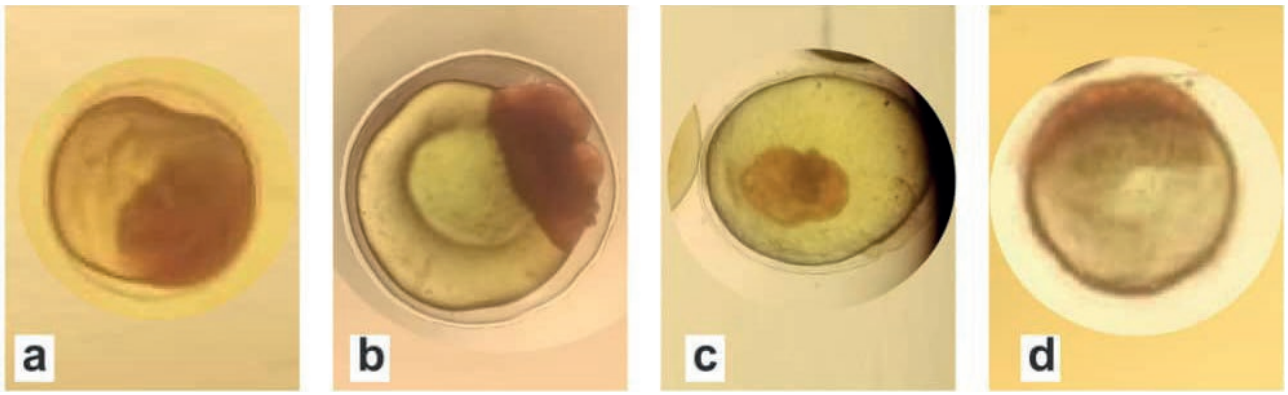

Figure 4. Abnormal egg development seen in eggs stored for 8 hours under different storage conditions.

(i.e., physiological saline) were tested in the second study. Unfortunately, all attempts to preserve the eggs' viability using these different storage approaches failed as the fertilization and hatchability rates were not improved, as observed in the second study. Contrary to this finding, the study by Samarin *et al.* (2017) reported that unfertilized eggs of Eurasian perch stored at low temperatures remained viable for 48 hours while that of salmonid eggs were viability for about 9 days as reported by Niksirat *et al.* (2007). Different species of fish may respond differently to different storage methods based on their biology.

Rothbard *et al.* (1996) also reported the storage of common carp, *Cyprinus carpio* eggs for short durations at low temperatures (6-9^{o}C), variable/high temperatures (12-31^{o}C) and at moderate-stable temperatures (20-24.5^{o}C). Their finding shows that *C. carpio* eggs stored at moderate and stable temperatures for a maximal duration of 6 hours yielded hatch-out larvae percentages higher than 50%. Similarly, the current results showed that the eggs of *C. gariepinus* preserved at room temperature responded better than those preserved with refrigeration. According to Nguenga *et al.* (2004), two strains of catfish eggs stored separately had better viability in warmer than colder temperatures. Linhart *et al.* (2001) evaluated the ova of tench *Tinca tinca* in various extenders at 21°C under aerobic conditions. Their findings show that the ova stored in the Dettlaff extender for one hour achieved 24-30% hatching compared to 58% recorded in the control. This is like the finding of our study with the physiological saline used. However, the severity of our finding compared to the report of Linhart *et al.* (2001) could be linked to the duration of exposure to the physiological saline storage aside from the differences in the species used.

The attempt of short-term storage with an extender may have also resulted in the closure of the micropyle of the eggs due to the nature of the liquid medium, hence triggering abnormal cell division without the presence of appropriate sperm, as noticed during the embryogenetic observation. This is probably the primary cause of the poor hatching recorded for the treatments with an extender. Like the current study, mass rupture of the cell structure of the eggs and uneven cell division were evident during the embryogenesis of the incubated eggs reported by (Rahman *et al.,* 2020) and Okomoda et al. (2018), respectively. The exact reason for such extensive disruption of cell metabolism, especially in treatments with extender, may result from the influx or presence of salt deposited in the cell. Normal embryogenic development was similar to those previously reported in the studies of Olaniyi and Omitogun (2014) and Okomoda et al. (2018) for the same species.

Ataguba *et al.* (2013) had earlier reported that the effect of egg size transcends beyond the developmental ability of the embryo to the characteristics of hatched fry. However, despite the significant differences in the egg size before and after fertilization of the different eggs delayed for fertilization, the attributes of normally hatched larvae in all the treatments of the first study were still similar. The larvae characteristics of the hatched fry in the second experiment were not taken since hatchability was close to zero in all the treatment groups except the positive control. Therefore, this study's findings suggest a four-hour window beyond which the viability of stripped eggs will be affected if not fertilized with appropriate sperm. Future studies can further research other short-term storage options not evaluated in this study, as all the current attempts failed to improve the viability of the ova under laboratory conditions.

ACKNOWLEDGEMENTS

The authors are profoundly grateful to the staff and students of the Department of Fisheries and Aquaculture,

Joseph Sarwuan Tarka University (formerly the Federal University of Agriculture Makurdi), who lend a helping hand during the tedious research process of this study. We would also like to thank the anonymous reviewers whose views and opinions have helped to modify this manuscript to its current level of acceptability for publication.

AUTHORS CONTRIBUTION

VTO SOO conceptualized and designed the study, FT and VTO experimented with assistance from several students and staffs, hence collecting the needed data for analysis which was done by VTO. Meanwhile, VTO wrote the draft of the manuscript. SGS, DAB, RY, IK validated the data, revised the manuscript, and approved it submission to be publication.

REFERENCES

Adebayo, O.T., Lawal, O.A., and Adeoye, O.A. (2015) Aspects of the Biology and Ecology of African Catfish (*Clarotes laticeps*) in the Lower Ogun River, Nigeria. *Journal of Aquatic Sciences* 30(1), 35-43.

Adeyemo, O. K., Adeyemo, O. A., Oyeyemi, M. O., and Gbede, S. A. (2007). Effect of semen extenders on the motility and viability of stored African catfish (*Clarias gariepinus*) spermatozoa. *Journal of Applied Science and Environmental Management* 11(1): 13-16.

Ataguba G.A., Okomoda V.T., and Onwuka M.C., (2013) Relationship Between Broodstock Weight Combination and Spawning Success in African catfish (*Clarias gariepinus*). *Croat Journal of Fisheries* 71:176–181.

Blaxter, J. H., and Hempel, G. (1963). The Influence of Egg Size on Herring Larvae (*Clupea harengus*). *ICES Journal of Marine Science* 28(2): 211-240.

Bobe J. and Labbe C., (2010) Egg and Sperm Quantity in Fish. *General and Comparative Endocrinology* 165: 535-548

Bromage N. R., and Roberts R. J., (1995) Broodstock Management and Egg and Larval Quality. Blackwell Science Company 2121 S (State Avenue, Ames, Iowa 500148300, USA): Iowa State University Press; p. 6-24: 76-93

Dauda AB, Natrah I, Karim M, Kamarudin MS, and Bichi AH, (2018) African Catfish Aquaculture in Malaysia and Nigeria: Status, Trend and Prospects. *Fisheries and Aquaculture Journal* 9: 237.

Dettlaff T.A., Ginsburg A.S., and O.I. Schmalhausen. (1993) Sturgeon Fishes. Developmental Biology and Aquaculture. Springer-Verlag, Berlin. 300 pp.

FAO, (2020). The State of World Fisheries and Aquaculture 2020. Sustainability in Action. Rome: FAO. https://doi.org/10.4060/ca9229en

Furuita, H., Ohta, H., Unuma, T., Tanaka, H., Kagawa, H., Suzuki, N., and Yamamoto, T. (2003) Biochemical Composition of Eggs in Relation to Egg Quality in the Japanese Eel, *Anguilla japonica*. *Fish Physiology and Biochemistry* 29: 37-46.

Harvey, B., and Kelley, R. N. (1984). Short-term Storage of *Sarotherodon mossambicus* Ova. *Aquaculture* 37(4): 391-395.

Hassan, A., Okomoda, V. T., and Nurhayati, M. N. (2018) Embryonic Development of Diploid and Triploid Eggs of *Clarias gariepinus* (Burchell, 1822). *Caryologia* 71(4): 372-379.

Idahor, K. O., Okunsebor, S. A., Sokunbi, O. A., Osaiyuwu, O. H., Osayande, U. D., Hamza, J., and Isah, N. (2018) Effect of Storage Temperature on African Catfish (*Clarias gariepinus* Burchell 1822) Milt Quality. *International Journal of Innovation Studies in Aquatic Biology and Fisheries* 4(1): 7-12.

Jensen, J. O. T., and Alderdice, D. F., (1984). Effect of Temperature on Short-term Storage of Eggs and Sperm of Chum Salmon (*Oncorhynchus keta*). *Aquaculture* 37(3): 251-265.

Kalinina, L., Zelenskaya, I., Trufanova, S., and Kalinin, N. (2020) Prospects of Development of Aquaculture in Russia and its Regions. In E3S Web of Conferences Volume 81, p. 01008. EDP Sciences.

Khedkar G.D. and Khedkar C.D. (2003) Encyclopedia of Food Science and Nutrition, Second Edition

Linhart O, Gela D, Rodina M, and Rodriguez GM (2001) Short-term Storage of Ova of Common Carp and Tench in Extenders. *Journal Fish Biology* 59(3): 616-623.

Megbowon, I., Fashina-Bombata, HA., Akinwale MA., Hammed, AM., Okunade OA., and Mojekwu TO. (2013) Breeding Performance of *Clarias gariepinus* Obtained from Nigerian Waters. *IOSR Journal of Agriculture and Veterinary Science* 6(3): 6-9.

Nguenga, D., Teugels, GG., Legendre, M., and Ollevier, F. (2004) Effects of Storage and Incubation Temperature on the Viability of Eggs, Embryos and Larvae in Two Strains of an African Catfish, *Heterobranchus longifilis* (Siluriformes, Clariidae). *Aquaculture Research* 35(14): 1358-1369.

Niksirat H, Sarvi K, Mojazi Amiri B, and Hatef A., (2007) Effects of Storage Duration and Storage Media on Initial and Post-eyeing Mortality of Stored Ova of Rainbow Trout *Oncorhynchus mykiss*. *Aquaculture* 262(2-4): 528-531.

Okomoda V.T, Koh ICC, Shahreza M.S. (2017) First Report on the Successful Hybridization of *Pangasian-*

odon hypophthalmus (Sauvage, 1878) and *Clarias gariepinus (Burchell, 1822). Zygote* 25(4): 443-452.

Okomoda V.T., Koh ICC, Shahreza M.S., (2018) A Simple Technique for Accurate Estimation of Fertilization Rate with Specific Application to *Clarias gariepinus (Burchell, 1822). Journal of Aquaculture Resources* 49: 1116e21.

Olaniyi, W. A., and Omitogun, O. G. (2014) Stages in the Early and Larval Development of the African Catfish *Clarias gariepinus* (Teleostei, Clariidae). *Zygote* 22(3): 314-330.

Olufeagba S. O. and Okomoda V. T. (2016). Cannibalism and performance evaluation of hybrids between Clarias batrachus and Clarias gariepinus. *Croatian Journal of Fisheries* 74(3): 124-129.

Olufeagba SO, Okomoda VT, Shaibu G. (2016) Embryogenesis and Early Growth of Pure Strains and Hybrids Between *Clarias gariepinus* (*Burchell*, *1822*) and *Heterobranchus longifilis Valenciennes*, *1840*. *North American Journal of Aquaculture* 78: 346-355.

Omoniyi, S.A., Adeyemi, O.A., and Okechi, J.K. (2018) Growth Performance and Survival Rate of African Catfish (*Clarotes laticeps*) Juveniles Reared in Concrete Tanks. *Nigerian Journal of Fisheries* 15(2): 233-238.

Rahman, S. M., Alsaquft, A. S., Alkhamis, Y. A., Rahman, M. M., Ahsan, M. N., Mathew, R. T., and Hossain, Q. Z. (2020) Short Term Storage of Asian Walking Catfish (*Clarias batrachus* linnaeus, 1758) Gametes. *Advances in Animal and Veterinary Sciences* 8(12): 1394-1401.

Rizzo, E., Godinho, H. P., and Sato, Y. (2003) Short-term Storage of Oocytes from the Neotropical Teleost Fish *Prochilodus marggravii*. *Theriogenology* 60(6): 1059-1070.

Rothbard, S., Rubinshtein, I., and Gelman, E. (1996) Storage of Common Carp, *Cyprinus carpio* Eggs for Short Durations. *Aquaculture Research* 27(3): 175-181.

Samarin AM, Żarski D, Palińska-Żarska K, Krejszeff S, Blecha M, Kucharczyk D, and Policar T (2017) Invitro Storage of Unfertilized Eggs of the Eurasian Perch and its Effect on Egg Viability Rates and the Occurrence of Larval Malformations. *Journal of Animal Sciences Volume* 11(1): 78-83.

Samarin AM, Policar T, Lahnsteiner F (2015) Fish Oocyte Ageing and its Effect on Egg Quality. *Review on Fisheries Science and Aquaculture* 23(3): 302-314.

Suquet M., Dreanno C., Fauvel C., Cosson J. and Billard R., (2000) Cryopreservation of Sperm in Marine Fish. *Aquaculture Research* 31: 231-243.

Tilahun, G., and Yalew, A. (2024). Cryopreservation and artificial insemination in African Catfish (Clarias gariepinus, Burchell 1822): A review. *Journal of Agriculture and Environmental Sciences* 9(1): 110-122.

Tacon, A. G. (2020). Trends in global aquaculture and aquafeed production: 2000–2017. *Rev. Fish. Sci. Aquac.* 28: 43-56. https://doi.org/10.1080/23308249.2019.1649634

Urbanyi B., Horvath A., Varga Z. and Horvath L., (1999) Effect of Extenders on Sperm Cryopreservation of African Catfish, *Clarias gariepinus* (*Burchell*). *Aquaculture Research* 30: 145-151

Withler, F. C., and Lim, L. C. (1982) Preliminary Observations of Chilled and Deep-frozen Storage of Grouper (*Epinephelus tauvina*) Sperm. *Aquaculture* 27(4): 389-392.

Yue K., and Shen Y., (2021) An Overview of Descriptive Technologies for Aquaculture. *Journal of Aquaculture and Fisheries* 7: 111-112.

Caryologia
International Journal of Cytology, Cytosystematics and Cytogenetics

Firenze University Press
https://riviste.fupress.net/index.php/caryologia

OPEN ACCESS

Citation: Abdo, A. S., Hamdy, R. S., El Garf, I. A., & Abd El Gawad, M. E. (2025). Taxonomic evaluation of three Egyptian *Solanum* species based on morphology, DNA sequences, and chromosome analysis. *Caryologia* 78(3): 15-28. doi: 10.36253/caryologia-3456

Received: April 11, 2025

Accepted: October 5, 2025

Published: December 24, 2025

Data Availability Statement: All relevant data are within the paper and its Supporting Information files.

Competing Interests: The Author(s) declare(s) no conflict of interest.

ORCID
ASA: 0000-0002-8470-8940
RSH: 0000-0001-7777-693X
IAEG: 0000-0002-8464-1125
MEAEG: 0000-0001-8267-8859

Taxonomic evaluation of three Egyptian *Solanum* species based on morphology, DNA sequences, and chromosome analysis

Amany S. Abdo[1,*], Rim S. Hamdy[2,3], Ibrahim A. El Garf[1], Mona E. Abd El Gawad[4]

[1] *Department of Botany and Microbiology, Faculty of Science, Cairo University, Egypt*
[2] *Biological science department, Faculty of Science, Galala University, Suez, Egypt*
[3] *Department of Botany and Microbiology, Faculty of Science, Cairo University, Giza, Egypt*
[4] *National Gene Bank, Agriculture Research Center (ARC), Egypt*
*Corresponding author. Email: amanysallam88@gmail.com

Abstract. We investigated the intra-specific relationships between three *Solanum* species in Egypt: *Solanum nigrum*, *Solanum villosum*, and *Solanum sinaicum*, in addition to the inter-specific relationships among the populations of the three studied species. These species' taxonomic difficulty is primarily due to its inconsistent infra-specific treatments in various floras. The morphological studies revealed distinguishing characteristics for the three investigated *Solanum* species mainly fruit and flower characteristics. The morphological differences allowed *S. villosum* to be divided into two subspecies: subsp. *villosum*, and subsp. *miniatum*. The genetic variation between the three *Solanum* species was clarified using AFLP technique. The ribosomal DNA ITS1-5.8S-ITS2 region of the three studied species was sequenced using the universal primers ITS4 and ITS5. The DNA sequences of *Solanum* species were counted. The karyotypes of the species under examination were established using the chromosome number and genome size acquired from mitotic chromosomal preparations.

Keywords: AFLP, karyotype, *Solanum*, *S. nigrum*, *S. sinaicum*, *S. villosum*.

INTRODUCTION

Solanaceae is one of the largest and most essential families of flowering plants. This family serves as a significant source for medicine, food, and spice (Afroz et al. 2020). It is extensively dispersed in both tropical and temperate regions; it has 100 genera and over 2500 species thriving in a variety of environments and ecologies and exhibits different morphologies (Nderitu et al. 2023). Solanaceae is represented in Egypt by eight genera including 30 species (Boulos 2002). *Solanum* L. is the family's largest genus (El-Shaboury et al. 2020). There are several species of *Solanum* that are used in traditional medicine, and some of these species are employed as sources of drugs in pharmacology (Jainu and Devi 2005). Due to its morphological plasticity and infraspecific genetic variation, *Solanum* possesses a taxonomic challenge (Jennifer and James 1997), also because of the 6,931 names that have been

published, many of which are connected to the cultivated and widely distributed species of the genus (Särkinen et al. 2018).

Solanum is represented in Egypt by 9 species (Boulos 2002). However, Täckholm (1974) recorded 10 species. Zohary (1966) recorded two subspecies of *Solanum villosum*: subsp. *villosum* and subsp. *puniceum*. Boulos (2002) recorded that *Solanum villosum* Mill. is represented in Egypt with two subspecies: subsp. *villosum* and subsp. *miniatum*. The name *Solanum sinaicum* is considered a synonym of *Solanum villosum* (Särkinen et al. 2018; powo.science.kew.org/) but the name is accepted by Khafagi et al. (2018) and (www.solanaceaesource.org).

Low taxonomic level phylogenetic relationships have been successfully solved using AFLP (Despres et al. 2003; Koopman 2005; Meudt and Clarke 2007). The use of AFLP offers numerous advantages. It generates data that is highly reproducible (Jones et al. 1997), and doesn't require a priori sequence knowledge. Previous attempts using AFLP markers have proved effective in resolving taxonomic issues and illuminating relationships among species of *Solanum* (Kardolus et al. 1998; Mace et al. 1999a, 1999b; Coulibaly et al. 2002; Jacoby et al. 2003; Dehmer and Hammer 2004; Olet 2004).

The objectives of this study are to investigate the morphological and genetic diversity found in the populations of the three selected *Solanum* species: *S. nigrum*, *S. villosum* and *S. sinaicum*, to solve the taxonomic problem of these species in Egypt due to the confused infraspecific groupings.

MATERIALS AND METHODS

Morphological study

This study was based on the examination of specimens deposited at Cairo University Herbarium (CAI), in addition to the authentic type specimens preserved in virtual herbaria that are accessible online (the JSTOR Global Plants database). Acronyms follow Index Herbariorum (http://sweetgum.nybg.org/ih/). In addition to the examination of fresh representative specimens of each of the three species collected between 2022–2024. These specimens belonging to 5 different localities from different phytogeographical regions of Egypt. The coordinates of these localities: 30°49'56" & 29°34'49"; 30°00'18" & 31°12'45"; 30°00'49" & 31°12'04"; 29°17'23"& 30°51'11"; and 28°33'38" & 33°58'20". All specimens were examined for morphological variations in all distribution localities. There were 44 different morphological features analyzed, including those for the stem, leaves, flower, and fruit. Scientific names for the species follow IPNI (http://www.ipni.org/). Vouchers Samples were placed in (CAI).

Data analysis

44 morphological characteristics were analyzed in order to establish a correlation between the samples of the three *Solanum* species. All samples had their characteristics measured and documented, and the software (R-4.3.1 for Windows) was used to analyze the data and create the heat map. A heatmap is a visual representation of numerical data where each value is represented as a square, with lighter squares representing smaller numerical values and darker squares representing larger values (Tiessen et al. 2017).

Cytogenetics study

Chromosomes number and Karyotype formulae

Chromosome preparations

Between 2022 and 2024, plant material was collected for cytogenetic analysis. A total of thirty specimens were sampled, comprising ten individuals from each of the three Solanum species. Seeds were extracted from the specimens and soaked in distilled water for 1 h prior to germination at room temperature. Root tips approximately 1 cm in length were excised and pretreated with 0.025% colchicine ($C_{22}H_{25}NO_6$) for 2 h at room temperature to arrest cells at metaphase, followed by rinsing with distilled water. The treated samples were subsequently fixed in a 3:1 (v/v) ethanol:glacial acetic acid solution.After thorough washing with distilled water, the root tips were hydrolyzed in 1 N HCl at 64 °C for 5 min. For slide preparation, the root tips were squashed in 45% acetic acid and stained with acetoorcein solution to visualize chromosomes. The procedure followed previously described protocols (Ibrahim et al., 2019; Elsayed et al., 2024).

Microscopic examination karyotyping, idiograming and signals imaging

Chromosomes examination was done via a vertical fluorescence microscope (Leica DM2500) equipped with a cooled monochrome digital camera (Leica DFC340FX). Twenty cells with clearly observed and well spread chromosomes were checked and photographed at 100X magnification under oil immersion. Chromosome counting and karyotype has performed via the automated Karyotype and FISH software processing (Leica

CW4000) system. Ideograms were constructed from complete chromosomes which showed the greatest possible banding pattern in at least ten different metaphase plates. (Ibrahim et al. 2019; Abdo et al. 2023).

Molecular study

DNA extraction

For the chosen samples of *Solanum nigrum*, *Solanum villosum* and *Solanum sinaicum*, genomic DNA was isolated from one gram of juvenile leaves using the CTAB (Cetyl-trimethyl ammonium bromide) extraction buffer approach as described by Doyle and Doyle (1990) and modified by Allen et al. (2006).

PCR reactions and data analysis

PCR amplification was carried according to Williams et al. (1990) with some modification. The reaction volume of 25 µl containing 12.5 µl Dream Taq Green PCR Master Mix (2X), 1 µl Forward primer, 1 µl Reverse primer, 2 µl Template DNA and completed to 25 µl with water (nuclease-free) was placed in a thin-walled PCR tube on ice, then gently vortex the samples and spin down. PCR reaction was performed using the recommended thermal cycling conditions: One cycle of initial denaturation at 95°C for 5 minutes, 35 cycles of denaturation at 95°C for 45 seconds followed by annealing at 57°C for 45 seconds, extension at 72°C for 60 seconds, and one cycle of final extension at 72°C for 10 minutes.

The reaction products were separated by electrophoresis on a 1.6% agarose gel in a 1x TBE buffer, run in the same buffer at 100 V for an hour, and then visualized by staining with 0.5 g/ml of ethidium bromide and being photographed under UV light.

To elucidate the genetic variation and construct the phylogeny of the studied *Solanum* species, the ribosomal DNA ITS1-5.8S-ITS2 region of the three species was sequenced using ABI377 DNA sequencer (ABI, USA). DNA was amplified using the universal primers ITS4 (5´-TCCTCCGCTTATTGATATGC-3´) and ITS5 (5´-GGAAGTAAAAGTCGTAACAAGG-3´), these primers described by White et al. (1990). Then, BLAST program was employed to look for sequence similarity in DNA databases. Multiple sequence alignment and the determination of genetic distances among the analyzed species were performed using MEGA5 software. Neighbour joining dendrogram was created to highlight the genetic links between the three species. The retrieved sequences were registered on the ncbi under accession numbers PP701899, PP707086, PP707087, and PP707088. The reference sequences from other countries of *Solanum nigrum* and *Solanum villosum* used to construct the heat map are available online in the Gene bank

RESULTS

Morphological diversity

Old herbarium specimens and 150 newly collected specimens of the three studied *Solanum* species were the subject of morphological studies and taxonomy revision based on 44 morphological traits, including plant height, leaf features, as well as inflorescence and fruit characters. The flower, fruit and leaf characters were the most distinctive characters between the species, and according to the variation in morphological characters we considered the two different forms of *Solanum villosum* as two different subspecies *Solanum villosum* subsp. *villosum* and *Solanum villosum* subsp. *miniatum* (Table 1, Figs 1-4).

***Solanum nigrum* L.,** Sp. Pl., ed. 1, 219 (1753).
Common name: Black nightshade

Annual erect herb; stem glabrous to pubescent, green, angular, woody, branched, up to 70 cm tall; leaves simple, alternate, petiolate, ovate or deltoid-rhomboid, entire or irregularly dentate, acute, base cuneate to truncate, 2-7 x 1.5-3.5 cm, petiole up to 2 cm, stipules absent; inflorescences unbranched cymes, number of flowers per inflorescence 5-10, peduncle length 1-1.5 cm; Flowers pentamerous, hermaphrodite; pedicel 3-10 mm; calyx lobes triangular with acute or rounded apex, green, (1.5-2.5 x 1 mm); corolla white with yellow midrib, oblong or ovate to lanceolate, 4-5 x 2-2.5 mm, acute; stamen filament 1.5-2 mm, anthers yellow, oblong, 1.5-2.5 x1 mm; ovary globose, 0.5-1 mm in diameter, style 2-3.5 mm long, stigma is small; fruit berry, globose, black, 6-7 mm in diameter, fruiting calyx lobes spreading to reflexed 2-3 x 2 mm; seeds ovoid, 1.5–2 mm in diameter; hairs non glandular unicellular papillose, or non-glandular basal cell with long narrow apical cell, or non-glandular bicellular uniseriate with hooked or obtuse apical cell.

Solanum villosum* subsp. *miniatum (Bernh. ex Willd.) J.M.Edmonds, Bot. J. Linn. Soc. 89: 166 (1984).
Common name: Woolly nightshade, Red-berried nightshade

Annual to perennial erect herb to small shrub; stem pubescent, green, angular, woody, branched, up to 70 cm tall; leaves simple, alternate, petiolate, broadly to narrowly ovate to elliptic or deltoid, entire or irregularly sinuate-dentate, acute to acuminate or obtuse, base

Table 1. Morphological variation among the studied *Solanum* species.

Character	*S. villosum* subsp. *miniatum*	*S. villosum* subsp. *villosum*	*S. nigrum*	*S. sinaicum*
Life cycle	Annual to perennial	Annual to perennial	Annual	perennial
Plant nature	Erect	Erect	Erect	Erect
Growth habit	herb to small shrub	herb to small shrub	herb	herb to small shrub
Plant surface	pubescent with multicellular glandualr hairs	pubescent	glabrous or with short hairs	sparsely pubescent
Stem length (cm)	up to 70	up to 70	up to 70	up to 60
Stem type	woody	woody	woody	woody
Stem shape	branched	branched	branched	branched
Stem outline	angular	angular	angular	angular
Stem color	green	green	green	green
Leaf structure	simple	simple	simple	simple
Leaf arrangement	alternate	alternate	alternate	alternate
Petiole length (cm)	up to 2	up to 2	up to 2	up to 3
Leaf shape	broadly to narrowly ovate to elliptic or deltoid	broadly to narrowly ovate to elliptic or deltoid	ovate or deltoid-rhomboid	oblong-rhombic to oblong-ovate
Leaf margin	entire or irregularly sinuate-dentate	entire or irregularly sinuate-dentate	entire or irregulary dentate	sinuate-dentate rarely entire
Leaf apex	acute to acuminate or obtuse	acute	acute	acute
Leaf base	cuneate to truncate or cordate	cuneate to truncate, cordate or hastate	cuneate to truncate	cuneate to truncate
Leaf color	green	green	green	green
Leaf length (cm)	2 to 6	2 to 8.5	2 to 7	2 to 6
Leaf width (cm)	1.5 to 5	1.5 to 6.5	1.5 to 3.5	1 to 3
stipules	absent	absent	absent	absent
number of lateral veins	4-7 per leaf	6-7 per leaf	6	6
Inflorescence type	unbranched cymes	unbranched cymes	unbranched cymes	unbranched cymes
number of flowers per inflorescence	2-5 flowers	3-6 flowers	5- 10 flowers	4-8 mostly 7
peduncle length (cm)	0.5-2.5	1-1.5	1-1.5	1.5-2.5
pedicel length	7-11 mm	9-12 mm	3-10 mm	8-11 mm
calyx lobes	rounded	rounded	triangular with acute or rounded apex	linear-oblong with acute or rounded apex
length	2.5 mm	2 mm	1.5-2.5 mm	1-2 mm
width	1 mm	1 mm	1 mm	1-2 mm
corolla color	white with black midrib	white with yellow midrib	white with yellow midrib	white with yellow midrib
corolla lobes length	8 mm	6-7 mm	4-5 mm	7-10 mm
corolla lobes width	4 mm	3 mm	2-2.5 mm	3-5 mm
filament length	2 mm	1.5 mm	1.5-2 mm	2 mm
anther length	2 .5 mm	3 mm	1.5-2.5 mm	2-3 mm
anther width	1 mm	1.5 mm	1 mm	1-1.5 mm
ovary shape	globose	globose	globose to ellipsoid	globose
ovary diameter	1 mm	1 mm	0.5-1 mm	1 mm
style	5 mm	5 mm	2-3.5 mm	5 mm
fruit type	berry	berry	berry	berry
fruit shape	globose	globose	globose	globose
fruit diameter	6-9 mm	6-9 mm	6-7 mm	7-9 mm
fruit color	bright red	orange	black	orange
friuting calyx legth	2-3 mm	3-4 mm	2-3 mm	4 mm

(Continued)

Table 1. (Continued).

Character	*S. villosum* subsp. *miniatum*	*S. villosum* subsp. *villosum*	*S. nigrum*	*S. sinaicum*
fruiting calyx width	1-2 mm	1.5-2 mm	2 mm	2 mm
hairs	non glandular bicellular uniseriate with hooked or obtuse apical cell	non glandular bicellular uniseriate with hooked or obtuse apical cell	non glandular unicellular papillose, or non-glandular basal cell with long narrow apical cell, or non-glandular bicellular uniseriate with hooked or obtuse apical cell	glandular, bicellular uniseriate stalk, with unicellular head, and glandular multicellular uniseriate stalk, unicellular head

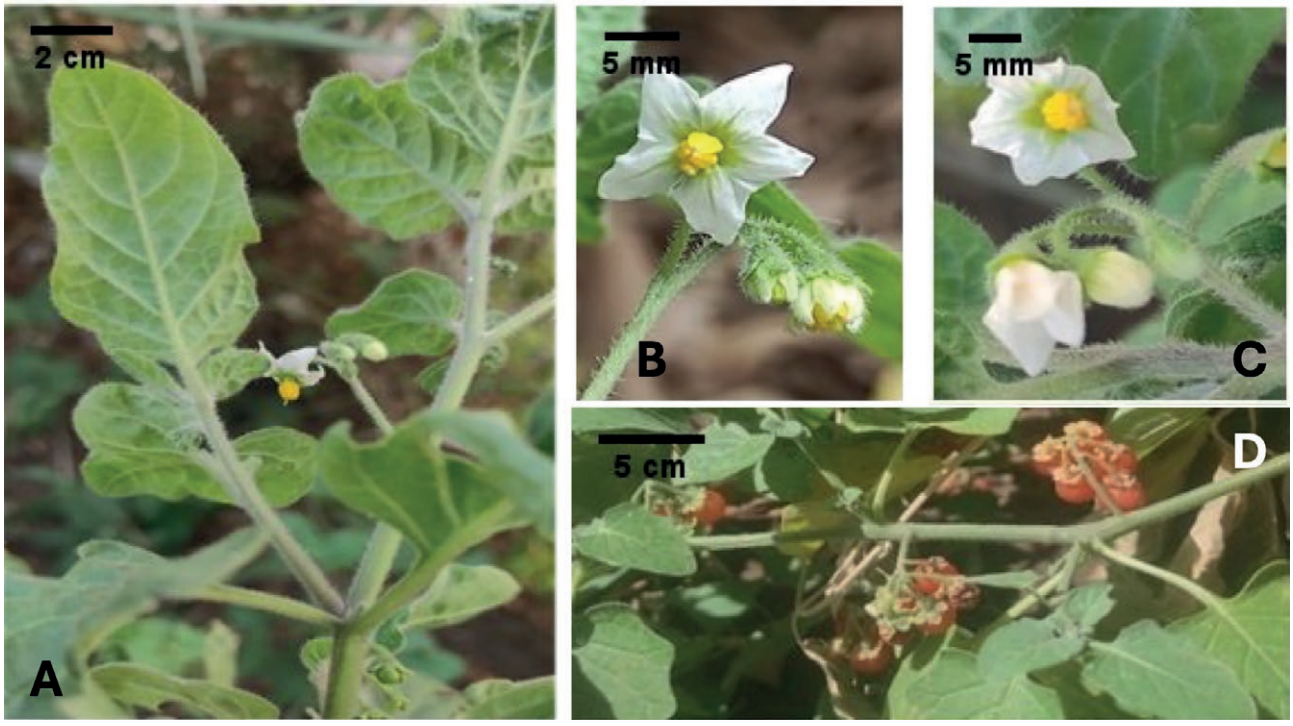

Figure 1. Specimen of *Solanum villosum* subsp. *villosum* showing the morphological features, (A) Leaf shape, (B), (C) flower shape, (D) fruit shape and color.

cuneate to truncate or cordate, 2-6 x 1.5-5 cm, petiole up to 2 cm, stipules absent; inflorescences unbranched cymes, number of flowers per inflorescence 2-5, peduncle length 0.5-2.5 cm; flowers pentamerous, hermaphrodite; pedicel 7-11 mm; calyx lobes rounded, green, (2.5 x 1 mm); corolla white with black midrib, oblong or ovate to lanceolate, 8 x 4 mm, acute; stamen filament 2 mm, anthers yellow, oblong, 2.5 x1 mm; ovary globose, 1 mm in diameter, style 5 mm long, stigma is small; fruit berry, globose, bright red, 6-9 mm in diameter, fruiting calyx lobes spreading to reflexed 2-3 x 1-2 mm; seeds 1.5–2.5 mm long, pale yellow; hairs non glandular bicellular uniseriate with hooked or obtuse apical cell.

Solanum villosum* subsp. *villosum Miller, Gard. Dict. 8th edn, no. 2 (1768)

It differs from subsp. *miniatum* in having acute leaves, base cuneate to truncate, cordate or hastate, 2-8.5 × 1.5-6.5; number of flowers per inflorescence 3-6 flowers, peduncle length 1-1.5 cm; pedicel 9-12 mm; calyx lobes 2 x 1 mm; corolla white with yellow midrib, 6-7 x 3 mm; stamen filament 1.5 mm, anthers 3 x1.5 mm; fruit orange, 3-4 x 1.5-2 mm.

Solanum sinaicum Boiss., Diagn. Pl. Orient. 11: 135 (1849)

Common name: Sinai Nightshade

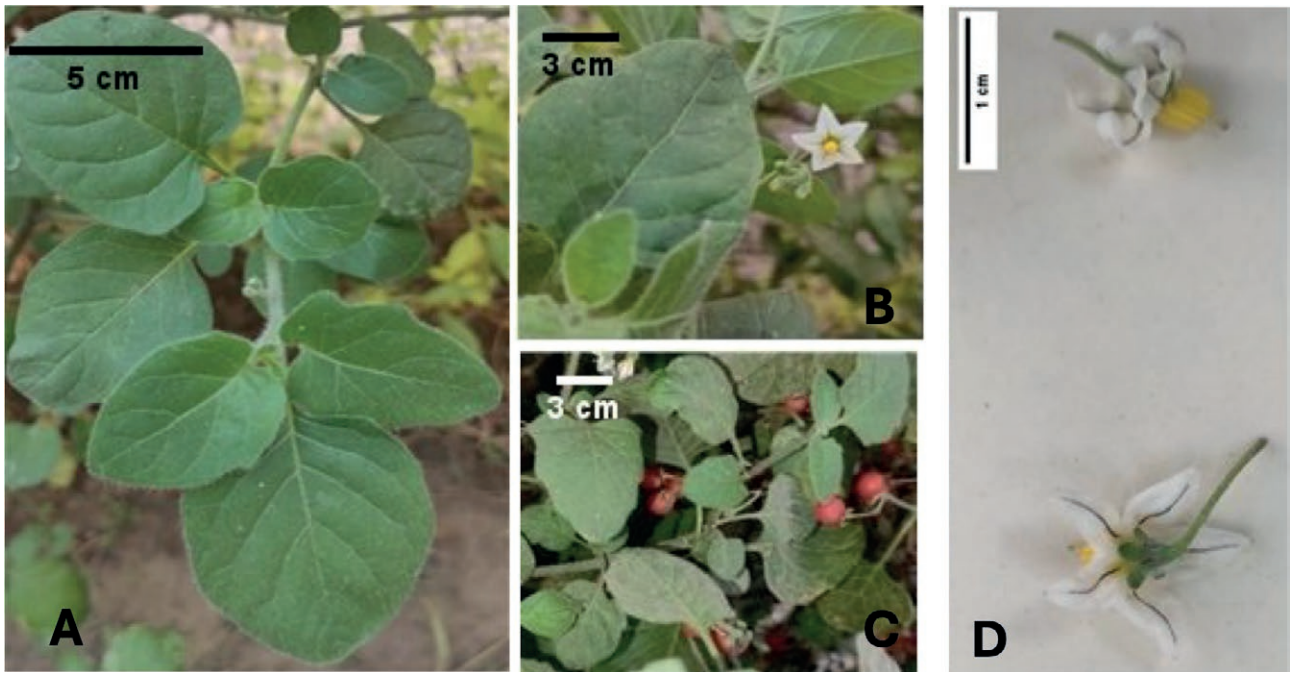

Figure 2. Specimen of *Solanum villosum* subsp. *miniatum* showing the morphological features, (A) Leaf shape, (B), (D) flower shape, (C) fruit shape and color.

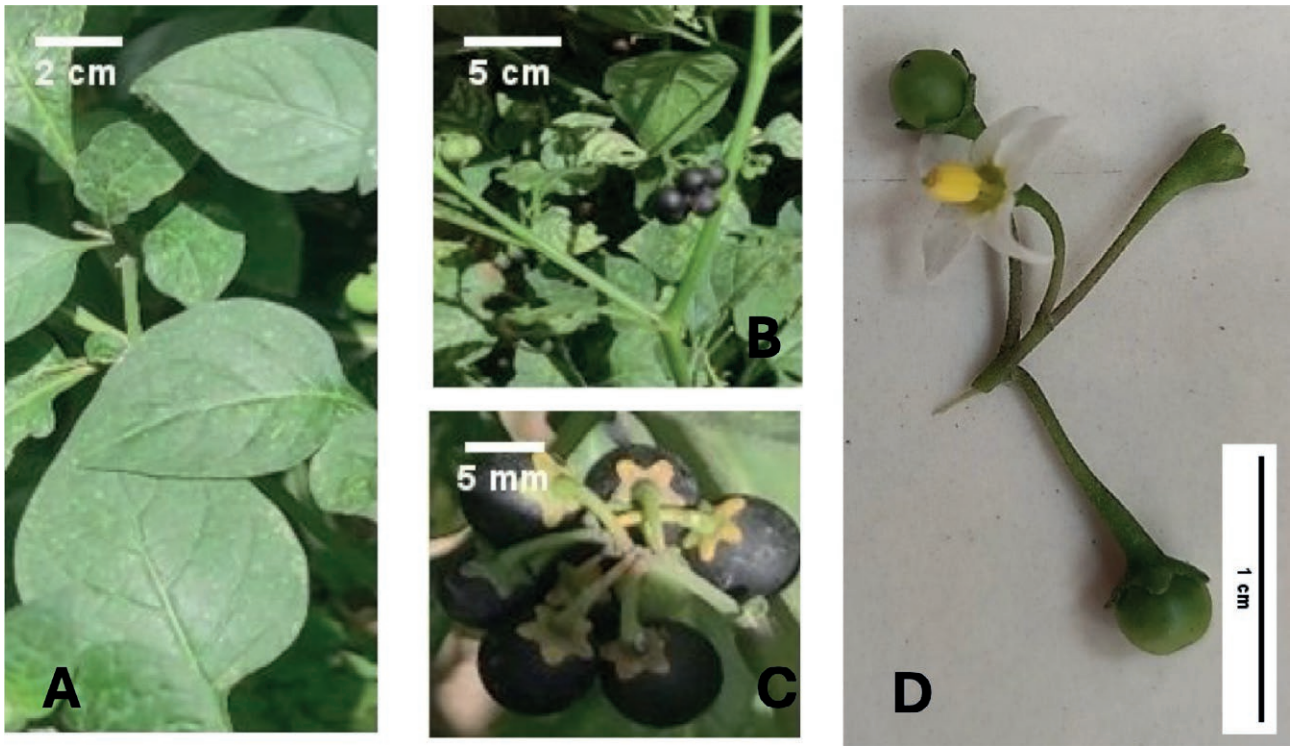

Figure 3. Specimen of *Solanum nigrum* showing the morphological features, (A) Leaf shape, (B), (C) fruit shape and color, (D) flower shape.

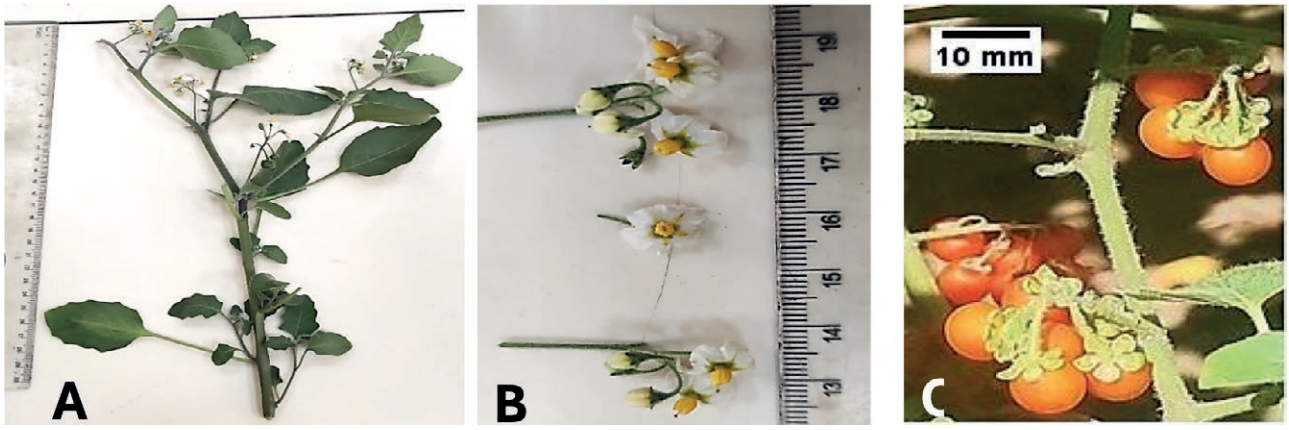

Figure 4. Specimen of *Solanum sinaicum* showing the morphological features, (A) Leaf shape, (B) Flower shape, (C) Fruit shape.

perennial erect herb to small shrub; stem sparsely pubescent, green, angular, woody, branched, up to 60 cm tall; leaves simple, alternate, petiolate, oblong-rhombic to oblong-ovate, sinuate-dentate rarely entire, acute, base cuneate to truncate, 2-6 x 1-3 cm, petiole up to 3 cm, stipules absent; inflorescences unbranched cymes, number of flowers per inflorescence 4-8 mostly 7, peduncle length 1.5-2.5 cm; flowers pentamerous, hermaphrodite; pedicel 8-11 mm; calyx lobes linear-oblong with acute or rounded apex, green, (1-2 x 1-2 mm); corolla white with yellow midrib, petals strongly recurved, 7-10 x 3-5 mm, acute; stamen filament 2 mm, anthers yellow, oblong, 2-3 x1-1.5 mm; ovary globose, 1 mm in diameter, style 5 mm long, stigma is small; fruit berry, globose, orange, 7-9 mm in diameter, fruiting calyx lobes spreading, 4 x 2 mm; seeds 1.5–2.5 mm long; hairs glandular, bicellular uniseriate stalk, with unicellular head, and glandular multicellular uniseriate stalk, unicellular head.

KEY TO STUDIED SPECIES OF THE GENUS *SOLANUM* IN EGYPT

1- Fruit berry black in color; calyx lobes triangular with acute or rounded apex ..... *S. nigrum*

- Fruit berry bright red or orange in color; calyx lobes rounded or linear-oblong 2

2- Fruit berry bright red in color; calyx lobes rounded; corolla white with black midrib ..... *S. villosum* subsp. *miniatum*

- Fruit berry orange in color; calyx lobes rounded or linear-oblong with acute or rounded apex; corolla white with yellow midrib 3

3- Leaves 2-8.5 × 1.5-6.5 cm, broadly to narrowly ovate to elliptic or deltoid; calyx lobes rounded; filament length 1.5 mm long ..... *S. villosum* subsp. *villosum*

- Leaves 2-6 × 1-3 cm, oblong-rhombic to oblong-ovate; calyx lobes linear-oblong with acute or rounded apex; filament length 2 mm long.. ..... *S. sinaicum*

Morphological correlation between the three Solanum species

Based on the 44 morphological characters that were investigated, the correlation between *S. nigrum*, *S. sinaicum*, *S. villosum* subsp. *miniatum*, and *S. villosum* subsp. *villosum* was constructed (Figure 5, Table 2). A clustering of the heat map identified two groups. *S. villosum* subsp. *miniatum* and *S. villosum* subsp. *villosum* together constituted the first group. *S. nigrum* and *S. sinaicum* were included in the second group. The heat map revealed that *S. nigrum* and *S. sinaicum* had the highest correlation (0.429), *S. villosum* subsp. *miniatum* and *S. villosum* subsp. *villosum* also have a high correlation of 0.415, followed by *S. sinaicum* and *S. villosum* subsp. *villosum* with correlation of 0.314**,** and there was a negative correlation (-0.127) between *S. villosum* subsp. *miniatum* and *S. nigrum*.

Cytogenetics study

Chromosomes number and Karyotype Formula

karyotype formula (Deanna et al., 2022), determined the fraction of m chromosomes for each of the three *Solanum* species (*S. nigrum*, *S. sinaicum* and two different subspecies of *S. villosum*) (Figure 6, Table 3) recorded highly variation. Chromosome counts from 10-20 well-scattered metaphase plates of each population of each species revealed interspecific differences in the diploid

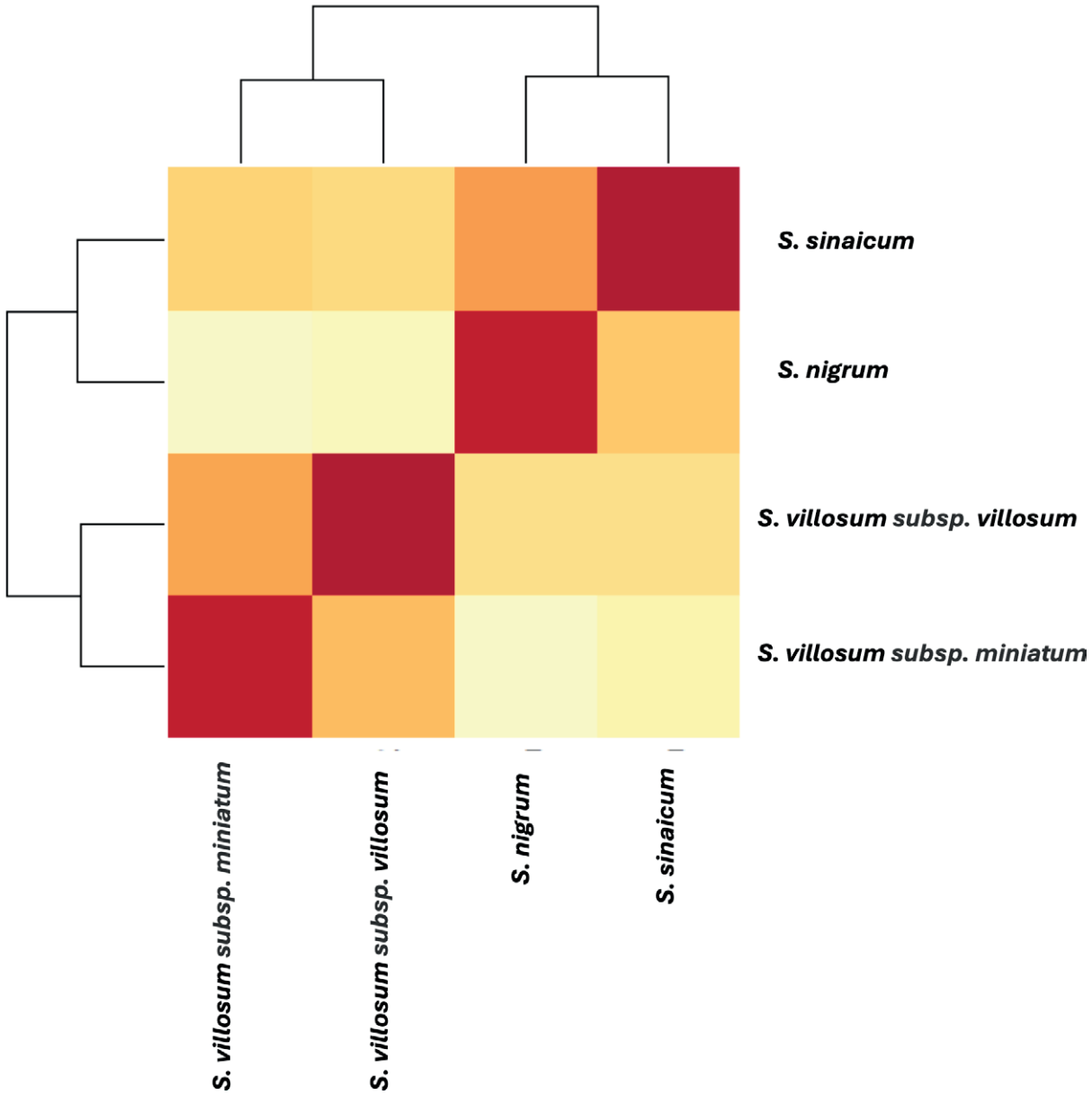

Figure 5. Heat map showing the correlation coefficients between morphological characters of the three studied *Solanum* species.

Table 2. Correlation coefficients between the three studied *Solanum* species, based on the investigated 44 morphological characters.

	S. villosum subsp. *miniatum*	*S. villosum* subsp. *villosum*	*S. nigrum*	*S. sinaicum*
S. villosum subsp. *miniatum*	1			
S. villosum subsp. *villosum*	0.415	1		
S. nigrum	-0.127	0.101	1	
S. sinaicum	0.217	0.314	0.429	1

chromosome number. *S. nigrum* showed 2n = 72 chromosomes, while *S. sinaicum* 2n= 24 chromosomes. The two different subspecies of *S. villosum* subsp. *villosum* and *S. villosum* subsp. *miniatum* showed 2n=24 and 2n= 48 chromosomes respectively. Accordingly, the x number of genome of the three *Solanum* species has been deter-

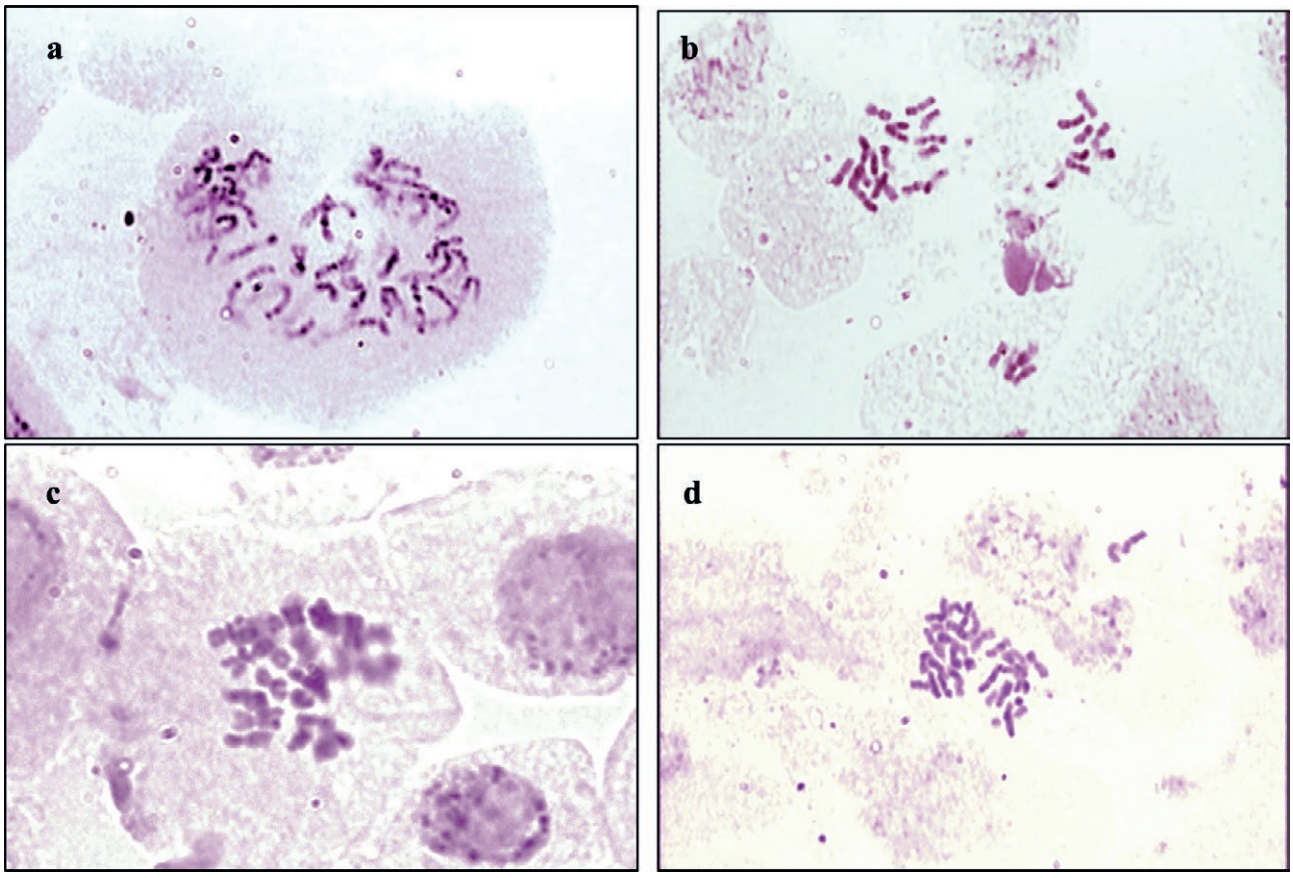

Figure 6. Photomicrographs showing well-spread mitotic metaphase of the three *Solanum* species, (a) *S. nigrum*, (b) *S. sinaicum*, (c) *S. villosum* subsp. *villosum*, (d) *S. villosum* subsp. *miniatum*.

Table 3. The chromosome number, genome size (x) and karyotype formula of the three *Solanum* species (*S. nigrum*, *S. sinaicum* and two different subspecies of *S. villosum*)

	Species	Chro. No. (2n)	Genome No. (x)	Karyotype Formula	Satellite chromosomes
1	*S. nigrum*	(2n=72)	6x	$M^{m}36+M^{sm}12+M^{ac}24$	-
2	*S. sinaicum*	(2n=24)	2x	$M^{m}12+M^{sm}4+M^{ac}8$	Chro. No. 5
3	*S. villosum* subsp. *villosum*	(2n=24)	2x	$M^{m}12+M^{sm}4+M^{ac}8$	Chro. No. 3
4	*S. villosum* subsp. *miniatum*	(2n=48)	4x	$M^{m}24+M^{sm}8+M^{ac}16$	Chro. No. 3 and 5

*M: medium, m: metacentric, sm: submetacentric, ac: acrocentric.

mined (Table 3). Both *S. nigrum* (6x) and *S. villosum* subsp. *miniatum* (4x) showed polyploidy, while *S. sinaicum* and *S. villosum* subsp. *villosum* showed diploid number (2x). (Figure 6, 7).

Molecular analysis

The PCR amplification products of the four investigated *Solanum* specimens produced four distinct, high-quality bands during gel electrophoresis. The DNA sequences ITS1-5.8S-ITS2 of 4 *Solanum* specimens that were the subject of molecular study have been registered on the National Center for Biotechnology Information (NCBI), and the following accession numbers PP701899, PP707086, PP707087, and PP707088 were given to these sequences.

Genetic correlation between the studied Solanum species

The phylogenetic dendrogram based on the ribosomal DNA ITS1-5.8S-ITS2 sequence of the three stud-

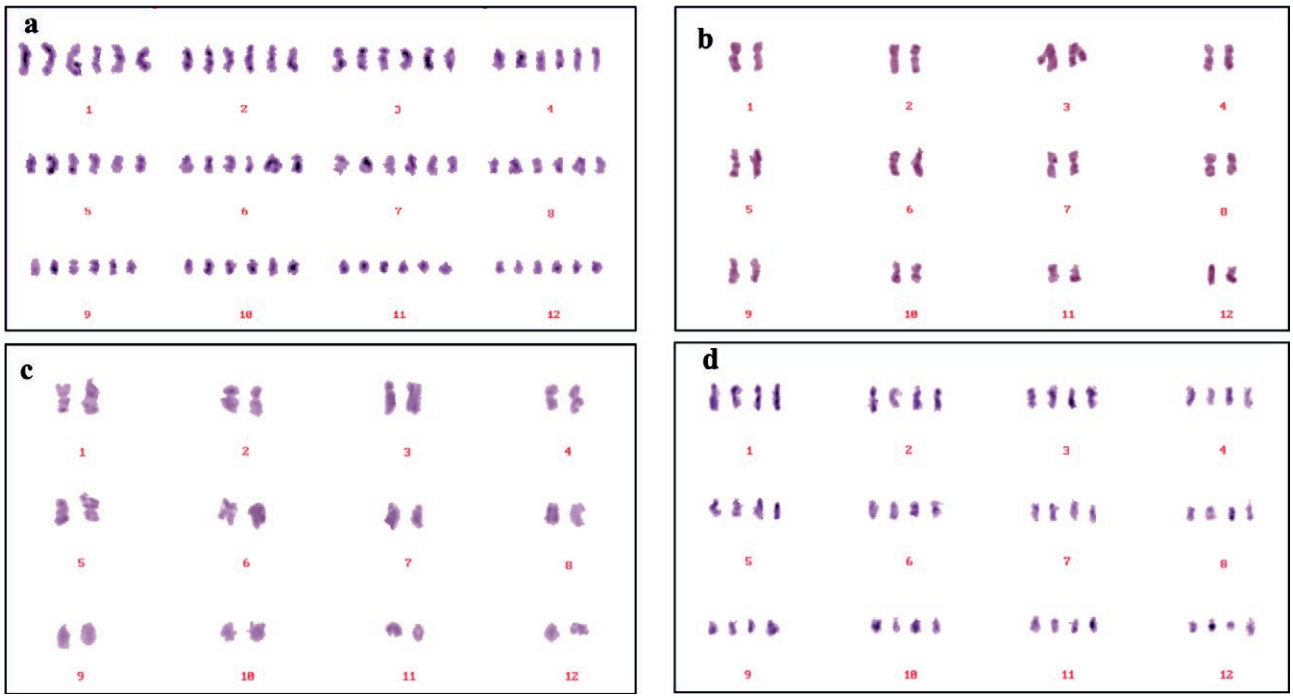

Figure 7. karyotypes of the three *Solanum* species, (a) *S. nigrum*, (b) *S. sinaicum*, (c) *S. villosum* subsp. *villosum*, (d) *S. villosum* subsp. *miniatum*.

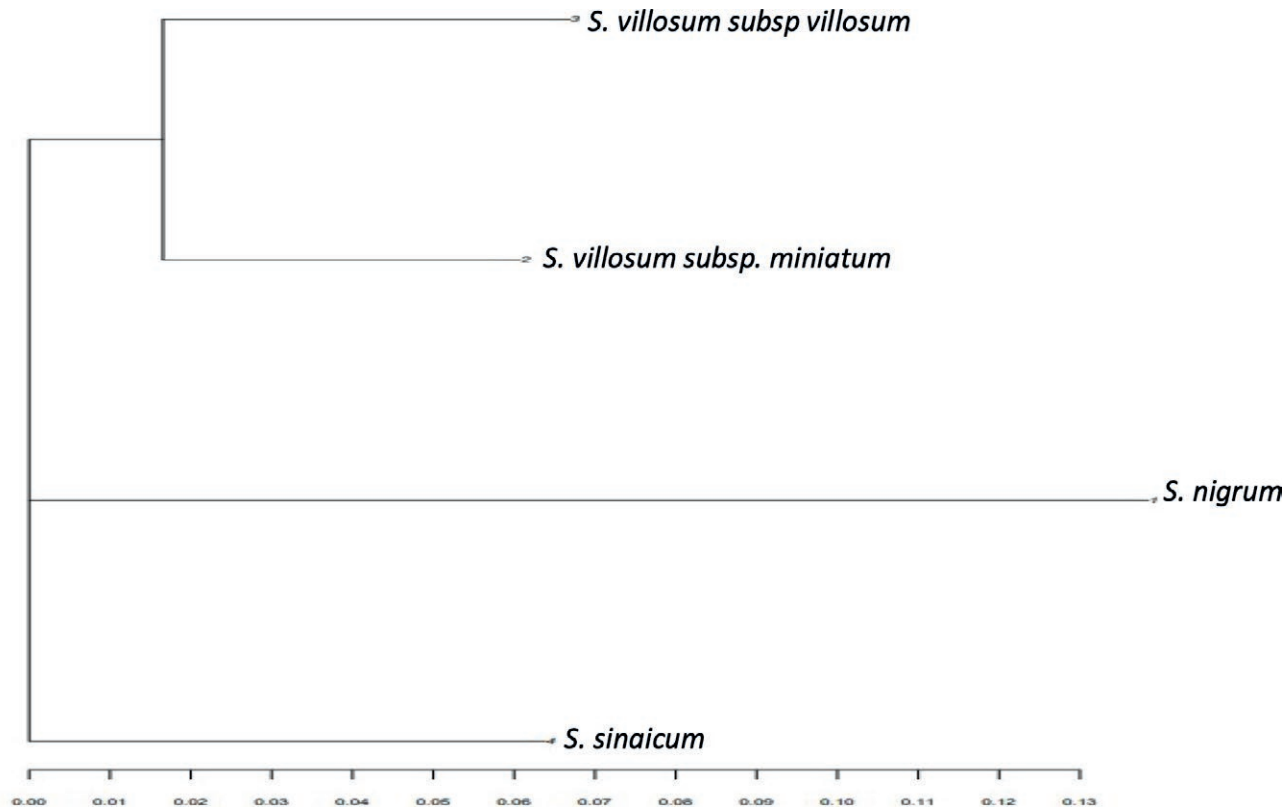

Figure 8. Phylogenetic dendrogram created by UPGMA using a combination of the ribosomal DNA ITS1-5.8S-ITS2 sequence data and values of the genetic dissimilarity distance between the investigated *Solanum* species.

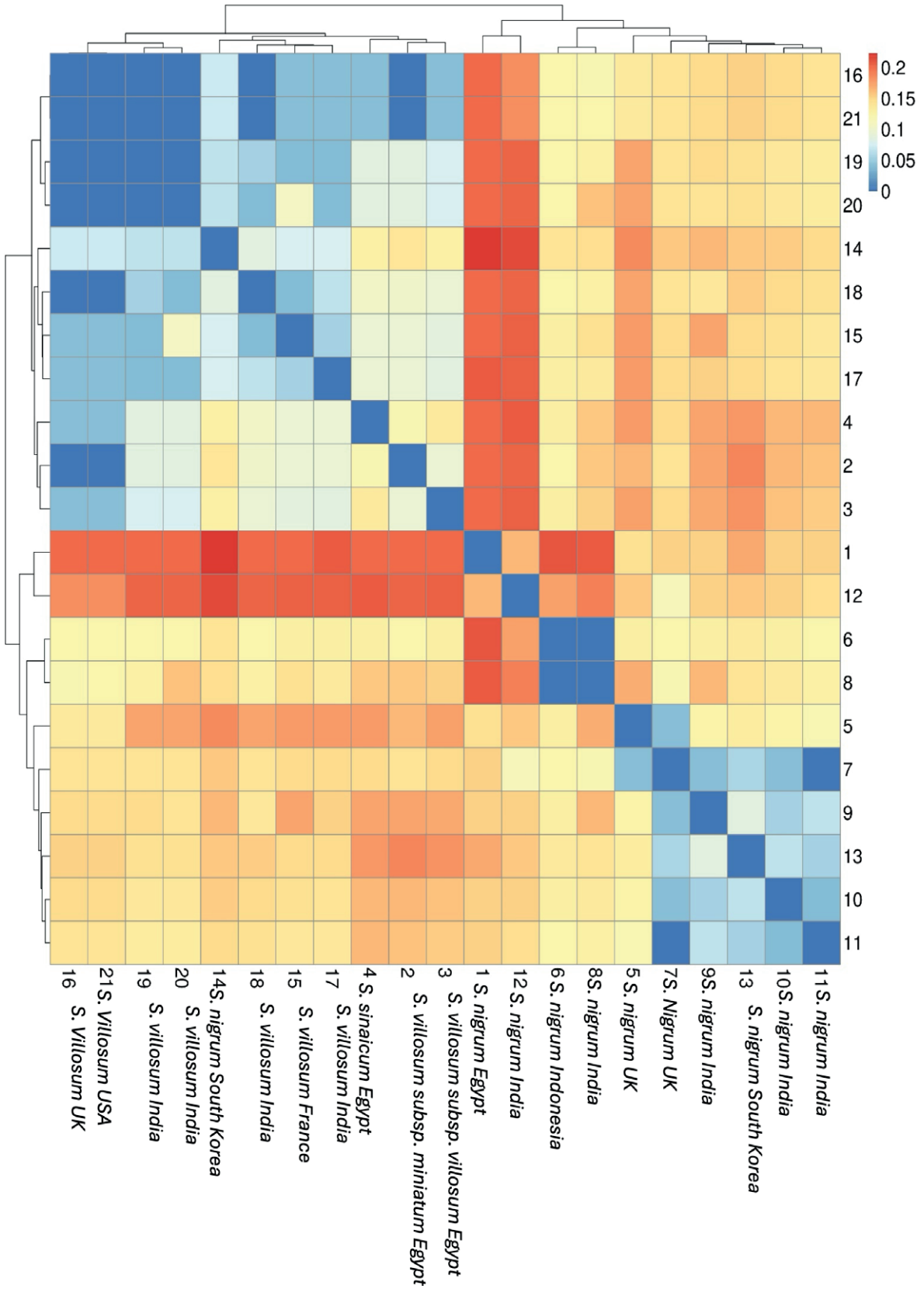

Figure 9. Heatmap of identity by state (IBS) distance matrix of 21 populations representing the three studied *Solanum* species worldwide.

ied species from Egypt (Figure 8), showed that these sequences generate three clusters. The first cluster included the two subspecies of *S. villosum* that showed close affinity with low divergence distance of 0.02. The second cluster included *S. nigrum* that showed high divergence distance from both *S. villosum* subspecies especially *S. villosum* subsp. *miniatum* and this result is consistent with the morphological correlations across these taxa. The third cluster included *S. sinaicum* which showed moderate genetic distance from *S. nigrum* and both *S. villosum* subspecies.

The genetic correlation between *S. nigrum* and *S. villosum* worldwide as shown in Figure 9 was indicated based on the constructed heat map using the ribosomal DNA ITS1-5.8S-ITS2 sequence and the genetic distance value between each two pairs, from the first sample to the last sample, is represented by each little square in the IBS distance matrix. The larger values of genetic distance between two specimens are closer to red, and smaller values are closer to blue. The heat map clustering separated two groups. The first group included specimens of *S. nigrum*, specimens 7 from UK and 11 from India have no genetic divergence, while specimens 9, 10 from India and specimen 13 from UK have very low genetic distance less 0.05, While other specimens of *S. nigrum* (Specimen 5 from UK, specimen 6 from Indonesia, specimens 6, 8 from India, specimen 1 from Egypt) have genetic distance from 0.05 to 0.2. *S. villosum* specimens comprised the second group, sp. 2 of *S. villosum* subsp. *miniatum*, sp. 3 of *S. villosum* subsp. *villosum*, and sp. 4 of *S. sinaicum* from Egypt comprised one subgroup with very low genetic distance less than 0.05, in addition the remaining specimens of *S. villosum* (sp. 17, 18, 19, 20 from India, sp. 15 from France, sp. 14 from South Korea, sp. 16 from UK, and sp. 21 from USA) also have low genetic distance less than 0.1.

DISCUSSION

Morphological identification might not be a trustworthy way to identify species in the Solanaceae because their members are cryptic and share phenotypic features that have been altered by genetic and environmental factors (Nderitu et al. 2023). However, Pojarkova (1997) and Yousaf et al. (2010) confirmed that an essential source for the classification of *Solanum* species was provided by morphological features. According to Knapp et al. 2019, *Solanum* L. possesses challenges for identification due to the lack of group-specific regional keys. There are 17 identified sections within the *Solanum* subgenus (Manoko 2007). About 50 global species make up the section *Solanum* (Child and Lester 2001), *the Solanum nigrum* complex is another name for the section *Solanum*. Since Linnaeus first described *S. nigrum* in 1753, the species in this section have undergone numerous reclassifications up till the present. The ploidy levels of the species, which range from diploid to hexaploid, the genetic variation between populations of the same species, and finally their naturally occurring inter-specific hybridization all contribute to the taxonomic complexity of this section (Edmonds and Chweya 1997).

Morphological studies of freshly collected species, in addition to the herbarium specimens of *S. nigrum*, *S. villosum*, and *S. sinaicum* based on 44 morphological characters (Table 1) showed that flower, fruit, and leaf characters were the most distinctive characters among the studied species. The examined *S. villosum* populations in Egypt exhibited inter-specific variations in morphology. These morphological differences allowed *S. villosum* to be divided into two subspecies: subsp. *villosum* has fruit with orange color, and white corolla with yellow midrib, while subsp. *miniatum* has fruit with a bright red color and white corolla with black midrib. These results agree with Boulos (2002). The morphological correlation of the three studied species as shown in Figure 5, Table 2 detected that *S. nigrum* and *S. sinaicum* had the highest correlation (0.429), followed by *S. villosum* subsp. *miniatum* and *S. villosum* subsp. *villosum* with a correlation of 0.415.

For each of the three *Solanum* species, we found the x number of genomes (Table 3). Polyploidy was demonstrated in *S. nigrum* (6x), This result agrees with Melo et al. (2011), Sultana and Alam (2007), and Särkinen et al. (2018), *S. sinaicum* and *S. villosum* subsp. *villosum* displayed diploid number (2x), however *S. villosum* subsp. *miniatum* displayed polyploidy (4x), this agrees with Sultana and Alam 2007 and Särkinen et al. 2018.

It is possible to determine the genetic diversity of individuals or populations by using morphological and molecular markers. Given that environmental factors and the stage of plant development determine morphological traits (El-Domyati et al. 2011). Previous research studies showed that ITS2 provides more accurate results on interspecific variation than intraspecific variation compared to RBCL (Duan et al. 2019). In this investigation, the ribosomal DNA ITS1-5.8S-ITS2 sequences of the studied species were used to examine the interspecific similarities showed the creation of three clusters (Figure 8), the two *S. villosum* subspecies that exhibited strong affinity and a low divergence distance of 0.02 were included in the first cluster. *S. nigrum* in the second cluster, had a high divergence distance from both *S. villosum* subspecies, particularly *S. villosum* subsp. *min-*

iatum. These findings were confirmed with the morphological correlation seen among these taxa Figure (5). *S. sinaicum* shows a moderate genetic divergence from *S. nigrum*, and both *S. villosum* subspecies were separated in the third cluster.

The heat map clustering based on the ribosomal DNA ITS1-5.8S-ITS2 sequence from worldwide specimens separated two groups (Figure 9). The first group included specimens of *S. nigrum* from Egypt and worldwide, the second group included specimens of *S. sinaicum*, *S. villosum* subsp. *miniatum*, and *S. villosum* subsp. *villosum* from Egypt in addition to worldwide specimens of *S. villosum*.

ACKNOWLEDGEMENTS

We are grateful to all members of Taxonomy and Flora section in Cairo University Herbarium (CAI) for their assistance and providing all possible facilities.

REFERENCES

Abdo AS, Ibrahim SD, Abd El Gawad ME. 2023. Biodiversity study of *Zilla spinosa* (L.) in Egypt. Egypt. J. Genet. Cytol. 52: 131-157.

Afroz M, Akter S, Ahmed A, Rouf R, Shilpi JA, Tiralongo E et al. 2020. Ethnobotany and Antimicrobial Peptides from Plants of the Solanaceae Family: An Update and Future Prospects. Front Pharmacol. 11. https://doi.org/10.3389/fphar.2020.00565

Bohs L. 2005. Major clades in Solanum based on ndhF sequences. In: Keating RC, Hollowell VC, Croat TB (eds) A Festschrift for William G. D'Arcy. the legacy of a taxonomist. Monographs in systematic botany from the Missouri Botanical Garden, vol 104. Missouri Botanical Garden, St. Louis. pp. 27-49.

Boulos L. 2002. Flora of Egypt. Verbenaceae - Compositae. Al-Hadara Publishing, Cairo. pp. 34-54.

Chiarini F, Bernardello G. 2006. Karyotype studies in South American species of *Solanum* subgen. *Leptostemonum* (Solanaceae). Plant Biol 8: 486-493. https://doi.org/10.1055/s-2006-923859

Child A, Lester RN. 2001. Synopsis of the genus *Solanum* L. and its infrageneric taxa. In: R. G. v. d. Berg, G. W. M. Barendse, G. M. v. d. Weerden, and C. Mariani (eds.), Solanaceae V: Advances in Taxonomy and Utilization. Nijmegen University Press. pp. 39-52.

Coulibaly S, Pasquet RS, Papa R, Gepts P. 2002. AFLP analysis of the phenetic organisation and genetic diversity of *Vigna unguiculata* (L.) Walp. reveals extensive gene flow between wild and domesticated types. Theor. Appl. Genet. 104: 358-366. https://doi.org/10.1007/s001220100740

Darlington CD, Wylie AP. 1955. Chromosome atlas of flowering plants. Allen & Unwin, London. pp. 325-326

Deanna R, Acosta, MC, Scaldaferro M, Chiarini F. 2022. Chromosome Evolution in the Family Solanaceae. Front. Plant Sci. 12: 787590. https://doi.org/10.3389/fpls.2021.787590

Despres L, Gielly L, Redoutet W, Taberlet P. 2003. Using AFLP to resolve phylogenetic relationships in a morphologically diversified plant species complex when nuclear and chloroplast sequences fail to reveal variability. Mol Phylogenet Evol. 27: 185-196. https://doi.org/10.1016/j.ympev.2003.09.006

Dehmer KJ, Hammer K. 2004. Taxonomic status and geographic provenance of germplasm accessions in *Solanum nigrum* L. complex: AFLP data. Gen. Res. Crop Evol. 51: 551-558.

Duan H, Wang W, Zeng Y, Guo M, Zhou Y. 2019. The screening and identification of DNA barcode sequences for Rehmannia. Sci Rep. 9(1): 1-12. https://doi.org/10.1038/s41598-019-53752-8

Edmonds JM. 1984. Botanical journal of the Linnean society. 89: 166.

Edmonds JM, Chweya JA. 1997. Black nightshades *Solanum nigrum* L. and related species. Institute of Plant Genetics and Crop Plant Research, Gatersleben / International Plant Genetic Resources Institute, Rome, Italy. pp. 5-113.

El-Domyati FM, Younis RAA, Edris S, Mansour A, Sabir J, Bahieldin A. 2011. Molecular markers associated with genetic diversity of some medicinal plants in Sinai. J Med Plants Res. 5(10): 1918-1929.

Elsayed SSA, Elshahawy IE, Hamden S, Abd Elgawad MEH, Sehsah MD. 2024. Genotoxicity by ear and kernel rots in three maize genotypes stored at different conditions. Egypt. J. Agric. Res. 102(1): 139-154. https://doi.org/10.21608/ejar.2024.250031.1467

El-Shaboury GA, Al-Wadi HM, Badr A. 2020. Biodiversity of some *Solanum* species from southwestern Saudi Arabia's highlands. Botany Letters. https://doi.org/10.1080/23818107.2020.1846614

Henderson RJ. 1973. *Solanum* and its close relatives in Florida. Ann Missouri Bot Gard 61: 819-867.

Ibrahim MA, Bekhit M, Hassan N, Refaat M, El-Akkad T. 2019, C-Banding Karyotype and Molecular Characterization on Cumin, Caraway and Coriander. Mol. Biol. 8: 229. https://doi.org/10.2139/ssrn.3388044

Jacoby A, Labuschagne MT, Viljoen CD. 2003. Genetic relationships between Southern African *Solanum ret-*

roflexum Dun. and other related species measured by morphological and DNA markers. Euphytica 132: 109-113.

Jainu M, Devi CS. 2005. Antiulcerogenic and ulcer healing effects of *Solanum nigrum* L. on experimental ulcer models: possible mechanism for the inhibition of acid formation. J Ethnopharmacol. 104: 156-163. https://doi.org/10. 1016/j.jep.2005.08.064

Jennifer ME, James AC. 1997. Black nightshades, *Solanum nigrum* L. and related species. Italy (Rome). IPGIR. pp. 5-113.

Jones CJ, Edwards KJ, Castaglione S, Winfield MO, Sala F, Wiel C, van de Bredemeijer G, Vosman B, Matthes M, Daly A, Brettschneider R, Bettini P, Buiatti M, Maestri E, Malcevschi A, Marmiroli N, Aert E, Volckaert G, Rueda J, Linacero R, Vazquez A, Karp A. 1997. Reproducibility testing of RAPD, AFLP and SSR markers in plants by a network of European laboratories. Mol Breed. 3: 381-390.

Kardolus JP, van Eck HJ, van den Berg RG. 1998. The potential of AFLPs in biosystematics: a first application in *Solanum* taxonomy (Solanaceae). Pl. Syst. Evol. 210: 87-103.

Khafagi AAF, El- Ghamery AA, Ghaly ON, Ragab OG. 2018. Fruit and seed morphology of some species of Solanaceae. Taeckholmia. 38: 123-140. https://doi.org/10.21608/taec.2018.13520

Knapp S, Vorontsova MS, Särkinen T. 2019. Dichotomous keys to the species of *Solanum* L. (Solanaceae) in continental Africa, Madagascar (incl. the Indian Ocean islands), Macaronesia and the Cape Verde Islands. PhytoKeys 127: 39-76. https://doi.org/10.3897/phytokeys.127.34326

Koopman WJM. 2005. Phylogenetic signal in AFLP Data Sets. Syst Biol. 54: 197-217. https://doi.org/10.1080/10635150590924181

Linnaeus C. 1753. Species Plantarum. Stockholm.

Mace ES, Lester RN, Gebhardt CG. 1999a. AFLP analysis of genetic relationships among the cultivated eggplant, *Solanum melongena* L., and wild relatives (Solanaceae). Theor. Appl. Genet. 99: 626-633.

Mace ES, Lester RN, Gebhardt CG. 1999b. AFLP analysis of genetic relationships in tribe Daturae (Solanaceae). Theor. Appl. Genet. 99: 634-633.

Manoko MLK. 2007. A systematic study of African *Solanum* section *Solanum* (Solanaceae). PhD thesis, Radboud University Nijmegen. http://dare.ubn.kun.nl/bitstream/2066/30032/1/30032.pdf

Meudt HM, Clarke AC. 2007. Almost Forgotten or latest Practice? AFLP applications, analyses and advances. Trends Plant Sci. 12: 106-117. https://doi.org/10.1016/j.tplants.2007.02.001

Miller P. 1768. The Gardeners Dictionary, 8th edn, no. 2. John & Francis Rivington. London.

Nderitu KW, Ager E, Mecha E, Nyachieo A. 2023. DNA Barcoding using ITS2 and RBCL markers for Solanaceae species identification. East Afr Med J. 100(1): 5567-5574.

Olet EA. 2004. Taxonomy of *Solanum* L. section *Solanum* in Uganda. Ph.D. thesis, Agricultural University of Norway.

Pinto-Magiio CAF, Pierozzi NL, Castro SCP, Soares-Scott MD. 1997. IOPB chromosome data 11. Newslett Int Organ PI Biosyst 26: 23-24.

Poczai P, Taller J, Szabó I. 2008. Analysis of phylogenetic relationship in the genus Solanum (Solanaceae) as revealed by RAPD markers. PI Svst Evol 275: 59-67. https://doi.org/10.1007/s00606-008-0051-x

Särkinen T, Poczai P, Barboza GE, Weerden GM, Baden M, Knapp S. 2018. A revision of the Old World black nightshades (Morelloid clade of *Solanum* L., Solanaceae). PhytoKeys 106: 1-223.

Täckholm V. 1974. Student's Flora of Egypt, 2nd edn. Cairo University Press, Egypt. pp. 473-474.

Tiessen A, Cubedo-Ruiz EA, Winkler R. 2017. Improved Representation of Biological Information by Using Correlation as Distance Function for Heatmap Cluster Analysis. Am J Plant Sci 8: 502-516. https://doi.org/10.4236/ajps.2017.83035

White TJ, Bruns T, Lee S, Taylor J. 1990. Amplification and direct sequencing of fungal ribosomal RNA genes for phylogenetics. In: PCR Protocols: a guide to methods and applications. (Innis MA, Gelfand DH, Sninsky JJ, White TJ, eds). Academic Press, New York, USA. pp. 315-322.

Williams JG, Kubelik AR, Livak KJ, Rafalski JA, Tingey SV. 1990. DNA polymorphisms amplified by arbitrary primers are useful as genetic markers. Nucleic Acid Res. 18: 6531-6535.

Zohary M. 1966. Flora Palaestina. The Israel Academy of Sciences and Humanities. pp. 402.

Caryologia
International Journal of Cytology, Cytosystematics and Cytogenetics

Firenze University Press
https://riviste.fupress.net/index.php/caryologia

OPEN ACCESS

Citation: Siddiqui, S. (2025). Lead and copper toxicity affecting chromosome structure, cell death, and micronucleus formation in *Glycine max* Cv-JS-355 root tip cells. *Caryologia* 78(3): 29-39. doi: 10.36253/caryologia-3423

Received: March 20, 2025

Accepted: November 10, 2025

Published: December 24, 2025

Data Availability Statement: All relevant data are within the paper and its Supporting Information files.

Competing Interests: The Author(s) declare(s) no conflict of interest.

ORCID
SS: 0000-0001-5448-7617

Lead and copper toxicity affecting chromosome structure, cell death, and micronucleus formation in *Glycine max* Cv-JS-355 root tip cells

Sazada Siddiqui

Department of Biology, College of Science, King Khalid University, Abha 61413, Saudi Arabia
Email: sasdeky@kku.edu.sa

Abstract. The rapid rise of heavy metals and their extensive industrial use have raised concerns because these metals are released into the environment from both intentional and unintentional sources. When present in the environment in high concentrations, heavy metals may threaten the plant kingdom, particularly staple food crops. Nevertheless, little research has been done to identify the effects of heavy metals. The current study aims to assess the cytological alterations caused by lead (Pb) and copper (Cu) heavy metals on *Glycine max* Cv-JS-355. For two hours, *Glycine max* seeds were subjected to different Pb and Cu concentrations (CN, 25, 50, 75, 100, and 125 ppm). They were examined for their effects on chromosomal aberrations (CAs), micronucleus index (MNI), radicle length (RL), mitotic index (MI), cell death (CD), and seed germination (SG). The findings show a dose-dependent rise in MNI, CAs, CD and a substantial decrease in SG, RL, and MI. Furthermore, the percentage of abnormal mitotic cells, including cell nucleic leaking (CNL), Multi-pole division (MPD), Chromosomal bridge at telophase (CBT), chromosome retarded in anaphase (CRA), Dissociate chromosome in metaphase (DCM), increased in the Pb and Cu treated groups.

Keywords: Heavy metals (Pb and Cu), seed germination, radicle length, mitotic index, genotoxicity, cell death, *Glycine max* Cv-JS-355.

INTRODUCTION

Heavy metals from mining, vehicle emissions, and agricultural effluents can pollute soil, affecting health of humans because of their noxious nature and higher bioaccumulation factor, potentially causing long-term ecosystem impacts (Dietrich et al. 2019; Neto et al. 2020). Heavy metal deficiency leads to environmental and toxicological issues due to increased contamination from industrialization and pesticide use. Contamination from agricultural waste, home sewage, and industrial discharges enters water bodies, reducing water quality and increasing metal availability in food chain (Hassan et al. 2020). Rapid industrialization and urbanization worldwide lead to the toxicity of dangerous metals in soil, including lead, copper, nickel, aluminum, and cadmium (Zhang et al. 2024), often resulting from irrigation from wastewater (Iqbal et al. 2016).

Increased levels of heavy metals in the soil have several detrimental impacts on plants, including decreased growth, inhibited root development, degradation of chlorophyll, altered biochemical activity, and reproductive diseases linked to oxidative damage (Colzi et al. 2015; Abdull et al. 2022). Furthermore, chromosomal irregularities, point mutations, and ploidy are among the genetic alterations that can result from the buildup of hazardous substances (Silveira et al. 2017). Programmed cell death (PCD), which is triggered by controlled intracellular signals, and nonprogrammed cell death as accidental cell death, which includes necrosis, are two types of cell death. Heavy metals are an example of an abiotic elemenst that can impact cells and cause necrosis or PCD (Brighigna 2006; van Doorn et al. 2011; Petrov et al. 2015).

Metals may have long-lasting negative effects on the ecosystem since they are non-biodegradable and can remain in soil for longer intervals of time. Former studies have shown that microorganisms present in soil, like plants growing in filthy locations, are vulnerable to high dosages of heavy metals, which can lead to malfunction, denaturation of protein, and compromised integrity of cell membranes (Hosseini et al. 2022). Accordingly, metals that are found in cationic forms interact with sulfhydryl radical (-SH) that are found in protein structures of enzymes, altering their characteristics and having detrimental effects on metabolism of plants (Nowicka 2022; Siddiqui 2025[a]). Metals play key functions in the metabolism of plants, and their characteristics are critical to the tridimensional maintenance of biomolecules and cell metabolism. Nevertheless, certain metals are required in trace amounts, others have no biological significance and may even cause metabolic harm (Neto et al. 2020).

In most countries around the world, Soybeans (*Glycine max* L.) are widely farmed for industrial, animal, and human purposes because of their higher protein and oil content (Siddiqui 2025[b]). Soybeans are frequently known as miracle crops since they are the world's main protein and vegetable oil source. Considering the growing global population and the need for increased crop productivity, this study aims to evaluate the effects of Pb and Cu on *Glycine max* L, seed germination, radicle length, mitotic index, cell death, micronucleus index, and chromosomal abnormalities.

METHODOLOGY

Glycine max seeds and chemicals procurement

Certified soybean seeds of *Glycine max* L Merr. Cv-JS-355 were purchased from CSIR (Council of Scientific and Industrial Research), Bhopal, India. Sigma-Aldrich Company was a supplier of heavy metals CuSO4 and PbSO4.

Experiment site, seed germination, and radicle length analysis

From October to December, the tests were carried out at King Khalid University's Botany Department, Al-Farra campus, Abha, Saudi Arabia. Six treatments of Pb and Cu were prepared: CN, 25, 50, 75, 100, and 125 ppm. The completely randomized methods comprise an experimental setup. In Petri dishes covered with a double layer of Whitman No. 2 paper, fifty *Glycine max* Cv-JS-355 seeds were planted. Ten milliliters of a solution with different Pb and Cu concentrations of CN, 25, 50, 75, 100, and 125 ppm were placed in each plate. Distilled water was taken as control (CN). The plates were maintained, with few adjustments, in a B.O.D. chamber (Cienlab®) at 18 °C ± 2 °C having a photo period of 12 hours, as per recommendations given by Siddiqui (2023). Seed germination was measured after 24, 48, and 72 h. Radicle length was measured after 24 h for three days with measuring scale.

Detection of mitotic index and chromosomal abnormality in root tips (RTs) of Glycine max

For cytogenetic assays, all plates were made utilizing the smashing technique, incorporating a slight modification as described by Siddiqui (2023). Root tips *Glycine max* were harvested after 72 hours of each treatment and subsequently fixed in a Carnoy's solution (3 parts ethanol : 1 part glacial acetic acid) and preserved at a temperature of 18 °C. Three samples, each containing 150 cells, were assessed, resulting in a total of 450 cells per replicate. The behavior of chromosomes were analyzed by quantifying the cell cycle stages. MI was calculated based on number of cells undergoing mitosis relative to total number of observed cells. Chromosomal irregularities were evaluated using specific criteria: cell nucleic leaking, multi-pole division, chromosomal bridge in telophase, chromosome retarded in anaphase, dissociate chromosome in metaphase with their frequencies determined by the total number of abnormalities and the overall cell count.

Detection of cell death in RTs of Glycine max

To assess cell death in RTs, uptake of non-permeable trypan blue dye was utilized. Trypan blue can only penetrate the membrane of a dead cell. Using the procedure described by Duan et al. (2010), RTs (0.1 cm) were

immersed in trypan blue (0.4%, w/v) for 15 minutes at room temperature. After that, they were twice rinsed with 2.5 g/mL chloral hydrate solution for ten minutes. Following sample preparation, pictures were captured, and analysis was done using an optical microscope (Olympus CX23, Japan).

Detection of micronucleus index in RTs of Glycine max

Each slide's 100 cells were scored to calculate the MN for assessment. A light binocular microscope (Olympus) with a magnification of 100x was used to investigate micronucleated cells. For scoring MNI, the technique stated by Tolbert et al. (1992) was utilized.

Statistical analysis

A one-way ANOVA test was used to examine the significance of differences between variables using the GPIS 1.13 program (GRAPHPAD, California, USA). All results were presented as mean ± standard error.

RESULTS

Effect of heavy metals on SG of Glycine max

In untreated seeds, after 2 h, germination percentage of seeds were 83.12%, 87.3%, and 99.3% at 24, 48, and 72 h respectively (Figure 1. A-C). Pb and Cu treatments of 25 to 125 ppm for 2 h caused a very significant SG decline ($p<0.01$) at 24 h relative to control. This pattern remained the same for SG at 48 and 72 h, where highest SG was recorded at 25 ppm at 24 h (Pb: 77.66 %, Cu: 75.65 %), 48 h (Pb: 80.33 %, Cu: 85.54 %), and 72 h (Pb: 90.65 %, Cu: 95.67 %), on treating with Pb and Cu for 2 h while lowest SG was found at 125 ppm at 24 h (Pb: 57.63%, Cu: 60.76%), at 48 h (Pb: 60.25%, Cu: 65.27%), and at 72 h (Pb: 65.35 %, Cu: 72.35 %) relative to control.

Effect of heavy metals on RL of Glycine max

Pb and Cu effect on untreated seeds show that RL rose with time on treating with double-distilled water (DDW) for 2 h: 0.94±0.020 at 24 h, 1.52±0.021 at 48 h, and 2.21±0.071 at 72 h (Figure 2. A-C). Pb and Cu treatments of 25 ppm to 125 ppm for 2 h caused significant RL decline ($p<0.05$ at 25 ppm and $p<0.01$ at 50 to 125 ppm) relative to control. This pattern remained the same for RL at 48 h and 72 h, where highest RL was recorded at 25 ppm at 24 h (Pb: 0.81±0.023, Cu: 0.89±0.053), at 48 h (Pb: 1.21±0.04, Cu: 1.35±0.04), and at 72 h (Pb: 1.55±0.06, Cu: 1.75±0.061) on treating with Pb and Cu for 2 h while lowest RL was found at 125 ppm at 24 h (Pb: 0.51±0.021, Cu: 0.55±0.041), at 48 h (Pb: 0.64±0.01, Cu: 0.67±0.01), and at 72 h (Pb: 0.90±0.02, Cu 0.99±0.02) relative to control.

Effect of heavy metals on MI of Glycine max

Figure 3 illustrates the impact of Pb and Cu on MI of root tip cells (*RTCs*) of *Glycine max*. In control, treatment with DDW for 2 h, exhibited MI values of about 65.90%. Seeds exposed to 25 ppm to 50 ppm of Pb and Cu for 2 h showed a significant reduction ($p<0.05$) in MI relative to control. A dose of 75 to 100 ppm of Pb and Cu for 2 h revealed a very significant reduction ($p <0.01$), while 125 ppm of Pb and Cu caused a highly significant reduction ($p<0.001$) in MI. Maximal MI was found at 25 ppm (Pb: 59.56%, Cu: 51.55%) and minimal MI was found at 125 ppm (Pb: 37.88%, Cu: 34.53%) relative to control.

Effect of heavy metals on CAs of Glycine max

No aberrant metaphase-anaphase plates were found in RTs of *Glycine max* in control (Table 1, Figure 4). Different types of CAs, such as cell nucleic leaking (CNL), multi-pole division (MPD), chromosomal bridge in telophase (CBT), chromosome retarded in anaphase (CRA), and dissociate chromosome in metaphase (DCM) were found in metaphase-anaphase plates. In seeds exposed to Pb and Cu for 2 h, there is a surge in ratio of aberrant metaphase-anaphase plates with a surge in Pb and Cu concentration. Cytological investigations disclose that level of CA steadily escalated with a surge in concentrations of Pb and Cu treatment for 2 hours. Investigations of varied stages of mitotic division reveal that all stages of the division were altered.

Percentage formation of CNL, MPD, CBT, CRA, and DCM were very significant ($p<0.01$) and maximal at 125 ppm such as CNL (2.25%), MPD (2.1%), CBT (0.40%), CRA (0.80%) and DCM (1.23%) after Pb treatment. Minimal percentage of chromosomal anomalies were at 25 ppm CNL (0.8%), CRA (0.21%), and MPD (0.40%), DCM (0.40%) at 75 ppm, CBT at 100 ppm (0.2%), at 2 h of Pb exposed seeds relative to control. Enhanced occurrence of CAs for Pb exposure were:

CNL > MPD >DCM >CRA> CBT

Similarly percentage formation of CNL, MPD, CBT, CRA, and DCM were very significant ($p<0.01$)

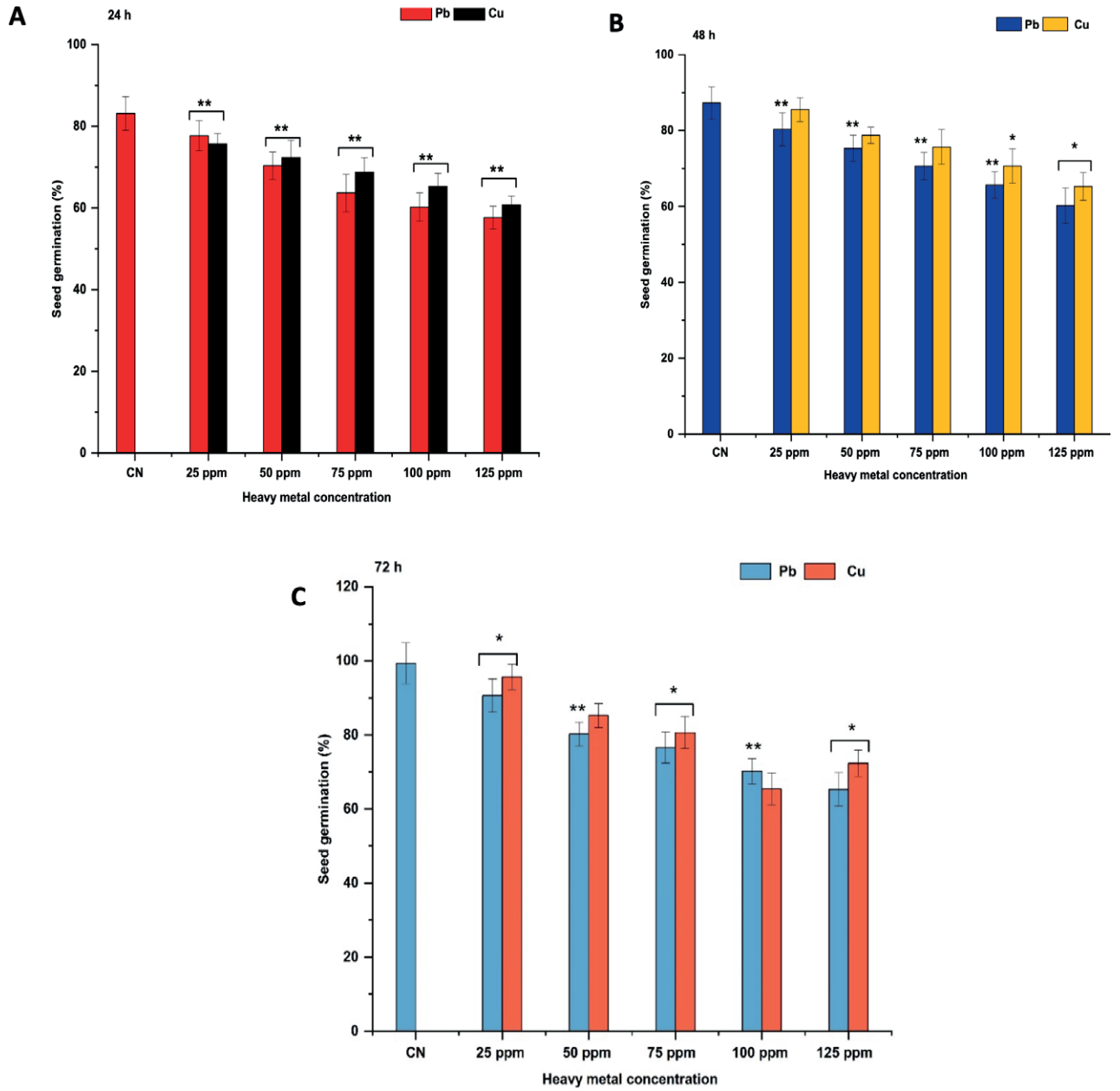

Figure 1. (A, B, C) Effect on SG of *Glycine max* treated with Pb and Cu for 2 h.*P<0.05; **P<0.01 compared to control group. Data are mean of three replicates ± SE, CN = control group.

and maximal at 125 ppm such as CNL (1.20%), MPD (1.40%), DCM (2.12%), and CBT (1.40%), and CRA (0.80%) at 100 ppm at 2 h of Cu treated seeds. Minimal percentage of chromosomal anomalies were reported at 100 ppm CNL (0.4%), MPD at 25 and 50 ppm (0.20%), BRT at 75 ppm (0.2%), CRA at 25 and 75 ppm (0.2%) and DCM at 25 ppm (0.40%) at 2 h of Cu exposed seeds relative to control. Enhanced occurrence of CAs for Cu exposure were:

DCM >MPD = CBT > CNL > CRA

Effect of Pb and Cu on CD in RTCs of Glycine max

Figure 5 illustrates the impact of Pb and Cu on CD in *Glycine max* RTCs. In control, treatment with DDW for 2 h, exhibited CD of 0.11%. Seeds exposed to 25 ppm of Pb for 2 h exhibited a nonsignificant rise in CD which

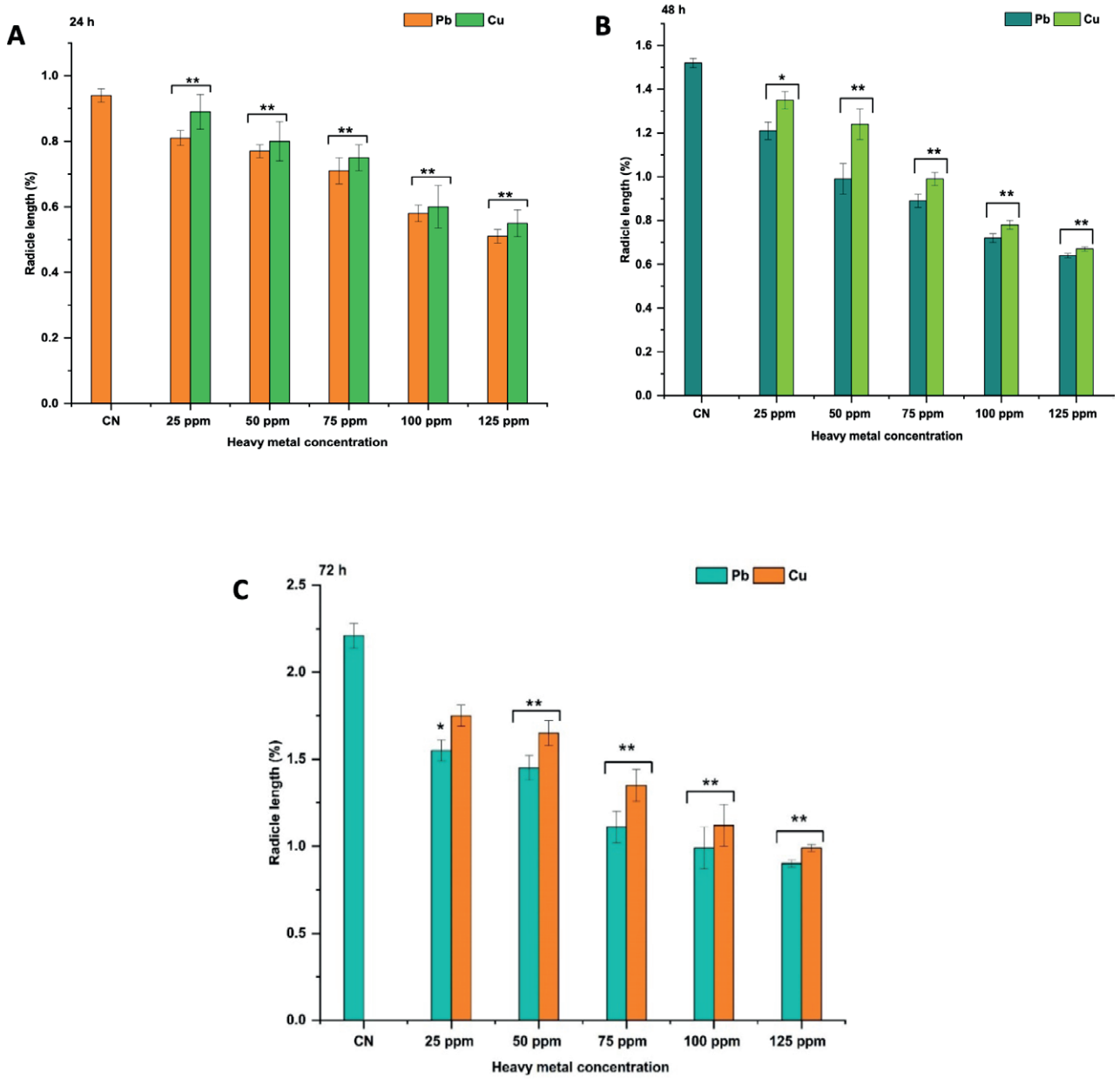

Figure 2. (A, B, C). Effect on RL of *Glycine max* treated with Pb and Cu for 2 h. *P<0.05; **P<0.01 compared to control group. Data are mean of three replicates ± SE, CN = control group.

was 1.40% in comparison to control. Seeds exposed to 50 ppm for 2 h with Pb exhibited a significant rise ($p<0.05$) in CD which was 2.80% relative to control. At 75 ppm to 100 ppm, a very significant rise ($p<0.01$) in CD was revealed which was 3.75% at 75 ppm and 4.90% at 100 ppm relative to control. At 125 ppm, a highly significant rise ($p<0.001$) in CD was revealed which was 5.85 % relative to control. Minimal CD was found at 25 ppm (1.40%), and maximal CD was found at 125 ppm (5.85%). Rise in CD was dose dependent.

Seeds exposed to 25 ppm of Cu for 2 h exhibited a nonsignificant rise in CD which was 1.23% relative to control. Seeds exposed to 50 ppm for 2 h with Cu exhibited a significant rise ($p<0.05$) in CD which was 2.2% relative to control. At 75 ppm to 100 ppm a very significant rise ($p<0.01$) in CD was revealed which was 3.2% at 75 ppm and 4.6% at 100 ppm as compared to control. At 125 ppm a highly significant rise ($p<0.001$)

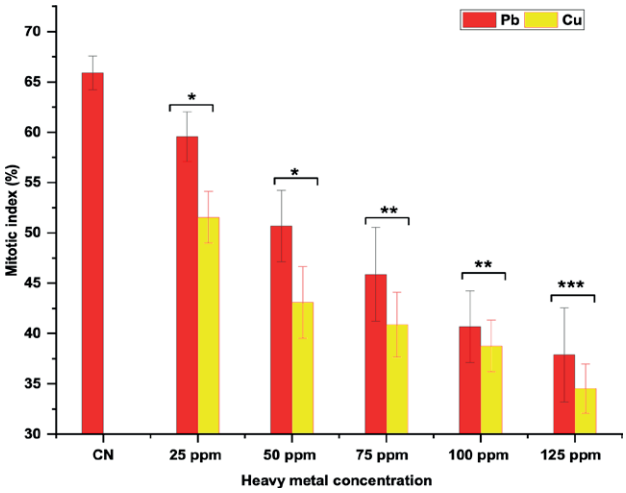

Figure 3. Effect on MI in RTCs of *Glycine max* treated with Pb and Cu for 2 h. *P<0.05; **P<0.01; **P<0.001 compared to control group. Data are mean of three replicates ± SE, CN = control group.

in CD was revealed which was 5.25% in comparison to control. Minimal CD was found at 25 ppm (1.23%), and maximal CD was found at 125 ppm (5.25%). The rise in CD was dose dependent.

Effect of Pb and Cu on MNI in RTCs of Glycine max

Figure 6 illustrates the impact of Pb and Cu on MNI of *Glycine max* in RTCs. In control, MNI was 0.15% of RTCs treated with DDW for 2 h. A significant rise ($p<0.05$) in MNI was found in RTCs treated for 2 h with Pb at 25 ppm which was 0.80% and very significant rise ($p<0.01$) in MNI was found at 50, 75 and 100 ppm which were 1.80 %, 2.80 %, and 3.92% respectively, and highly significant rise ($p<0.001$) in MNI was found at 125 ppm which was 5.23%, in comparison to control. Minimal MNI was found at 25 ppm (0.80%), and maximal MNI was found at 125 ppm (5.23%). Rise in MNI was dose dependent.

A significant rise ($p<0.05$) in MNI was found in RTCs treated for 2 h with Cu at 25 ppm which was 0.52% and a very significant rise ($p<0.01$) in MNI was found at 50, 75 and 100 ppm which were 1.30%, 2.23%, and 3.40% respectively and highly significant rise ($p<0.001$) in MNI was found at 125 ppm which was 4.80%, in comparison to control. Minimal MNI was found at 25 ppm (0.52%), and maximal MNI was found at 125 ppm (4.80%). Rise in MNI was dose dependent.

DISCUSSION

This study noticed delayed SG, RL, MI, increased CD, MNI, and CA in *Glycine max* root tip cells. According to previous research, Pb and Cu reduces germination (Siddiqui et al. 2009; Siddiqui 2013; Sarac et al. 2019; Nouri et al 2019) and causes toxicity and mutagenicity in various plant species (da Cunha Neto 2020; Siddiqui and Sulaiman 22021; da Cunha Neto et al. 2023). When seeds are sown in high Cd environments, their ability to survive is hampered, preventing the development of the embryonic axis and radicle. This impacts activity of α and β amylases (Karmous et al. 2015). Numerous factors

Table 1. Effect on CAs of *Glycine max* treated with Pb and Cu for 2 h.

Conc. (ppm)	CNL	MPD	CBT	CRA	DCM
CN	0.00±0.00	0.00±0.00	0.00±0.00	0.00±0.00	0.00±0.00
Pb					
25 ppm	0.80±0.02*	0.42±0.01*	0.42±0.01*	0.21±0.02	0.80±0.04*
50 ppm	1.20±0.04**	0.80±0.24**	0.31±0.24**	0.80±0.24*	0.80±0.02**
75 ppm	1.20±0.04*	0.40±0.02*	0.40±0.02*	1.00±0.10*	0.40±0.02**
100 ppm	1.60±0.37*	0.80±0.10*	0.20±0.01*	0.40±0.01**	1.22±0.40**
125 ppm	2.25±0.54**	2.10±0.44***	0.40±0.01**	0.80±0.04 ***	1.23±0.21**
Cu					
25 ppm	0.80±0.02*	0.20±0.01	0.30±0.01*	0.20±0.01*	0.40± 0.06*
50 ppm	1.20±0.03*	0.20±0.42	0.40±0.03*	0.40±0.02*	0.80±0.02*
75 ppm	1.20±0.03*	0.80±0.21*	0.20±0.05*	0.20±0.01**	1.20±0.24**
100 ppm	0.40±0.04**	0.80±0.24**	0.30±0.21**	0.80±0.22**	1.20±0.24**
125 ppm	1.20±0.15***	1.40±0.12***	1.40±0.15**	0.40± 0.21***	2.12± 0.63***

*P<0.05; **P<0.01; ***P<0.001 compared to control group. Data are mean of three replicates ± SE, CN = control group, where CNL (Cell nucleic leaking); MPD (Multi-pole division); CBT (Chromosomal bridge in telophase), CRA (chromosome retarded in anaphase), DCM (Dissociate chromosome in metaphase).

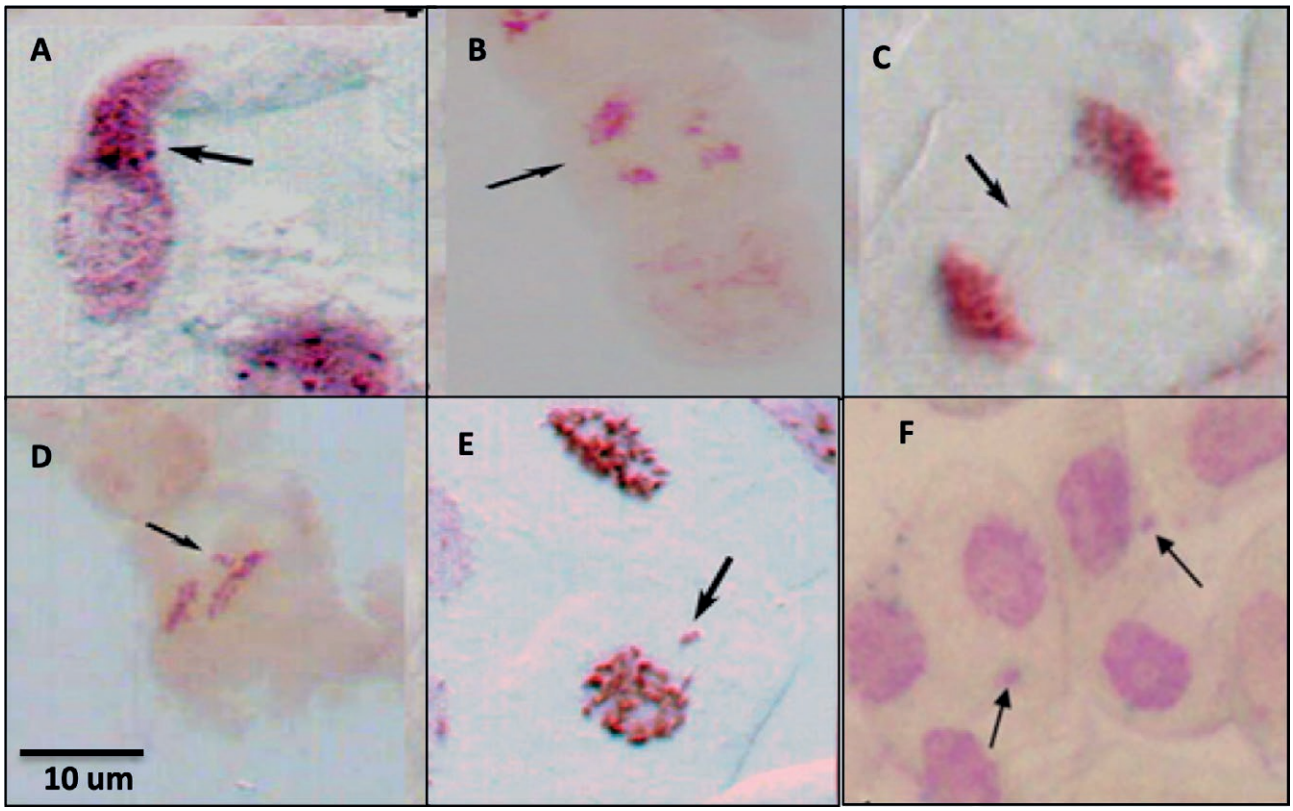

Figure 4. Micrograph of CA and MNF in RTCs of *Glycine max* treated with Pb and Cu for 2 h. A- CNL (Cell nucleic leaking); B- MPD (Multi-pole division); C- CBT (Chromosomal bridge in telophase); D- CRA (chromosome retarded in anaphase); E- DCM (Dissociate chromosome in metaphase); F- Micronuclei.

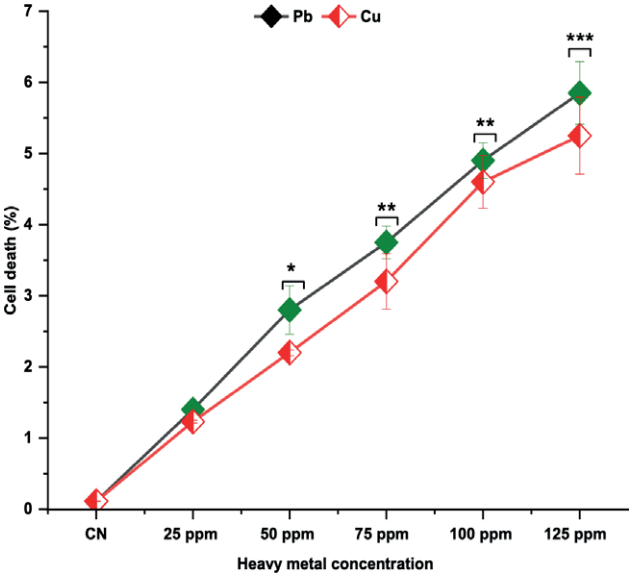

Figure 5. Effect on CD of *Glycine max RTCs* treated with Pb and Cu for 2 h. *P<0.05; **P<0.01; *P<0.001 compared to control group. Data are mean of three replicates ± SE, CN = control group.

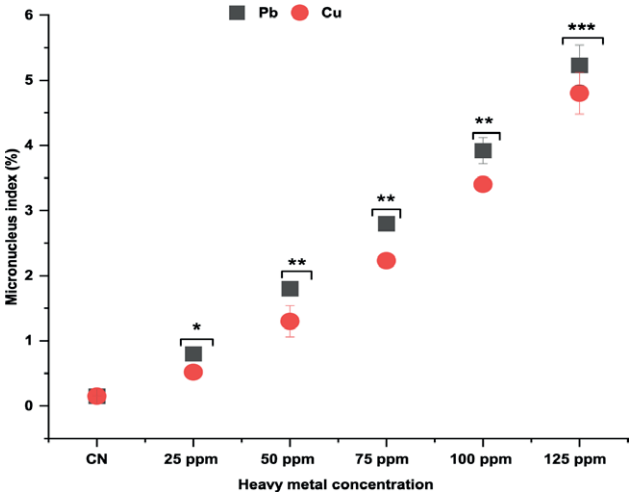

Figure 6. Effect on MNI of *Glycine max RTCs* treated with Pb and Cu for 2 h. *P<0.05; **P<0.01; **P<0.001 compared to control group. Data are mean of three replicates ± SE, CN = control group.

are known to affect seed germination, including light, moisture content, oxygen concentration, and incubation temperature (Siddiqui 2024 [a] and [b]; Anwar et al. 2025). It has been demonstrated that heavy metals prevent seeds from germinating at higher concentrations (Siddiqui 2012; 2015; Akbaş 2024). A decrease in RL is thought to be caused by heavy metal-induced root cell death, specifically because of inadequate energy synthesis in root cells (Siddiqui 2018; Siddiqui et al. 2021; Tasar et al. 2022; Qin et al. 2024). In *Brassica napus* seedlings, heavy metals caused cell death and formation of callose in addition to lowering the micronutrient concentrations (Pramanik et al. 2018).

MI is a crucial factor in determining the genotoxic potential of heavy metals. In *Glycine max*, cytotoxicity elucidates delay in growth, whereas genotoxicity explicates chromosomal abnormalities. Pesticides, heavy metals and other chemical pollutants exposure were linked to the decline in MI in *Pisum sativum* (Siddiqui et al. 2007; Siddiqui et al. 2020 a and b, 2022 a, b and c). Delays in cell cycle or chromatin disorder brought on by metal-DNA interaction causes a decrease in MI (Siddiqui et al. 2012; Ditika and Anila 2013). During cell division, heavy metal affects mitosis and causes spindle-related chromosomal aberrations (Siddiqui 2012; 2015). Numerous findings have demonstrated that differences in the mitotic cycle's duration may be the cause of a decline in cell activity. A rise in the S phase's duration has been attributed by some researchers to mitotic inhibition (Siddiqui et al. 2012; Periakaruppan et al. 2023). As per Das et al. (2023), heavy metals can reach DNA by nuclear pores or when nuclear membrane splits into cells undergoing mitotic divide.

Our results show that CD in the RTs of *Glycine max* exposed to heavy metals at all doses from 25, 50, 75, 100, and 125 ppm increases in a dose-dependent manner. For programmed cell death, plants use vacuolar content and vacuoles in two ways: destructively and non-destructively (Yang et al. 2023). Direct and immediate cell death results from the release of vacuolar hydrolytic enzymes into the cytoplasm following the rupture of the vacuolar membrane (Brighigna et al. 2006). As organelles that generate energy, mitochondria help cells divide, operate, and elongate by metabolizing energy (Fenech et al. 2011; Siddiqui 2024[a]).

Presence of micronuclei in the root tip cells of *Glycine max* further confirmed the genotoxicity caused by heavy metals. After two hours of exposure to heavy metals concentration being increased from 25 to 125 ppm, they significantly increased the number of MNI. The precise mechanism by which heavy metals induce the formation of micronuclei is still unknown. Conversely, micronuclei form during mitosis because of lagging chromosomes or acentric fragments. (Fenech et al. 2011; Yan 2011; Sabeen et al. 2020). Heavy metal-induced damage to parental cells that are either unrepaired or improperly healed and may have a mutagenic effect (Shobha et al 2020). Similar genotoxic effects of heavy metals on *Triticum sativum, Glycine max*, *Vicia faba*, and Allium cepa have been reported by other studies (Bapi et al. 2018; Abdelkader et al. 2022).

The formation of chromosomal aberrations are a useful way to analyze genotoxicity. To assess the extent of chromosomal damage, this study looked at changes in chromosomal behavior brought on by heavy metals. Although the control plant lacked CAs, treated plants showed several abnormalities, such as cell nucleic leaking, multi-pole division, chromosomal bridge at telophase, chromosome retarded in anaphase, dissociate chromosome in metaphase even at the lowest dosage. The frequency of these abnormalities suggests that they have aneugenic, tubergenic, and clastogenic effects (Siddiqui 2019; Liu et al. 2021; Abdelsalam et al. 2022). They are brought on by chromosomal breakage (fragments, micronuclei) and spindle apparatus disorders, anomalous metaphase, telophase, anaphase, and bridges (Zhang et al. 2024; Leng et al. 2025)

CONCLUSION

The dosage of exposure to heavy metals was directly correlated with their cytotoxicity. It is suggested that ambient heavy metals are readily absorbed and finally move up the food chain and higher concentrations of these heavy metals may harm plant by inducing chromosomal aberrations, cell death, alterations in mitotic index, micronucleus index radicle length, and seed germination. Additionally, they impede plant growth by causing oxidative stress, heavy metals have the potential to harm the ecosystem by causing DNA damage. These results are important for the proper disposal of heavy metals and the levels at which they become dangerous.

FUNDING

The authors extend their appreciation to the Deanship of Research and Graduate Studies at King Khalid University for funding this work through the Large Group Project under grant number (RGP2/89/46)

REFERENCES

1. Abdelkader M, Geioushy RA, Fouad OA, Khaled AG. 2022. Investigation of the activities of photosyn-

thetic pigments, antioxidant enzymes and inducing genotoxicity of cucumber seedling exposed to copper oxides nanoparticles stress. Sci. Hortic. 305:111364.
2. Abdelsalam NR, Abdel-Megeed A, Ghareeb RY, Ali HM, Salem MZ, Akrami M, Al-Hayalif, MF, Desoky ESM. 2022. Genotoxicity assessment of amino zinc nanoparticles in wheat (*Triticum aestivum* L.) as cytogenetical perspective. Saudi J. Biol. Sci. 29: 2306–2313.
3. Abdull SR, Rashid SH, Ghafoor BS, Khdhir BS. 2022. Effect of Ag Nanoparticles on morphological and physio-biochemical traits of the medicinal plant *Stevia rebaudiana*. Caryologia. 75(2): 15–22.
4. Akbaş. 2024. effects of different concentrations OF Cu+, Mn+, and Ni+ ions on *Glycine max* germination. Bilim Armonisi. 7(2): 26–36.
5. Anwar A, Akhtar J, Aleem S, Aleem M, Razzaq MK, Alamri S, Raza Q, Sharif I, Iftikhar A, Naseer S, Ahmed Z. 2025. Genome-wide identification of MGT gene family in soybean (*Glycine max*) and their expression analyses under magnesium stress conditions. BMC Plant Biology. 25(1): 83.
6. Brighigna L, Papini A, Milocani E, Vesprini JL. 2006. Programmed cell death in the nucellus of Tillandsia (Bromeliaceae). Caryologia. 59(4): 334-9.
7. Bapi G, Kumar DA, Debadrito D, Vishambhar KD, Ankita P. 2018. Assessment of nanoparticles (copper, cadmium sulphide, copper oxide and zinc oxide) mediated toxicity in a plant system (Indigofera tinctoria L.; Fabaceae). Res. J. Chem. Environ. 22: 34–48.
8. Colzi I, Pignattelli S, Giorni E, Papini A, Gonnelli C. 2015. Linking root traits to copper exclusion mechanisms in Silene paradoxa L.(Caryophyllaceae). Plant and Soil. 390(1): 1–5.
9. da Cunha Neto AR, Carvalho M, Morais GM, Guaraldo MM, Dos Santos HO, Pereira WV, Barbosa S. 2023. Changes in chromosome complement and germination of lettuce (Lactuca sativa L.) exposed to heavy metal stress. Water, Air, & Soil Pollution. 234(4): 243.
10. da Cunha Neto, AR, Ambrósio, ADS, Wolowski, M, Westin TB, Govêa, KP, Carvalho, M, Barbosa, S. 2020. Negative effects on photosynthesis and chloroplast pigments exposed to lead and aluminum: A meta-analysis. CERNE. 26(2): 232–37. https://doi.org/10.1590/01047 760202026022711
11. Das D, Bisht K, Chauhan A, Gautam S, Jaiswal JP, Salvi P, Lohani P. 2023. Morpho-physiological and biochemical responses in wheat foliar sprayed with zinc-chitosan-salicylic acid nanoparticles during drought stress. Plant Nano Biol. 4: 100034.
12. Dietrich M, Wolfe A, Burke M, Krekeler MPS. 2019. The first pollution investigation of road sediment in Gary, Indiana: anthropogenic metals and possible health implications for a socioeconomically disadvantaged area. Environ. Int. 128: 175–192. https://doi.org/10.1016/J.ENVINT.2019.04.042
13. Ditika K, Anila M. 2013. Assessment of cytotoxic and genotoxic potency of Cr (VI)-doped river water of Nen-Shkodra lowland, Albania, on *Allium cepa* L. J Environ. Res. Dev. 7(4): 1322–1332
14. Duan Y, Zhang W, Li B, Wang Y, Li K, Sodmergen, HC, Li X. 2010. An endoplasmic reticulum response pathway mediates programmed cell death of root tip induced by water stress in Arabidopsis. New Phytol. 186: 681–695. https://doi.org/10.1111/j.1469-8137.2010.03207.x
15. Fenech M, Krisch-Volders M, Natarajan AT, Surralles J, Crott JW, Parry J, Noppa H, Eastmond DA, Tucker JD, Thomas P. 2011. Molecular mechanism of micronucleus, nucleoplasmic bridge and nuclear bud formation in mammalian and human cells. Mutagenesis. 26: 125–132.
16. Hassan MM, Haleem N, Baig MA, JamalY. 2020. Phytoaccumulation of heavy metals from municipal solid waste leachate using different grasses under hydroponic condition. Sci. Rep. 10(1): 1–8. https://doi.org/10.1038/s41598-020-72800-2
17. Hosseini, S. M., Kalatejari, S., Kafi, M., & Motesharezadeh, B. (2023). Assessment of the absorption ability of nitrate and lead by japanese raisin under salt stress conditions. Caryologia 75(4). https://doi.org/10.36253/caryologia-1827
18. Iqbal HH, Taseer R, Anwar S, Qadir A, Shahid N. 2016. Human health risk assessment: heavy metal contamination of vegetables in Bahawalpur, Pakistan Hafiza. Bull. Environ. Stud. 1(1): 10–17
19. Karmous I, Bellani LM, Chaoui A, El Ferjani E, Muccifora S. 2015. Effects of copper on reserve mobilization in embryo of Phaseolus vulgaris L. Environ. Sci. Pollut. Res. 22(13): 10159–10165. https://doi.org/10.1007/S11356-015-4208-1/FIGURES/7
20. Leng Y, Niu ZB, Liu SH, Qiao FJ, Liu GF, Cheng B, Li SW. 2025. Characterisation of cytochrome c oxidase-coding genes from mung bean and their response to cadmium stress based on genome-wide identification and transcriptome analysis. Mol. Biol. Rep. 52(1): 17.
21. Liu C, Yu Y, Liu H, Xin H. 2021. Effect of different copper oxide particles on cell division and related genes of soybean roots. Plant Physiol. Biochem. 163: 205–14.
22. Neto AR, da Ambrósio C, Wolowski ADS, Westin M, Govêa TB, Carvalho KP, Barbosa MS. 2020. Negative effects on photosynthesis and chloroplast pigments

exposed to lead and aluminum: a meta-analysis. CERNE 26(2): 232–237. https://doi.org/10.1590/01047760202026022711
23. Nouri M, El Rasafi T, Haddioui A. 2019. Responses of two barley subspecies to induced heavy metal stress: seeds germination, seedlings growth and cytotoxicity assay. Agriculture 65(3) 107–18.
24. Nowicka B. 2022. Heavy metal–induced stress in eukaryotic algae—Mechanisms of heavy metal toxicity and tolerance with particular emphasis on oxidative stress in exposed cells and the role of antioxidant response. Environ. Sci. Pollut. Res. 29(12): 16860–16911. https://doi.org/10.1007/s11356-021-18419-w
25. Periakaruppan R, Vanathi P, Priyanka G, Vidhya D. 2023. Toxicity in plants by metal oxide nanoparticles. In Nanometal Oxides in Horticulture and Agronomy; Academic Press: Cambridge, MA, USA. 241–273.
26. Pramanik A, Datta AK, Gupta S, Ghosh B. 2018. Copper oxide nanoparticles induced fertile desynaptic mutant line in Coriandrum sativum L. (Apiaceae). Cytologia. 83: 103–107.
27. Qin C, Lian H, Alqahtani FM, Ahanger MA. 2024. Chromium-mediated damaging effects on growth, nitrogen metabolism and chlorophyll synthesis in tomato can be alleviated by foliar application of melatonin and jasmonic acid priming. Sci. Hortic. 323: 112494.
28. Sabeen M, Mahmood Q, Bhatti ZA, Irshad M, Bilal M, Hayat MT, Irshad U, Akbar TA, Arslan M, Shahid N. 2020. *Allium cepa* assay-based comparative study of selected vegetables and the chromosomal aberrations due to heavy metal accumulation. Saudi J. Biol. Sci. 27(5): 1368–4.
29. Sarac I, Bonciu E, Butnariu M, Petrescu I, Madosa E. 2019. Evaluation of the cytotoxic and genotoxic potential of some heavy metals by use of allium test. Caryologia. 72(2): 37–43. https://doi.org/10.13128/cayologia-256.
30. Shobha G, Shashidhara KS, Naik C. 2020. Cuprous oxide nanoparticles induced antioxidant response and genotoxicity in *Lycopersicum esculentum*. Bio Nanosci. 10: 1128–1137
31. Siddiqui S, 2023. Phenthoate toxicity evaluation in root meristem of *Pisum sativum* L. Caryologia. 76(1): 57–66.
32. Siddiqui S, Meghvansi MK, Khan SS. 2012. Glyphosate, alachor and maleic hydrazide have genotoxic effect on *Trigonella foenum-graecum* L. Bull. Environ. Contam. Toxicol. 88(5): 659-65.
33. Siddiqui S. 2013. Exposure of Cu and Mn to *Cicer arietinum* L. Var. BGD-72 seeds induces morphological and biochemical changes in the plant. South Asian J. Exp. Biol. 3(1): 31–36.
34. Siddiqui S. 2018. Cytotoxicity induced by aluminum sulfate in cells of root meristem of *Pisum sativum* cv. arikil. Bangl. J. Bot. 1: 47:219.
35. Siddiqui S, Meghvansi MK, Wani MA, Jabee F. 2009. Evaluating cadmium toxicity in the root meristem of *Pisum sativum* L. Acta Physiol. Plant. 31: 531–6.
36. Siddiqui S. 2025[a]. Global patterns and drivers of species and genera richness of Fabaceae. Front. Plant Sci. 16: 1581814.
37. Siddiqui S. 2025[b]. Unlocking the environmental potential of biochar: production, applications, and limitations. Frontiers in Sustainable Food Systems. 9: 1569941
38. Siddiqui S, Al Amri SAM, Al Ghamdy HA, Alqahtani WSS, Alquyr SM, Yassin HM. 2021. Impact of Bisphenol A on seed germination, radicle length and cytogenetic alterations in *Pisum sativum* L. Caryologia. 74(2): 103–109.
39. Siddiqui S, Al-Rumman S. 2020[a]. Clethodim induced pollen sterility and meiotic abnormalities in vegetable crop *Pisum sativum* L. Caryologia. 73: 37–44.
40. Siddiqui S, Al-Rumman S. 2020[b]. Cytological changes induced by clethodim in *Pisum sativum* plant. Bangladesh J. Bot. 49(2): 367–374.
41. Siddiqui S, Al-Rumman S. 2022[a]. Methomyl, imbraclaobrid and clethodim induced cytomixis and syncytes behaviors in PMCs of *Pisum sativum* L: Causes and outcomes. Saudi J Biol Sci. 29(9): 103390. https://doi.org/10.1016/j.sjbs.2022.103390.
42. Siddiqui S, Al-Rumman S. 2022[b]. Exposure of *Pisum sativum* L. seeds to methomyl and imidacloprid cause genotoxic effects in pollen-mother cells. Biology. 11: 1549. https://doi.org/10.3390/ biology11111549
43. Siddiqui S, Al-Rumman S. 2022[c]. Methomyl has clastogenic and aneugenic effects and alters the mitotic kinetics in *Pisum sativum* L. Caryologia. 75(3): 91–99.
44. Siddiqui S, Meghvansi MK, Hasan Z. 2007. Cytogenetic changes induced by sodium azide (NaN3) on *Trigonella foenum-graecum* L. seeds. S. Afr. J. Bot. 73(4): 632–5.
45. Siddiqui S. 2012. Lead-induced genotoxicity in Vigna mungo var. HD-94. J. Saudi Soc. Agric. Sci. 11(2): 107–12.
46. Siddiqui S. 2015. DNA damage in Cicer plant grown on soil polluted with heavy metals. J. King Saud Univ. Sci. 27(3): 217–23.
47. Siddiqui S. 2024[a]. DNA Damage, cell death, and alteration of cell proliferation insights caused by cop-

per oxide nanoparticles using a plant-based model. Biology. 13(10): 805.
48. Siddiqui S. 2024[b]. Effects of cypermethrin on morphological, physiological and biochemical attributes of *Cicer arietinum* (Fabales: Fabaceae). Front. Sustain. Food Syst. 8: 1446308.
49. Silveira GL, Lima MGF, Reis GB, Palmieri MJ, Andrade-Vieria LF. 2017. Toxic effects of environmental pollutants: a comparative investigation using *Allium cepa* L. and *Lactuca sativa* L. Chemosphere. 178: 359–367. https://doi.org/10.1016/J.CHEMOSPHERE.2017.03.048
50. Tasar N. 2022. Mitotic effects of copper oxide nanoparticle on root development and root tip cells of *Phaseolus vulgaris* L. seeds. Microsc. Res. Tech. 85: 3895–3907.
51. Tolbert PE, Shy CM, Allen JW. 1992. Micronuclei and other nuclear anomalies in buccal smears: Methods development. Mutat. Res. 271: 69–77.
52. Zhang Y, Li T, Fu Q, Hou R, Li M, Liu D, Shi G, Yang X, Xue P. 2024. Drip irrigation reduces the toxicity of heavy metals to soybean: By moving heavy metals out of the root zone and improving physiological metabolism. Agric. Water Manag. 292: 108670
53. van Doorn WG, Beers EP, Dangl JL, Franklin-Tong VE, Gallois P, Hara-Nishimura I, Jones AM, Kawai-Yamada M, Lam E, Mundy J, Mur LA. 2011.Morphological classification of plant cell deaths. Cell Death Differ. 18(8): 1241–6.
54. Petrov V, Hille J, Mueller-Roeber B, Gechev TS. 2015. ROS-mediated abiotic stress-induced programmed cell death in plants. Front. Plant Sci. 6: 69.

Caryologia
International Journal of Cytology, Cytosystematics and Cytogenetics

Firenze University Press
https://riviste.fupress.net/index.php/caryologia

OPEN ACCESS

Citation: Siddiqui, S. (2025). Cytotoxicity and genotoxicity of manganese in meristematic cells of Glycine max L. root. *Caryologia* 78(3): 41-50. doi: 10.36253/caryologia-3775

Received: April 12, 2025

Accepted: October 14, 2025

Published: December 24, 2025

Data Availability Statement: All relevant data are within the paper and its Supporting Information files.

Competing Interests: The Author(s) declare(s) no conflict of interest.

ORCID
SS: 0000-0001-5448-7617

Cytotoxicity and genotoxicity of manganese in meristematic cells of *Glycine max* L. root

Sazada Siddiqui

Department of Biology, College of Science, King Khalid University, Abha 61413, Saudi Arabia
Email: sasdeky@kku.edu.sa

Abstract. A crucial method for evaluating the potential harm to the genome caused by contaminants at levels exceeding the optimal threshold is the chromosomal plant assay. This paper reports on a study that examined the effects of varying concentrations of manganese (Mn) on the mitotic index (MI), cell kinetics index (CKI), and abnormality index (AI) in *Glycine max* L. root tip cells. Percentage of mitotic index, abnormality index, cell kinetics index, in root meristems of *Glycine max* L. at control and varying concentrations of Mn were evaluated. The findings showed that Mn doses that were utilized for seed treatment caused distinct differences in chromosomal activity of *Glycine max* L. root tip cells, with a decreased mitotic index and cell kinetics, and an increased abnormality index. Treatment was conducted at room temperature for 24 hours, 48 hours, and 72 hours at four different concentrations of Mn: CN (Control), 5µM, 10µM, 15µM, and 20µM. The control group was treated with distilled water. The findings demonstrated that Mn has cytotoxic and genotoxic effects on Glycine *max L.* root tip cells.

Keywords: Manganese (Mn), *Glycine max* L, mitotic index, abnormality index, cell kinetics.

INTRODUCTION

In many parts of the world, heavy metal contamination has an adverse effect on the biosphere, which is hazardous for environment. Metal contamination can come from a variety of sources, including mining, industry, agricultural chemicals, fuel, combustion byproducts, etc. (Siddiqui 2013; Siddiqui 2025a; Lee et al. 2024). Additionally, industrialization created industrial effluents that contained various pollutants, such as organic, inorganic, and radioactive trace elements, microbes, which might potentially contaminate soil (Siddiqui 2012; Siddiqui 2015; Chukwu et al. 2025). Heavy metals like Mn, Pb, Cd, Hg, and Ni are the most problematic worldwide pollutants. Industries release heavy metals and other pollutants into the environment, which are harmful to humans, animals, and plants. Although they are trace elements, these heavy metals are crucial to many physiological processes in living beings (Siddiqui et al. 2007; Siddiqui et al. 2009; Siddiqui et al. 2021; Hafeez et al. 2023; Espinola et al. 2025; Elik and Gül 2025). There is a sig-

nificant qualitative difference between natural environmental changes seen in the past and those seen in the present, especially when considering the current overextended anthropogenic activity (Siddiqui 2018; Siddiqui and Suliman 2021). These days, neither humans nor other superior organisms have developed genetic defenses against anthropogenic pollutants, such as chemicals released by industry, some of which are xenobiotics – things that have never existed in nature (Üstündağ et al. 2023; Siddiqui 2025 b; Vieira et al. 2025).

Although Mn is a chemical element that is necessary for proper nutrition, it can also be hazardous under some circumstances. Scientists are still trying to comprehend the various effects of its toxicity and deficiency on living things. However, Mn is unquestionably extremely hazardous at high concentrations, leading to several diseases dependent on the production of reactive oxygen species (ROS) (Ertürk et al. 2021; Vijaya Kumar et al. 2025; Rao et al. 2025; Xia et al. 2025). Additionally, Mn may build up inside cell, leading to cytotoxicity and eventual cell death. Following alterations in gene expression and enzyme activity, Mn causes intracellular changes such as lipid peroxidation, chromosomal disintegration, and DNA helix breakage (Siddiqui and Al rumman 2020 a and b; Perfileva and Krutovsky 2024; Aseef and Venkatkumar 2025). The pathophysiology and toxicity of various diseases, including atherosclerosis, diabetes, chronic inflammatory diseases, neurological disorders, and cardiovascular diseases, have been linked to long-term oxidative stress in humans (Dorman 2023). Lactate dehydrogenase and lipid peroxidation, two cytotoxic measures, show that Mn causes oxidative stress in a time and concentration-dependent way (Jomova et al. 2025; Sobańska et al. 2021). Our study used cytogenetic analysis in *Glycine max* L. as a plant indicator for the degree of heavy metal pollution in crops to identify the mutagenic effects of Mn.

METHODOLOGY

Procurement of chemicals

Mn is supplied by Sigma-Aldrich (MERCK). Local distributor Bayouni sells Sigma-Aldrich (MERK) products in Saudi Arabia. *Glycine max* L (Fabaceae) seeds with 2n = 40 chromosomes, cultivar JS 335, were collected from Indian Ministry of Agriculture.

Plant material and treatment

For cytological examination, a homogeneous batch of *Glycine max* L (Fabaceae) seeds with 2n = 40 chromosomes, cultivar JS 335, were collected. *Glycine max* seeds were immersed in water overnight. The seeds were then treated with various concentrations of Mn (CN, 5µM, 10µM, 15µM, and 20µM) for 2 hours with CN serving as control with only distilled water. For root tip germination, the seeds were placed in a Petri dish lined with filter paper, covered, and incubated at 22-25 °C for 2-3 days. The root tips were properly cleaned with distilled water, then fixed in Carnoy's fixative (1 glacial acetic acid: 3 ethanol) for 24 hours and stored in 90% alcohol.

Glycine max L. test

For germination, 30 *Glycine max* seeds were put in Petri Plates with 3 mL of each of the test solutions of Mn. The seeds were subjected to treatments in a germination chamber (Quimis) with regulated temperatures of 23±3 °C every 96 hours. The size of the roots were measured using a digital calliper (Digmess), and the number of seeds that germinated were manually counted. The roots were subsequently gathered and preserved in Carnoy fixative. The microscope slides were prepared by Siddiqui et al. (2022 a), and they were stained for 1 hour and 30 minutes using Schiff's reagent based on Feulgen method. Ten slides containing *Glycine max*. root meristems were made for each treatment, and 500 cells were counted from each slide, for a total of 5000 cells per treatment. The slides were examined using an optical microscope that had a 400x magnification.

Analysis of cytotoxicity and genotoxicity

For cytotoxicity analysis, MI and CKI were evaluated. The indices were calculated using the formulas described below:

$$\text{Mitotic Index (MI)} = \frac{\text{No. of cells in cell division} \times 100}{\text{Total No. of counted cells}}$$

Formula for calculating cell kinetics index (CKI)

$$\text{Interphase index} = \frac{\text{No. of interphase cells} \times 100}{\text{Total No. of cells analyzed}}$$

$$\text{Prophase index} = \frac{\text{No. of prophase cells} \times 100}{\text{Total No. of cells analyzed}}$$

$$\text{Metaphase index} = \frac{\text{No. of metaphase cells} \times 100}{\text{Total No. of cells analyzed}}$$

$$\text{Anaphase index} = \frac{\text{No. of anaphase cells} \times 100}{\text{Total No. of cells analyzed}}$$

$$\text{Telophase index} = \frac{\text{No. of telophase cells} \times 100}{\text{Total No. of cells analyzed}}$$

For genotoxicity analysis, chromosomal abnormality index was evaluated. AI was calculated using the formulas described below:

$$\text{AI} = \frac{(\text{No. of cells with chromosomal alteration} \times 100)}{\text{Total No. of counted cells}}$$

Statistical analysis

A one-way ANOVA test was used to examine the significance of differences between variables using the GPIS 1.13 program (GRAPHPAD, California, USA). All results were presented as mean ± SE.

RESULT

Effect of Mn on MI in Glycine max root tips

The control samples had the highest MI values, which reached 1.52% after 24 h (Figure 1 A), 1.35% after 48 h (Figure1 B), and 72 h (Figure 1 C). After Mn treatment for 24 h, MI decreased significantly ($p<0.05$) dose-dependently from 10 µM (1.01±0.10), 15 µM (0.98±0.10), and 20 µM (0.97±0.09) concentrations, with no significant difference ($p>0.05$) observed at 5 µM (1.48±0.15) concentration. After 48 h, MI decreased significantly ($p<0.05$) dose-dependently from 10 µM (1.02±0.10), 15 µM (1.05±0.13), and 20µM (0.87±0.13) concentrations, with no significant difference ($p>0.05$) observed at 5µM (1.28±0.13). Similarly, on Mn treatment for 72 h, MI decreased significantly ($p<0.05$) dose-dependently from 10 µM (1.17±0.22), 15 µM (1.07±0.11), and 20 µM (0.70±0.08) concentrations, with no significant difference ($p>0.05$) observed at 5 µM (1.25±0.22) as compared to control.

Effect of Mn on Abnormality Index, in Glycine max root tips

In our study, we found that AI, such as anaphase bridges, dissociated chromosomes in metaphase and anaphase, chromosomal bridging, were caused by incorrect separation and retarded chromosomes in anaphase (Figure 3). These were the most common abnormalities after treating root meristematic cells of *Glycine max* with Mn.

The control samples showed AI values of (0.0±0.0) at 24 h, 48 h, and 72 h. Following a 24 h Mn treatment, AI increased significantly ($p<0.05$) dose-dependently at 5 µM (0.39±0.059), 10 µM (0.40±0.049), 15 µM (0.46±0.050), and very significantly ($p<0.01$) at 20 µM (0.65±0.087) (Figure 2A). The AI increases significantly ($p<0.05$) from 5 µM (0.25±0.08), 10 µM (0.29±0.07), and very significantly ($p<0.05$) at 15 µM (0.42±0.06), and at 20 µM (0.53±0.07) dose-dependently following 48 h of Mn treatment (Figure 2B). AI increased significantly ($P<0.05$) dose-dependently from 5µM, which is (0.17±0.042), 10 µM (0.290.092), and 15 µM (0.410.093), and very significantly ($p<0.01$) at 20 µM (0.46±0.065) following 72 h of Mn treatment as compared to control (Figure 2C).

Effect of Mn on cell kinetics index in Glycine max root tips

Table 1 shows that Mn decreases CKI of *Glycine max* root tip cells in interphase, prophase, metaphase, anaphase, and telophase at 24 h, 48 h, and 72 h from 5 µM to 20 µM (Table 1). At 24 h of exposure to Mn, prophase (1.43±0.24), metaphase (0.83±0.06) and telophase (0.60±0.08) increased very significantly ($p<0.01$) in 5 µM. However, at 10 µM (0.15±0.02), there was a significant decrease ($p<0.05$) in telophase and at 15 µM (0.10±0.01 and 20 µM (0.13±0.01), there was a very significant decrease in telophase. Non-significant ($p>0.05$) decreases were reported in interphase and anaphase from 5 µM to 20 µM as compared to control.

After 48 h, in prophase, metaphase, anaphase, and telophase, very significant ($p<0.01$) increase was reported at 5 µM. In the case of interphase and prophase, non-significant ($p> 0.05$) decreases were reported from 5 µM to 20 µM. But in the case of anaphase and telophase, there was a significant decrease ($p<0.05$) at 10 µM to 20 µM as compared to control. After 72 h of exposure to Mn, interphase and telophase were very significantly ($p<0.01$) decreased from 5 µM to 20 µM. However, at anaphase at 20 µM, significant ($p<0.05$) decrease was reported. But in the case of prophase and metaphase, there was a non-significant decrease ($p> 0.05$) from 5 µM to 20 µM as compared to control.

Pearson correlation coefficients between MI, AI, and CKI on Mn treatments with different time intervals

The heat map of Pearson correlation coefficients displays the correlation among measured MI, AI, and CKI in Figure 4 (24 h), Figure 5 (48 h) and Figure 6 (72 h). The blue and red squares signify positive and nega-

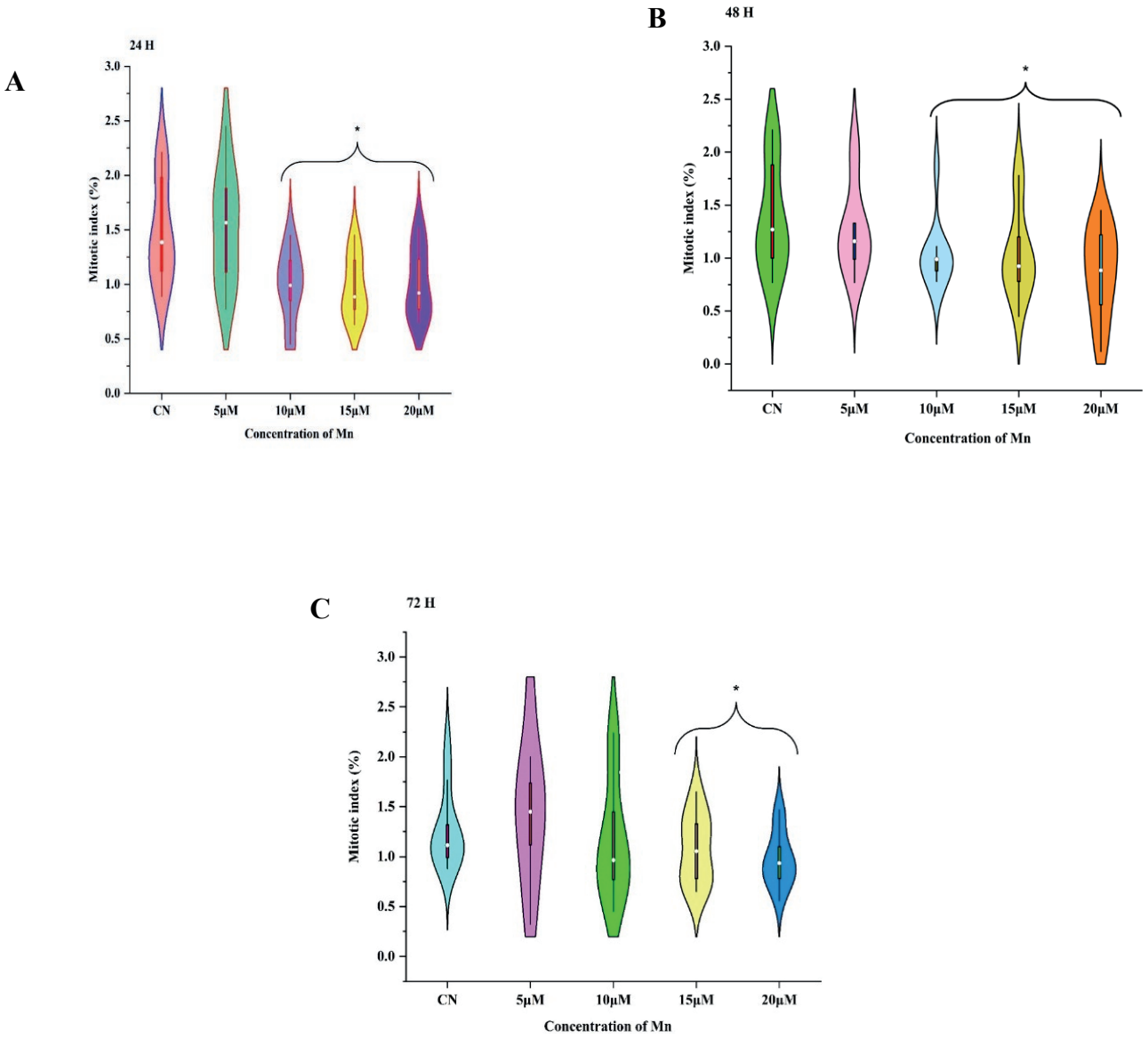

Figure 1. Effect of Mn on MI in *Glycine max* root tips at 24 h (A), 48 h (B), and 72 h (C).

tive correlations, respectively. Negative correlations were reported between MI and AI (-0.020) after treatment of Mn for 24 h. A negative correlation was noticed in MI and interphase of CKI (-0.02). On the other hand, a strong positive correlation was noticed between MI and CKI (prophase (0.51), metaphase (0.31), anaphase (0.56), and telophase (0.26) (Figure 4). However, positive correlations were noticed between AI and different phases of CKI, interphase (0.22), metaphase (0.24), anaphase (0.04), and telophase (0.29) and a negative correlation in prophase (-0.05), after treatment of Mn for 24 h.

Negative correlations were reported between MI and AI (-0.07) after treatment of Mn for 48 h. On the other hand, a positive correlation was noticed between MI and phases of CKI (Interphase (0.07), prophase (0.15), metaphase (0.01), anaphase (0.22) and telophase (0.40) (Figure 5). However, negative correlations were reported between AI and different phases of CKI: interphase (-0.20), prophase (-0.32), metaphase (-0.16), anaphase (-0.24), and telophase (-0.26) after treatment of Mn for 48 h (Figure 5). These two parameters are negatively correlated with each other.

A negative correlation was reported between MI and AI (-0.05) after treatment of Mn for 72 h. On the other hand, negative and positive correlations were noticed between MI and phases of CKI: interphase (-0.14), pro-

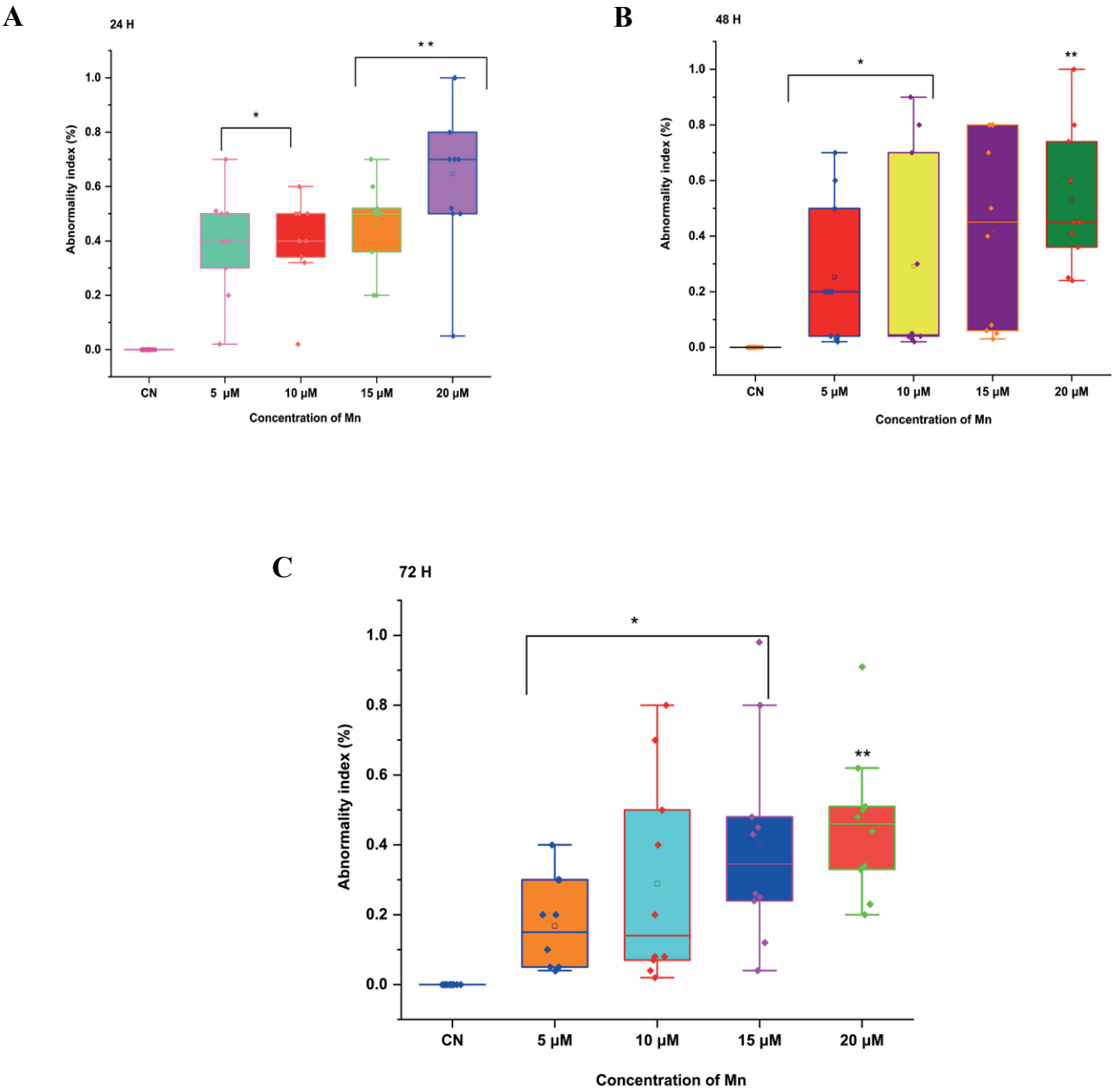

Figure 2. Effect of Mn on AI in *Glycine max* root tips at 24 h (A), 48 h (B), and 72 h (C).

phase (-0.15), metaphase (0.09), anaphase (-0.15) and telophase (0.06) (Figure 6). A positive correlation was reported between AI and interphase (0.17) of CKI, and negative correlations were noticed in prophase (-0.07), metaphase (-0.39), anaphase (-0.28), and telophase (-0.27) after treatment of Mn for 72 h (Figure 6).

DISCUSSION

On the basis of above data, it is obvious that Mn, a heavy metal, can cause cytotoxic and genotoxic effects on root tip cells of *Glycine max*. Findings indicate that when treatment dosages increase, the frequency of MI, CKI decreases and AI rises. It is practically obvious from this decrease in MI and increase in AI that Mn has a clastogenic impact on chromosomes at DNA level. How-

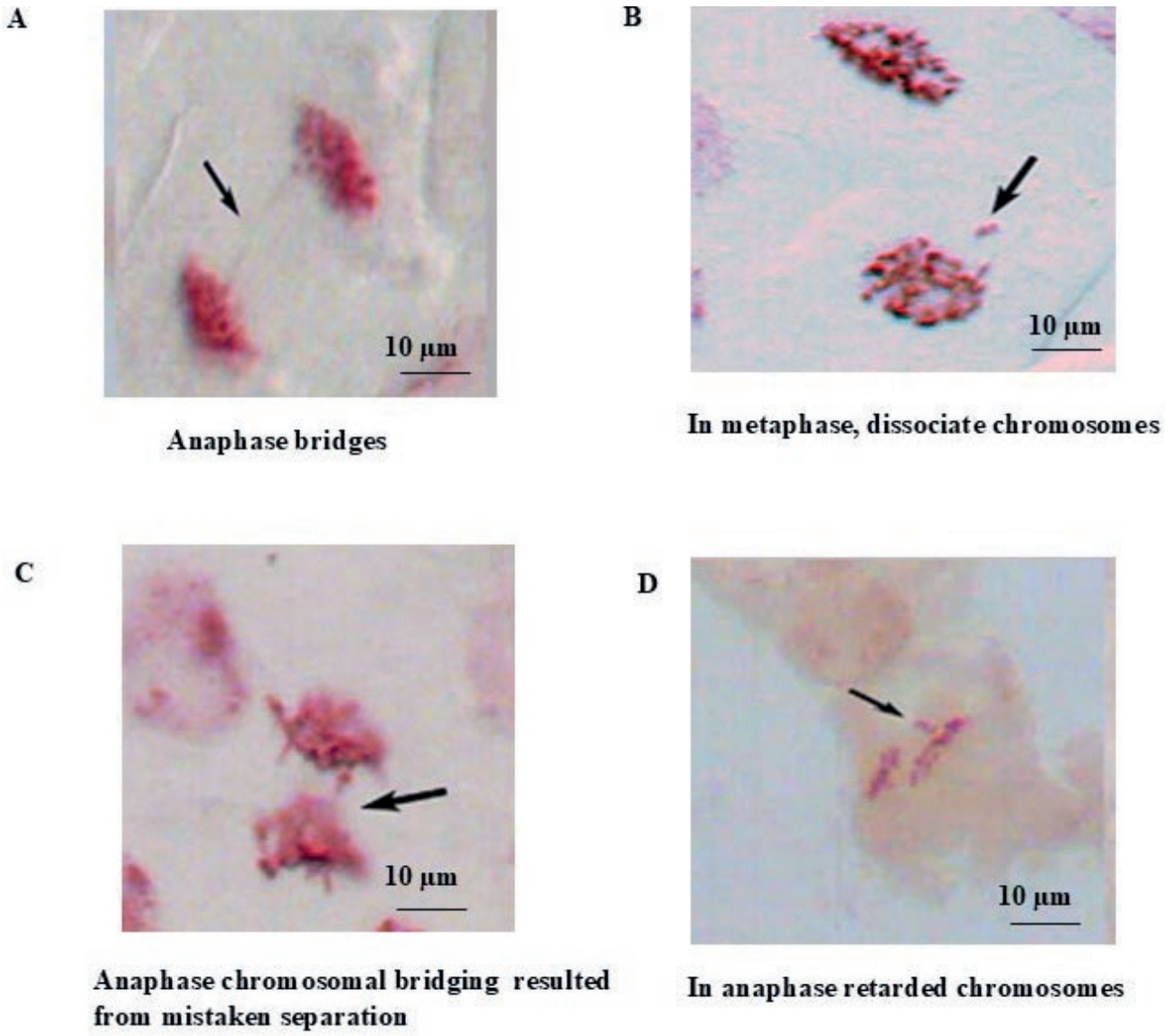

Figure 3. Chromosomal abnormality in Mn-treated *Glycine max* root tips. A. Anaphase bridges B. In metaphase, dissociate chromosomes C. Anaphase chromosomal bridging resulted from mistaken separation D. In anaphase retarded chromosomes. Bar. 10 µm.

ever, excessive and negligent use of these heavy metals and agrochemicals often leads to their selective accumulation on agricultural fields topsoil layers (Mauser et al. 2025; Shahwar and Ansari 2022; Aslam and Aslam et al. 2021; Sarkar et al. 2022), which eventually reduces soil fertility. The rapid emergence of pathogen resistance to these agrochemicals lowers the effectiveness of pesticides and causes more harmful side effects. One of these consequences is the problem of eliminating insects that are beneficial to environment from the ecosystem (Fairoj et al. 2024; Yu et al. 2025).

MI is a crucial indicator for determining heavy metal's potential for genotoxicity. Exposure to pesticides, heavy metals, and other chemical pollutants was linked to a decrease in MI in many plant species (Siddiqui and Al-Rumman, 2022a, b, and c; Siddiqui 2025 b). Chromatin abnormalities brought on by metal-DNA interaction or cell cycle delays result in decreased MI (Siddiqui 2023; Siddiqui 2024 a). Spindle-related chromosomal abnormality during cell division is also a result of primary mechanism of action of pesticides and heavy metals in mitosis (Firbas and Amon 2014). In this work, Mn demonstrated cytotoxicity by lowering MI dose-dependently. This implies that Mn causes mito-depression in *Glycine max*. Numerous investigations have demonstrated that differences in mitotic cycle's duration may be

Table 1. CKI in *Glycine max*, treated with different concentrations of Mn for 24 h, 48 h, and 72 h.

Conc.	FI	FP	FM	FA	FT
24 h					
CN	10.19 ± 0.56	0.71±0.08	0.20 ± 0.03	0.28±0.06	0.33±0.03
5 µM	10.30 ± 0.63	1.43±0.24**	0.83 ± 0.06**	0.45±0.07	0.60±0.08**
10 µM	9.10 ± 0.73	0.49±0.14	0.25 ± 0.07	0.16±0.02	0.15±.020*
15 µM	5.50 ± 0.17	0.55±0.17	0.15 ± 0.02	0.12±0.02	0.10±0.01**
20 µM	3.70 ± 0.12	0.37±0.13	0.15 ± 0.02	0.12±0.01	0.13±0.01**
48 h					
CN	10.20±0.56	0.73±0.07	0.17±0.03	0.28±0.06	0.31±0.05
5 µM	10.29±0.63	1.06±0.16	0.56±0.08**	0.32±0.06	0.35±0.04
10 µM	9.13±0.65	0.42±0.128	0.15±0.018	0.11±0.01*	0.14±0.02**
15 µM	8.32±0.53	0.39±0.12	0.15±0.010	0.13±0.01*	0.12±0.11**
20 µM	8.32±0.53	0.38±0.12	0.16±0.017	0.12±0.01*	0.12±0.01**
72 h					
CN	10.28±0.08	0.85±0.07	0.79±0.05	0.49±0.08	0.74± 0.05
5 µM	9.49±0.71**	0.37±0.74	0.45±0.06	0.21±0.03	0.24±0.04**
10 µM	8.24±0.04**	0.69±0.26	0.141±0.02	0.31±0.13	0.31±0.14**
15 µM	8.78±0.43**	0.79±0.26	0.15±0.03	0.41±0.13	0.41±0.14**
20 µM	7.80±0.84**	0.39±0.13	1.23±0.12	0.11±0.01*	0.11±0.03**

Where CN = control, FI (Frequency of interphase), FP (Frequency of prophase), FM (Frequency of metaphase), FA (Frequency of anaphase), and FT (Frequency of telophase).

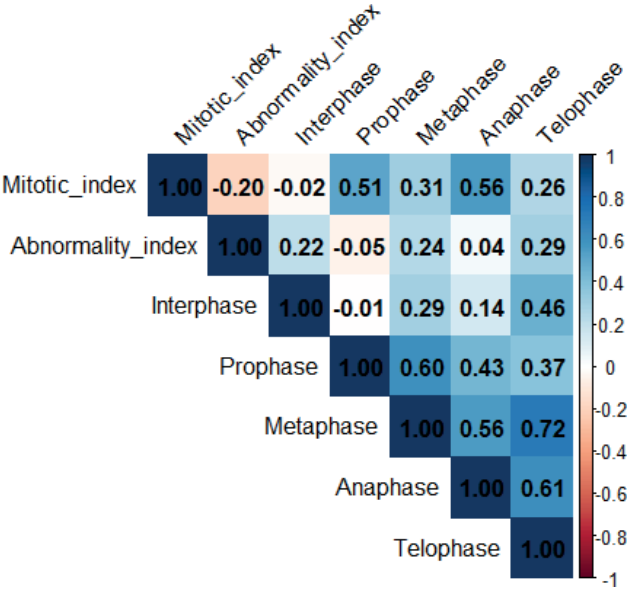

Figure 4. Pearson's correlation coefficients were calculated to assess the relationships among different variables (MI, AI, and CKI) under Mn treatments for 24 hours.

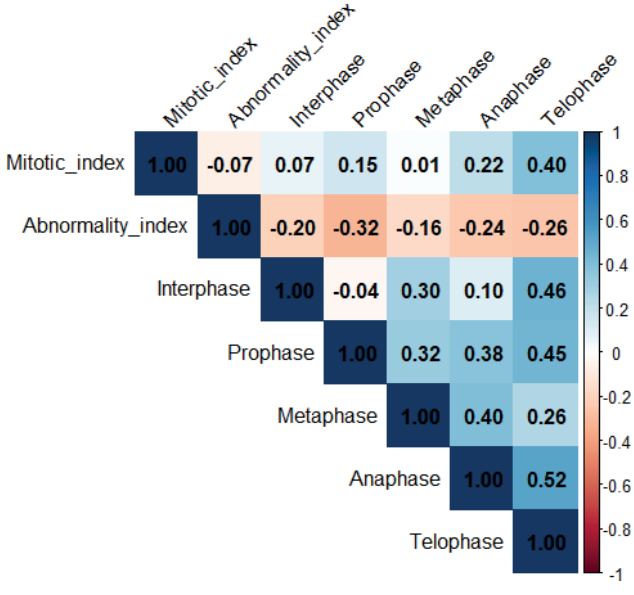

Figure 5. Pearson's correlation coefficients were calculated to assess the relationships among different variables (MI, AI, and CKI) under Mn treatments for 48 h.

the cause of decline in cell activity. A longer S phase has been associated by certain researchers with mitotic inhibition (Siddiqui 2024 ; Periakaruppan et al. 2023; Qian 2024). According to Das et al. (2023), heavy metals can enter DNA through nuclear pores or when the nuclear membrane splits into cells undergoing mitosis.

Aneugenic, tubergenic, and clastogenic effects are caused by the prevalence of these abnormalities (Sid-

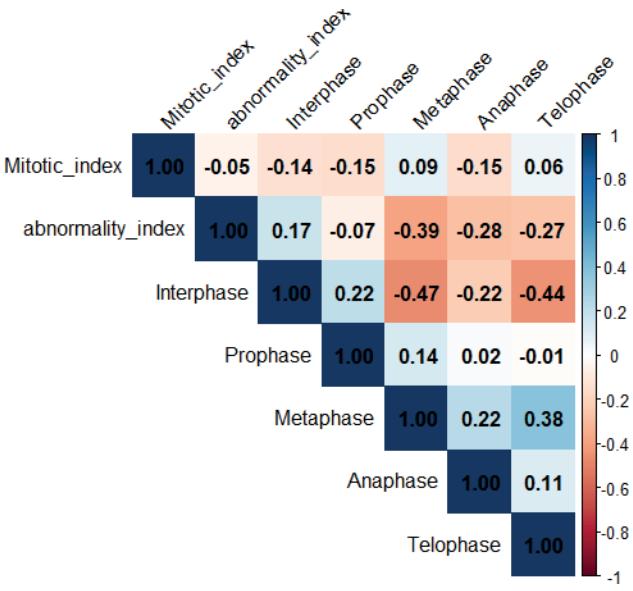

Figure 6. Pearson's correlation coefficients were calculated to assess the relationships among different variables (MI, AI, and CKI) under Mn treatments for 72 h.

diqui 2024 b; Siddiqui et al. 2012;–Bonciu et al. 2018; Bonciu et al. 2022). They are caused by spindle apparatus disorders, abnormal metaphase, telophase, anaphase, and bridges, as well as chromosomal breakage (fragments, micronuclei) (Hossain et al.2022; Faizan M, et al. 2022). The rising occurrence of AI has resulted from suppression of DNA synthesis during S-phase (Tumer et al., 2022). In the current study, different types of AI, such as anaphase bridges, dissociated chromosomes in metaphase and anaphase, chromosomal bridging was caused by incorrect separation and retarded chromosomes in anaphase were reported in *Glycine max* after treatment with Mn. Based on the results of proportions of distribution of mitotic phases, Mn reduced the percentage of interphase, prophase, metaphase, anaphase, and telophase in all concentrations dose-dependently.

The results align with those of (Liman et al. 2022; Munir et al. 2021; Yu et al. 2025). The percentage of telophase stage was reduced as compared to control. These results imply that a decrease in cell development during mitosis or the stoppage of one or more mitotic stages may be the cause of decline in telophase stages and, thereafter, MI (Ping et al. 2012; Siddiqui 2018 a and b). The results suggest that a reduction in cell development and the arrest of one or more mitotic phases may be the source of a drop in the proportion of prophase, metaphase, anaphase, and telophase at all doses, and therefore MI (Siddiqui 2014; Siddiqui 2016; Sarac et al. 2019).

CONCLUSION

The cytotoxic and genotoxic properties of Mn, which is commonly added to our agricultural fields due to environmental pollution, can cause mutations in *Glycine max*. The above studies suggest that natural resources pollution, industrial effluents, and agricultural practices for comforts should be curtailed, as incidence of heavy metal increases soil pollution, resulting in grave cytogenetic effects in plants and higher organisms. Thus, mutagenesis data obtained from plant tests are critical for genetic studies aimed at maintaining a stable ecosystem.

FUNDING

The authors extend their appreciation to the Deanship of Research and Graduate Studies at King Khalid University for funding this work through the Large Group Project under grant number (RGP2/89/46).

REFERENCES

Aseef A, Venkatkumar S. 2025. Staggering cytotoxic effects of manganese oxide nanoparticles from Bacillus thuringiensis. Microb. Pathog. 198:107184.

Aslam M, Aslam A, Sheraz M, Ali B, Ulhassan Z, Najeeb U, Zhou W, Gill RA. 2021. Lead toxicity in cereals: mechanistic insight into toxicity, mode of action, and management. Front. Plant Sci. 11:587785.

Bonciu E, Firbas P, Fontanetti CS, Wusheng J, Karaismailoğlu MC, Liu D, Menicucci F, Pesnya DS, Popescu A, Romanovsky AV, Schiff S, Ślusarczyk J, de Souza CP, Srivastava A, Sutan A, Papini A. 2018. An evaluation for the standardization of the *Allium cepa* test as cytotoxicity and genotoxicity assay. Caryologia. 71(3): 191-209

Bonciu E, Paraschivu M, Şuțan NA, Olaru AL. 2022. Cytotoxicity of sunset yellow and brilliant blue food dyes in a plant test system. Caryologia. 75(2):143-9.

Chukwu EC, Gulser C. 2025. Morphological, physiological, and anatomical effects of heavy metals on soil and plant health and possible remediation technologies. Soil Sec. 100178.

Das D, Bisht K, Chauhan A, Gautam S, Jaiswal JP, Salvi P, Lohani P. 2023. Morpho-physiological and Biochemical responses in wheat foliar sprayed with zinc-chitosan-salicylic acid nanoparticles during drought stress. Plant Nano Biol. 4:100034.

Dorman DC. 2023. The role of oxidative stress in manganese neurotoxicity: a literature review focused on

contributions made by Professor Michael Aschner. Biomolecules. 13(8), p.1176.

Elik Ü, Gül Z. 2025. Accumulation potential of lead and cadmium metals in maize (*Zea mays* L.) and effects on physiological-morphological characteristics. Life. 15(2):310.

Ertürk FA, Sunar S. 2021. Determination of cytogenetic and epigenetic effects of manganese and copper on Zea mays L. ISPEC J. Agric. Sci. 5(3):529-43.

Espinola EC, Cabreros MM, Redillas MC. 2025. Morpho-Physiological Adaptations of Rice Cultivars Under Heavy Metal Stress: A Systematic Review and Meta-Analysis. Life. 15(2):189.

Fairoj SA, Ghosh UK, Islam MM, Jahan K, Siddiqui S, Alshaharani MO, Siddiqua A, Yassin HM.2024. Amelioration strategy of saline stress in wheat with salicylic acid: a review. Caryologia. 77(3):11-25.

Faizan M, Bhat JA, El-Serehy HA, Moustakas M, Ahmad P. 2022. Magnesium oxide nanoparticles (MgO-NPs) alleviate arsenic toxicity in soybean by modulating photosynthetic function, nutrient uptake and antioxidant potential. Metals. 12(12):2030.

Firbas P, Amon T. 2014. Chromosome damage studies in the onion plant *Allium cepa* L. Caryologia. 67(1): 25-35

Hafeez A, Rasheed R, Ashraf MA, Qureshi FF, Hussain I, Iqbal M. 2023 Effect of heavy metals on growth, physiological and biochemical responses of plants. In Plants and their interaction to environmental pollution. (pp. 139-159). Elsevier.

Hossain J, Azam MG, Gaber A, Aftab T, Hossain A. 2022. Cytotoxicity of metal/metalloids' pollution in plants. In Metals Metalloids, Soil Plant Water Systems. 371-394. Academic Press.

Jomova K, Alomar SY, Valko R, Nepovimova E, Kuca K, Valko M. 2025. The role of redox-active iron, copper, manganese, and redox-inactive zinc in toxicity, oxidative stress, and human diseases. EXCLI Journal. 24:880-954.

Lee SY, Lee YY, Cho KS. 2024. Inoculation effect of heavy metal-tolerant and plant growth-promoting rhizobacteria for rhizoremediation. Int. J. Environ. Sci. Technol. (2):1419-34.

Liman R, Ali MM, Istifli ES, Ciğerci İH, Bonciu E. 2022. Genotoxic and cytotoxic effects of pethoxamid herbicide on Allium cepa cells and its molecular docking studies to unravel genotoxicity mechanism. Environ. Sci. Pollut. Res. 29: 63127–63140.

Mauser KM, Wolfram J, Spaak JW, Honert C, Brühl CA. 2025. Current-use pesticides in vegetation, topsoil and water reveal contaminated landscapes of the Upper Rhine Valley, Germany. Commun. Earth Environ. 6(1):166.

Munir N, Jahangeer M, Bouyahya A, El Omari N, Ghchime R, Balahbib A, Aboulaghras S, Mahmood Z, Akram M, Ali Shah SM, Mikolaychik IN. 2021. Heavy metal contamination of natural foods is a serious health issue: A review. Sustainability. 14(1):161.

Perfileva AI, Krutovsky KV. 2024. Manganese nanoparticles: synthesis, mechanisms of influence on plant resistance to stress, and prospects for application in agricultural chemistry. J. Agric. Food Chem. 72(14):7564-85.

Periakaruppan R, Vanathi P, Priyanka G, Vidhya D. 2023. Toxicity in plants by metal oxide nanoparticles. In Nanometal Oxides in Horticulture and Agronomy; Academic Press: Cambridge, MA, USA, 2023; pp. 241–273.

Ping KY, Darah I, Yusuf UK, Yeng C, Sasidharan S. 2012. Genotoxicity of Euphorbia hirta: an *Allium cepa* assay. Molecules. 17(7):7782–7791.

Qian YA, Haipeng LI, Yinghao LI, Helian LI. 2024. Wheat morphological and biochemical responses to copper oxide nanoparticles in two soils. Pedosphere. 34(4):814-25.

Rao MJ, Duan M, Zhou C, Jiao J, Cheng P, Yang L, Wei W, Shen Q, Ji P, Yang Y, Conteh O. 2025. Antioxidant defense system in plants: Reactive oxygen species production, signaling, and scavenging during abiotic stress-induced oxidative damage. Horticulturae. 11(5):477.

Sarac I, Bonciu E, Butnariu M, Petrescu I, Madosa E. 2019. Evaluation of the cytotoxic and genotoxic potential of some heavy metals by use of *Allium* test. Caryologia. 72(2):37-43.

Sarkar AK, Saha R, Halder R. 2022. Chromosomes damage by sewage water studies in the Allium cepa L. and Zea mays L. Caryologia. 75(1):55-63.

Shahwar D, Khan Z, Ansari MY. 2022. Cadmium induced genotoxicity and antioxidative defense system in lentil (*Lens culinaris* Medik.) genotype. Caryologia. 75(3):47-64.

Siddiqui S, Al Amri SAM, Al Ghamdy HA, Alqahtani WSS, Alquyr SM, Yassin HM. 2021. Impact of Bisphenol A on seed germination, radicle length and cytogenetic alterations in *Pisum sativum* L. Caryologia. 74(2): 103–109.

Siddiqui S, Alamri S, Al-Rumman S, Moustafa M. 2018. Allelopathic and cytotoxic effects of medicinal plants on vegetable crop pea (*Pisum sativum*). Cytologia.83(3):277-82.

Siddiqui S, Al-Rumman S. 2020[a]. Clethodim induced pollen sterility and meiotic abnormalities in vegetable crop *Pisum sativum* L. Caryologia. 73: 37–44.

Siddiqui S, Al-Rumman S. 2020[b]. Cytological changes induced by clethodim in *Pisum sativum* plant. Bangladesh J. Bot. 49(2):367–374.

Siddiqui S, Al-Rumman S. 2022[a]. Methomyl, imbraclaobrid and clethodim induced cytomixis and syncytes behaviors in PMCs of *Pisum sativum* L: Causes and outcomes. Saudi J Biol Sci. 29(9):103390.

Siddiqui S, Al-Rumman S. 2022[b]. Exposure of *Pisum sativum* L. seeds to methomyl and imidacloprid cause genotoxic effects in pollen-mother cells. Biology. 11: 1549.

Siddiqui S, Al-Rumman S. 2022[c]. Methomyl has clastogenic and aneugenic effects and alters the mitotic kinetics in *Pisum sativum* L. Caryologia. 75(3): 91–99.

Siddiqui S, Meghvansi MK, Hasan Z. 2007. Cytogenetic changes induced by sodium azide (NaN3) on *Trigonella foenum-graecum* L. seeds. S. Afr. J. Bot. 73(4):632–5.

Siddiqui S, Meghvansi MK, Khan SS. 2012. Glyphosate, alachor and maleic hydrazide have genotoxic effect on *Trigonella foenum-graecum* L. Bull. Environ. Contam. Toxicol. 88(5):659-65.

Siddiqui S, Meghvansi MK, Wani MA, Jabee F. 2009. Evaluating cadmium toxicity in the root meristem of *Pisum sativum* L. Acta Physiol. Plant. 31:531-6.

Siddiqui S, Sulaiman AA. 2021. Influence of nanoparticles on food: An analytical assessment. Journal of King Saud University-Science, 33;(6):101530.

Siddiqui S. 2012. Lead-induced genotoxicity in *Vigna mungo* var. HD-94. J. Saudi Soc. Agric. Sci. 11(2):107–12.

Siddiqui S. 2013. Exposure of Cu and Mn to Cicer arietinum L. Var. BGD-72 seeds induces morphological and biochemical changes in the plant. South Asian J. Exp. Biol. 3 (1): 31-36.

Siddiqui S. 2015. DNA damage in *Cicer* plant grown on soil polluted with heavy metals. J. King Saud Univ. Sci. 27(3):217–23.

Siddiqui S. 2018. Cytotoxicity induced by aluminum sulfate in cells of root meristem of *Pisum sativum* cv. arikil. Bangl. J. Bot. 1:47:219.

Siddiqui S. 2023. Phenthoate toxicity evaluation in root meristem of *Pisum sativum* L. Caryologia. 76(1):57–66.

Siddiqui S. 2024 [a]. DNA Damage, cell death, and alteration of cell proliferation insights caused by copper oxide nanoparticles using a plant-based model. Biology. 13(10): 805.

Siddiqui S. 2025[a]. Global patterns and drivers of species and genera richness of Fabaceae. Front. Plant Sci. 16:1581814.

Siddiqui S. 2025 [b]. Unlocking the environmental potential of biochar: production, applications, and limitations. Frontiers in Sustainable Food Systems. 9:1569941.

Siddiqui S. 2024[b]. Effects of cypermethrin on morphological, physiological, and biochemical attributes of *Cicer arietinum* (Fabales: Fabaceae). Front. Sustain. Food Syst. 8: 1446308.

Siddiqui S. 2014. Genotoxic effect of four medicinal plant extracts on *Pisum sativum* cv. Arikil. Bangl. J. Bot. 43(1): 107-111.

Siddiqui S. 2016. Inhibitory effects of leaf extracts on morphology of *Pisum sativum* cv. Arikil. Bangl. J. Bot. 45(1): pp.243-246.

Sobańska Z, Roszak J, Kowalczyk K, Stępnik M. 2021. Applications and biological activity of nanoparticles of manganese and manganese oxides in in vitro and in vivo models. Nanomaterials. 11(5):1084.

Tümer C, Çavuşoğlu K. and Yalcin E. 2022. Screening the toxicity profile and genotoxicity mechanism of excess manganese confirmed by spectral shift. Scientific Reports, 12(1):.20986.

Üstündağ Ü, Macar O, Kalefetoğlu Macar T, Yalçın E, Çavuşoğlu K. 2023. Effect of Melissa officinalis L. leaf extract on manganese-induced cyto-genotoxicity on *Allium cepa* L. Sci. Rep. 13(1):22110.

Vieira IT, Nascimento AL, Sampaio RA, Pegoraro RF. 2025. Vermicompost from sewage sludge: effects on heavy metal presence in soil and bioaccumulation in castor bean. Int. J. Environ. Sci. Technol. 1-4.

Vijaya Kumar M, Prasad Raju H. 2025. Heavy Metals in the Environment: Sources, Fate, and Health Implications. In-Groundwater Resource Management Planning Strategies: A Geospatial Approach: Volume 1 2025 Jun 17 (pp. 135-153). Cham: Springer Nature Switzerland.

Xia Z, Xue C, Liu R, Hui Q, Hu B, Rennenberg H. 2025. Lead accumulation and concomitant reactive oxygen species (ROS) scavenging in Robinia pseudoacacia are dependent on nitrogen nutrition. Plant Physiol. Biochem. 219:109388.

Yu JA, Chen Z, Gao W, He S, Xiao D, Fan W, Huo M, Nugroho WA. 2025. Global trends and prospects in research on heavy metal pollution at contaminated sites. J. Environ. Manag. 1;383:125402.

Caryologia
International Journal of Cytology, Cytosystematics and Cytogenetics

Firenze University Press
https://riviste.fupress.net/index.php/caryologia

OPEN ACCESS

Citation: Author (2025). Spontaneous stickiness in somatic metaphase cells suggests chromosomal instability in a Mexican population of *Aeschynomene* sp. prope *villosa* (Fabaceae: Papilionoideae: Dalbergieae). *Caryologia* 78(3): 51-59. doi: 10.36253/caryologia-3492

Received: May 11, 2025

Accepted: November 1, 2025

Published: December 24, 2025

Data Availability Statement: All relevant data are within the paper and its Supporting Information files.

Competing Interests: The Author(s) declare(s) no conflict of interest.

ORCID
FTP: 0000-0003-0232-2110

Spontaneous stickiness in somatic metaphase cells suggests chromosomal instability in a Mexican population of *Aeschynomene* sp. prope *villosa* (Fabaceae: Papilionoideae: Dalbergieae)

Fernando Tapia-Pastrana*

Facultad de Estudios Superiores Zaragoza, Universidad Nacional Autónoma de México, Laboratorio de Genecología, Batalla 5 de mayo s/n esquina Fuerte de Loreto, Col. Ejército de Oriente, Alcaldía Iztapalapa, C.P. 09230, Ciudad de México, Mexico
Email: pasfer@unam.mx

Abstract. *Aeschynomene* sp. prope *villosa* (a dalbergioid legume) represents a group of populations with morphological characteristics similar to those of *Aeschynomene villosa*, but without complete overlap, and whose cytogenetic characteristics subtly differ from both the latter and other related taxa. In this study, conventional surface spread and air-drying techniques, along with Giemsa staining, were used to analyze metaphase chromosome complements and karyotypes of individuals belonging to a population of *A.* sp. prope *villosa*, a taxon included in the Americanae series of *Aeschynomene*. The results confirm a previously obtained karyotypic formula. Differences observed in chromosome sizes do not modify the karyotype or its symmetry. They are interpreted here as a loss of gene flow between populations or adaptations to different ecogeographic conditions. The presence of chromosome stickiness in 7.4% of the nuclei analyzed is noteworthy. This aberration, not previously observed in *Aeschynomene*, primarily involves areas near the telomeres of apparently homologous and non-homologous chromosomes. This phenomenon, observed mainly in meiosis, has been linked to the tendency of chromosomes to clump together during cellular divisions following plant hybridization events. The same criterion of chromosomal interaction after hybridization could explain the changes in the number and position of satellites recorded in a previous study. Although unexpected, these results should not be surprising, since intergradation between *A. villosa* and *A. americana,* species with which it overlaps in its distribution area, has been suspected for at least 70 years. Furthermore, hybridization and allopolyploidy have already been demonstrated in other morphological series of *Aeschynomene*.

Keywords: Chromosomal instability, chromosome stickiness, hybridization, interchromosomal connections, karyotype, SAT-chromosomes.

INTRODUCTION

Aeschynomene L. is a genus of flowering plants in Leguminosae, subfamily Papilionoideae, and recently assigned to the tribe Dalbergieae. It

includes around 130 species of pantropical distribution, commonly referred to as joint vetch (Lavin et al. 2001; Wojciechowski et al. 2004; Cardoso et al. 2012, 2020; WFO 2025). It includes herbaceous and woody species, annual, perennial, and repetitive, with different ecological requirements and of increasing economic importance as green manure by supplementing nitrogen to the soil through nodulating stems and roots in symbiosis with nitrogen-fixing bacteria (Alazar and Becker 1987; Fernandes 1996; Souza et al. 2012; Tapia-Pastrana and Delgado-Salinas 2020).

In the New World, *Aeschynomene villosa* Poir. and its three varieties (included in the Americanae series, a taxon defined on morphological basis) constitute a group widely distributed from southern Arizona through Mexico (mostly on the Pacific side) and Central America to northern South America and the West Indies. (Rudd 1955; McVaugh 1987; Rodríguez 1990). It also occurs, apparently as an introduced species, in the tropics of the Old World. It is highly variable, and often weedy (McVaugh 1987). On the other hand, Rudd (1955) observed a close relationship between *A. villosa* and *A. americana* L. (also in the Americanae series) and anticipated probable intergradation due to divergence.

In Mexico, the distribution of *A. villosa* overlaps in many areas with that of *A. americana* and its varieties *flabellata* and *glandulosa*, which are also widely distributed (Rudd 1955). This overlap also extends to some morphological features, confusing fieldwork, especially when the two taxa lack fruit (Rudd 1955; Reynolds 1990; Olvera-Luna et al. 2012). Additionally, phylogenetic analyses consistently indicate that both species are closely related (Chaintreuil et al. 2013; Brottier et al. 2018; Cardoso et al. 2020). It is important to note here that *A. villosa* Poir. was initially described as *Aeschynomene americana* var. *villosa* (Urban 1905, cited by Rudd 1955) and as *Aeschynomene americana* var. *longifolia* (Micheli 1895, cited by McVaugh 1987); however, its specific status, as well as that of its varieties, was confirmed by morphological (Rudd 1955) and chromosomal (Tapia-Pastrana et al. 2020) characters and are currently accepted names in the genus *Aeschynomene* (WFO).

Morphological similarities between species of the Americanae series, particularly between *A. americana* and *A. villosa*, were recognized during a cytogenetic analysis that included, among others, seven taxa of this series that thrive in Mexico. Two of them were described as *A.* sp. prope *americana* and *A.* sp. prope *villosa*, whose karyotypic characteristics supported their taxonomic identity; however, they also showed some similarities concerning the typical species (Tapia-Pastrana et al. 2020). In this research, the taxonomic criteria of Rudd (1955) and McVaugh (1987) for species in the morphological Americanae series of *Aeschynomene* were followed, in addition to the available cytogenetic information. It was considered that the individuals under study fit better in the description of *Aeschynomene* sp. prope *villosa* (Tapia-Pastrana et al. 2020).

Aeschynomene sp. prope *villosa* can be confused with the typical variety (*A. villosa*) and with *A. americana*; however, there are sufficient morphological differences to allow them to be differentiated, particularly the length of the inflorescence and the abundance of glandular hairs on vegetative structures, flowers, and fruits (Rudd, 1955). In some descriptions, *A. villosa* var. *longifolia* is considered a synonym of *A. villosa* var. *villosa* (WFO 2025). Additionally, the possible hybridization between the typical variety and *A. americana* is proposed (Rudd 1955; WFO 2025).

Aeschynomene sp. prope *villosa* comprises erect, branching subshrubs that reach up to 1.6 m in height. Stems are green or slightly reddish, with abundant glandular hairs. The stipules are hispid on mature plants, 12-20 mm long, striated, and ciliate, with the upper portion up to three times longer than the lower portion. Leaves 2.5-6 cm long, 18-66 foliolate, oblong, ciliate, with reddish edges; inflorescences with axillary flowers shorter than the underlying leaves; bracts cordate, slightly hispid, ciliate; bracteoles lanceolate 2.0 x 1.0 mm, serrate-ciliate, with reddish edges; peach-yellow or rusty yellow flowers 8.0-9.0 x 5.5-7.5 mm, glandular hairs on the margins; calyx deeply bilabiate, adaxial lip ciliate 3.5 mm x 1.5 mm, nearly glabrous; carinal lip 3.5-4.5 mm x 1.5 mm, glandular hairs on the outer surface; standard petal sub orbiculate to reniform, 6 mm long, 4.5 mm wide, claw less than 1 mm, macule dark yellow with reddish semicircular margins, nectar guides reddish; wing petals 6 x 2.5-3.0 mm, sculptured on the distal portion suprabasal-medial; claws 0.7 mm wide; keel petals 6.0 x 2.5 mm, lower margin slightly ciliate, claw less than 1 mm; stamens 5.0-5.5 mm long, pistil 6 mm long, ovary profusely hispid; fruits slightly curved with persistent style, commonly 4-6 jointed, articles 4 x 3 mm, hispid in early stages of development, verrucose during ripening; seeds 2.5 x 2.0 mm, brown or light olive (Fig. 1A-J).

This research aims to: (1) present the relevant morphological characters of individuals belonging to a population initially identified as *Aeschynomene villosa* var. *longifolia*, but which, after a thorough review, are finally treated as *A.* sp. prope *villosa*, (2) corroborate cytogenetic characteristics and karyotype, (3) discuss the possible hybrid origin of the individuals under study based on morphological and chromosomal evidence, and (4) offer some data on their phenology.

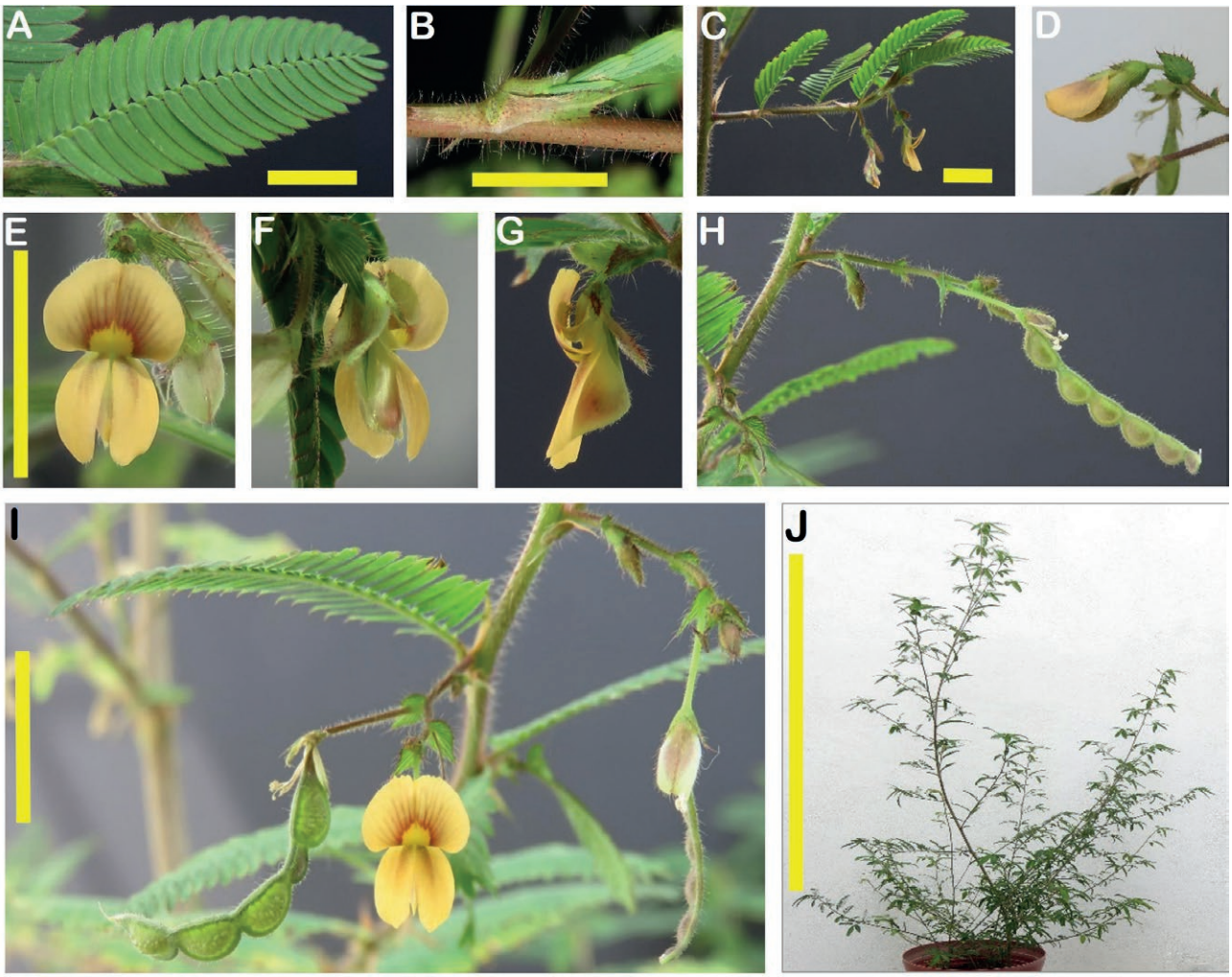

Figure 1. Morphological traits of *Aeschynomene* sp. prope *villosa*. (**A**). Leaf and leaflets. **(B)**. Branch and stipule are covered with abundant glandular hairs. **(C)**. Fertile branch, the shortened inflorescence is obvious. **(D)**. Flower in preanthesis with cordate bracts and lanceolate bracteoles. **(E-G)**. Peach-yellow or rust-yellow papilionate flowers. Front, dorsal, and side views, respectively. Petals with glandular hairs on the edges. Keel's petal is shorter than the wings. **(H-I)**. Inflorescence with clusters of two to four flowers. Peduncles and pedicels hispid. Fruits are villous-hispid, commonly 4 to 6-seeded. **(J)**. General appearance of a mature plant. In **A**, **B**, **C**, **E**, and **I**, the scale bar = 1 cm. In **J**, the scale bar = 1 m.

MATERIALS AND METHODS

Plant material

Cytogenetic studies were performed on seeds collected in January 2017 in the Locality of Los Mangos, Municipality of Hueyapan de Ocampo, State of Veracruz, Mexico (18°14'37" N; 95°7'22" W. 350 m asl; Fig. 2). The identity of the plants was established after comparing them with specimens deposited in the National Herbarium (MEXU) collection. Specimens prepared from plants grown in greenhouse conditions were entered as vouchers in the same collection.

Chromosome and karyotype procedures

The mitotic cells were obtained from radicular meristems of seeds from five individuals, germinated in Petri dishes lined with cotton moistened in distilled water. Chromosomes at metaphase were obtained following the splash method by Tapia-Pastrana and Mercado-Ruaro (2001) briefly described as follows: the meristems were separated from the root when it reached between 3-5 mm in length and were pretreated with fresh solution of 0.002M 8-hydroxyquinoline for 5 h at room temperature and fixed in the fixative Farmer´s solution (ethanol: acetic acid, 3:1). Then they were treated in a mixture of

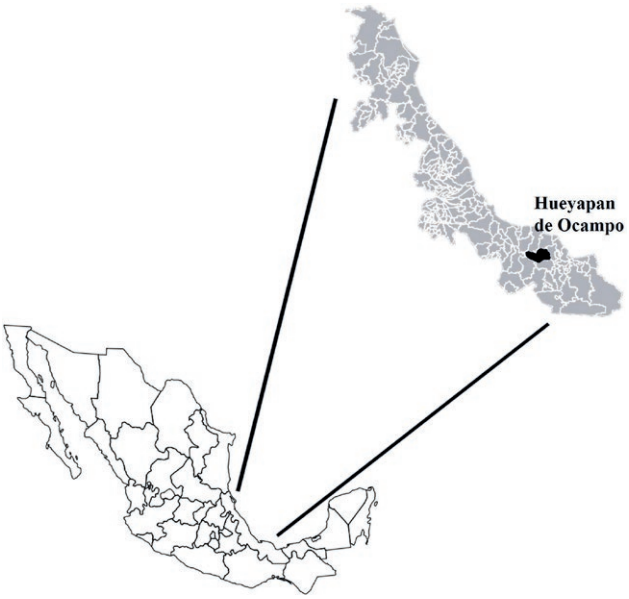

Figure 2. The Municipality of Hueyapan de Ocampo is in the south of the State of Veracruz, in the Los Tuxtlas, southeastern Mexico region.

2% cellulase (w/w, Sigma) and 20% pectinase (v/w, Sigma) in 75 mM KCl for 2 h at 37 °C. After centrifugation at 1500 rpm for 10 min, the cell pellet was transferred to 75 mM KCl solution for 20 min at 37 °C. After two successive rinses with KCl solution, they were again fixed in Farmer´s solution and rinsed twice more. Two drops of the suspension of the pellet were placed on clean slides, air dried, and stained in 10% Giemsa for 10 min. Preparations were made permanent using a synthetic resin (solution in xylol Hycel). At least ten well-spread metaphase plates, no chromosome overlapping, were photographed, using a Carl Zeiss Axioscope A1, and analyzed for chromosome number. Five photographs of metaphases with chromosomes having comparable degrees of contraction and centromeres localized were used to obtain mean values in the following chromosomal parameters: the difference in length between the longest chromosome and the shortest chromosome (Range), total haploid chromosome length (THC), average chromosomal size (AC) and ratio of the longest/shortest chromosome (Ratio, L/S). The asymmetry index (TF%) was obtained following Huziwara (1962). Chromosomes were classified as metacentric (m), submetacentric (sm), and subtelocentric according to their morphology and arm proportions (Levan et al. 1964). Chromosome size was estimated using a Mitutoyo Digimatic Caliper. A karyotype is prepared from a photomicrograph by cutting individual chromosomes, organizing them in descending order of length, and matching based on morphology.

RESULTS

108 typical metaphase nuclei exhibiting a $2n = 20$ were examined (Fig. 3 A-D). The complements showed a predominance of m chromosomes, few sm chromosomes, and a single pair of st chromosomes carrying secondary constriction and satellites on short arms (Table 1; Fig. 3A, B, and D). The chromosome formula and other cytogenetic parameters are summarized in Table 2. The karyotype obtained is shown in Fig. 3E. Eight metaphase complements (7.4%) exhibited chromosomes of different shapes and sizes linked by chromatin strands (interchromosomal connections) in regions close to the telomeres (Fig. 3A-D) and an apparent satellite association between the st chromosomes (Fig. 3D). Interphase cells exhibited one or two nucleoli.

DISCUSSION

The chromosome number $2n = 20$ obtained for *Aeschynomene* sp. prope *villosa* confirms the predominance of n=10 in dalbergioid legumes. It adds to the records showing that the species and subspecific taxa in the Americanae series of *Aeschynomene* cytogenetically analyzed are strictly diploid. Its karyotypic formula (7m + 2sm + 1st) confirms the chromosomal architecture observed in a previous study for another Mexican population also registered as *A.* sp. prope *villosa*. Although it shows slight differences in some cytogenetic parameters such as THC and AC, this does not substantially affect either the chromosomal formula or the asymmetry index (TF%) and instead suggests a loss of genetic inter-

Table 1. Mean chromosome measures in *Aeschynomene* sp. prope *villosa.*

CP	TCL (μm)	LLA (μm)	LSA (μm)	r	S
01	2.25±0.19	1.26±0.18	0.98±0.09	1.63	m
02	2.10±0.13	1.21±0.10	0.89±0.05	1.35	m
03	1.96±0.08	1.13±0.06	0.87±0.08	1.29	m
04	1.75±0.13	0.99±0.12	0.75±0.04	1.32	m
05	1.67±0.13	0.89±0.09	0.77±0.04	1.15	m
06	1.58±0.11	0.90±0.11	0.67±0.04	1.34	m
07	1.51±0.12	1.02±0.09	0.48±0.04	2.12	sm
08	1.40±0.13	0.74±0.09	0.64±0.04	1.15	m
09	1.30±0.20	1.02±0.16	0.27±0.05	3.77	st*
10	1.25±0.14	0.87±0.08	0.37±0.07	2.35	sm

CP=Chromosome pair; TCL=total chromosome length; LLA=length long arm; LSA=length short arm; ±=SD; r=arms ratio; S=shape after Levan et al. (1964). *Chromosomes with secondary constrictions on the short arm.

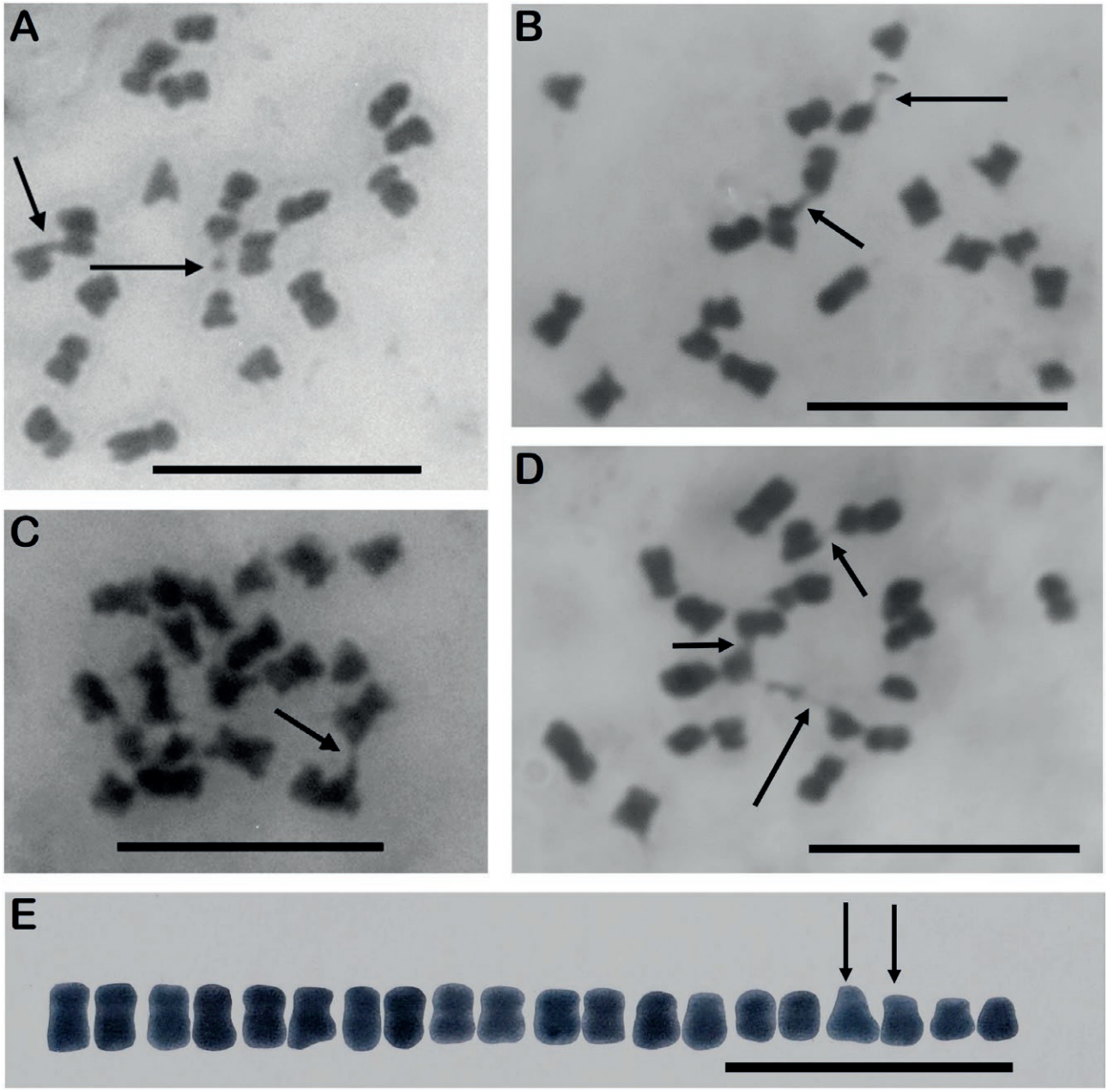

Figure 3. Metaphase nuclei of *Aeschynomene* sp. prope *villosa* 2*n* = 20. **A-D**. Evidence of chromosome stickiness linking telomeric regions of some homologous and non-homologous chromosomes. Short arrows indicate sticky chromatin strands, while long arrows indicate isolated secondary constrictions or satellite associations. **E**. Karyotype. Scale bar = 10 μm.

Table 2. Karyotypic analysis of *Aeschynomene* sp. prope *villosa*.

NA	2*n*	Karyotype formula	Sat	THC ± SD (μm)	AC ± SD (μm)	Range ± SD (μm)	L/S ± SD	TF% ± SD
108	20	7m + 2sm+1st	2	16.79±1.18	1.67±0.11	1.03 ± 0.14	1.85 ± 0.20	40.08 ± 1.45

NA = Nuclei analyzed; Sat = Number of satellites; THC = Total haploid chromosome length; AC = Average chromosome size; TF% = Asymmetry index.

action between populations or adaptations to different eco-geographic factors (Tapia-Pastrana et al. 2020). However, the most striking difference is the presence of a single SAT chromosome pair observed here, in which the microsatellites are located on the short arms of the st chromosomes (Fig. 3A and D), whereas, in the previous description, the complements also showed microsatellites on a pair of m chromosomes. The observation of up to two nucleoli in interphase could indicate the presence of two NOR regions, thus coinciding with the record of two pairs of SAT chromosomes described previously. In *Aeschynomene*, SAT chromosomes are considered to carry, at least in part, the NOR regions (Tapia-Pastrana et al. 2020).

Although this might suggest a new cytotype in *A.* sp. prope *villosa*, evidence of chromosomes linked by chromatin strands, a phenomenon known as chromosome stickiness, might offer another explanation. Stickiness is a chromatid aberration resulting from the induction of breaks and exchanges in chromosomes during their folding in mitotic prophase, when chromatin fibers remain bound in a three-dimensional organization and do not unfold due to some physical interference. The result is an intermingling of fibers and chromosomes joined by chromatidic bridges. That is when chromosome fibers do not condense correctly, in preparation for mitosis, they become trapped and physically entangled with fibers from other chromosomes (McGill et al. 1974; Pathak et al. 1975; Klášterská et al. 1976; Grant 1978; Gaulden 1987; Al-Achkar et al. 1989). Even more, Evans (1962) considered stickiness as a chromatid aberration, where the localized junction points represent sites in which different parts of the chromatids have undergone exchanges that occur naturally in plants and animals, especially after genetic instability due to hybridization.

For example, in plants, there are records of chromosomal stickiness after hybridization in *Rosa* (Klášterská and Natarajan 1975), *Panicum maximum* (Pessim et al. 2015), and *Brassica napus* (Sheidai et al. 2003). Furthermore, hybridization between plant species has been reported to cause cytological alterations, chromosomal instability, loss of somatic chromosomes, heritable changes in their size and staining, and abnormalities in meiotic behavior, although the exact mechanisms of such phenomena are unknown (Moav 1961; Moav et al. 1968; Wagenaar 1969; Klášterská and Natarajan 1975; Klášterská et al. 1976; Rao et al. 1990; Kiihl et al. 2011).

Today, there is a broad record of chromosomal alterations in plants that involve close contact between chromosomes or parts thereof. For example, the proximity of homologous chromosomes in metaphase is referred to as somatic associations (Therman 1951; Hiraoka 1958; Mitra and Steward 1961; Chauhan and Abel 1968; Wagenaar 1969). Dicentric chromosomes, anaphase bridges, and acentric fragments have also been recorded, recognizable as lagging chromatin during the separation of daughter nuclei due to instability in mitotic cells (Puizina et al. 2004). Other types of metaphase chromosome associations include somatic syndesis observed in *Daphne odora* (Hiraoka 1958), somatic pairing of homologous chromosomes recorded in *Impatiens balsamina* and *Salvia nemorosa* (Chauhan and Abel 1968) or *Ornithogalum graminifolium* and *O. caudatum* (Therman 1951). However, Fig. 3 A-D shows that the type of association observed in the mitotic chromosomes of *Aeschynomene* sp. prope *villosa* involves the telomeric regions of both homologous and non-homologous chromosomes. In this respect, the phenomenon observed here also differs from the associations observed in *Allium cepa*, where the ends of adjacent homologous chromosomes join in pairs to form chromosome chains (Wagenaar 1969).

The evidence of chromosome stickiness observed in *Aeschynomene sp. prope villosa* fits well with the chromatid bridges model described above and is interpreted as the result of a molecular event that can occur at different phases of the cell cycle (including prophase contraction) recognizable in prometaphase, metaphase, and anaphase in both mitosis and meiosis (Gaulden 1987). Furthermore, given the number of chromosomes involved, it would correspond to the moderate type of chromosome stickiness (Dowd et al. 1986; Gaulden 1987), facilitating an accurate chromosome count and the establishment of the karyotypic formula in the analyzed nuclei.

Other explanations consider chromosomal stickiness under genetic control due to the mutation of a recessive gene called sticky (Beadle 1932; Mehra and Rai 1970; Sosnikhina 1973; Golubovskaya 1989; Rao et al. 1990), and under this approach, it has been studied in several species of higher plants (Mendes-Bonato et al. 2001; Kaur and Singhal 2019). Likewise, the deficient functioning of non-histone proteins such as DNA topoisomerase and peripheral proteins, which are integral components of the chromosome whose function is necessary for the separation and segregation of chromatids, has been suggested (Gaulden 1987). However, given the supposed hybrid origin of *Aeschynomene* sp. prope *villosa* studied here, it is more likely that the observed chromosome stickiness results from improper folding of chromosome fibers, as mentioned above.

It is known that inter- or intraspecific hybridization events lead to genomic instability, which results in *de novo* chromosomal rearrangements due to changes in chromatin structure among other aspects (Fontdevila 1992, 2005; Metcalfe et al. 2007). Thus, changes in the

number and position of NORs have been recorded in species of the genus *Allium* and their hybrids (Sato 1981; Loidl and Greilhuber 1983; Schubert et al. 1983; Schubert 1984; Schubert and Wobus 1985; Pich et al. 1996), in subspecies of *Turnera sidoides* (Arbo 1985; Solís Neffa and Fernández 2002), and recently in the so-called *Aeschynomene americana* complex (Tapia-Pastrana et al. 2020).

Today, it is recognized that the Americanae morphological series of *Aeschynomene* includes taxa that are difficult to identify, but whose karyotypes confirm the evolutionary relationships rescued in phylogenies that use molecular data (Rudd 1955; Chaintreuil et al. 2013; Tapia-Pastrana et al. 2020). The suspicion that this group includes taxa that have not yet been described remains in force, so a more inclusive taxonomic revision is needed that considers morphological characters such as floral morphotypes and macule geometry in the standard petal, in addition to cytogenetic and ecological information (Tapia-Pastrana et al. 2020).

The present study shows for the first time the occurrence of chromosomal stickiness in a taxon of *Aeschynomene* L., an unsuspected cytogenetic event with various implications, particularly related to hybridization, an evolutionary pathway already described in other morphological series and phylogenetic clades of *Aeschynomene* (Arrighi et al. 2014; Tapia-Pastrana and Delgado-Salinas 2020).

ACKNOWLEDGEMENTS

The author is grateful for the support of the Division of Postgraduate Studies and Research, Faculty of Higher Studies Zaragoza.

REFERENCES

Alazar D, Becker M. 1987. *Aeschynomene* as green manure for rice. Plant Soil 101:141-143. https://doi.org/10.1007/BF02371043

Al-Achkar W, Sabatier L, Dutrillaux B. 1989. How are sticky chromosomes formed? Ann Genet. 32:10-15.

Arbo MM. 1985. Notas taxonómicas sobre Turneráceas Sudamericanas. Candollea 40(1):175-191.

Arrighi JF, Chaintreuil C, Cartieaux F, Cardi C, Rodier-Goud M, Brown SC, Boursot M, D´Hont A, Dreyfus B, Giraud E. 2014. Radiation of the Nod-independent *Aeschynomene* relies on multiple allopolyploid speciation events. New Phytol. 201(4):1457-1468. https://doi.org/10.1111/nph.12594

Beadle GW. 1932. A gene in *Zea mays* for failure of cytokinesis during meiosis. Cytologia 3(2):142-155. https://doi.org/10.1508/cytologia.3.142

Brottier L, Chaintreuil C, Simion P, Scornavacca C, Rivallan R, Mournet P, Moulin L, Lewis GP, Fardoux J, Brown SC, et al. 2018. A phylogenetic framework of the legume genus *Aeschynomene* for comparative genetic analysis of the Nod-dependent and Nod-independent symbioses. BMC Plant Biol. 18:333. https://doi.org/10.1186/s12870-018-1567-z

Cardoso D, de Queiroz LP, Pennington RT, de Lima HC, Fonty E, Wojciechowski MF, Lavin M. 2012. Revisiting the phylogeny of papilionoid legumes: New insights from comprehensively sampled early-branching lineages. Am J Bot. 99(12):1991-2013. https://doi.org/10.3732/ajb.1200380

Cardoso DBOS, Mattos CMJ, Filardi F, Delgado-Salinas A, Lavin M, Moraes PLR, Tapia-Pastrana F, Lima HC. 2020. A molecular phylogeny of the pantropical papilionoid legume *Aeschynomene* supports reinstating the ecologically and morphologically coherent genus *Ctenodon*. Neodiversity 13:1-38. https://doi.org/10.13102/neod.131.1

Chaintreuil C, Arrighi JF, Giraud E, Miché L, Moulin L, Dreyfus B, Munive-Hernández JA, Villegas-Hernández MC, Béna G. 2013. Evolution of symbiosis in the legume genus *Aeschynomene*. New Phytol. 200(4):1247-1259. https://doi.org/10.1111/nph.12424

Chauhan KPS, Abel WO. 1968. Evidence for the association of homologous chromosomes during premeiotic stages in *Impatiens* and *Salvia*. Chromosoma 25:297-302. https://doi.org/10.1007/BF01183122

Dowd MA, Gaulden ME, Proctor BL, Seibert GB. 1986. Formaldehyde-induced acentric chromosome fragments and chromosome stickiness in *Chortophaga* neuroblasts. Environ Mutagen. 8:401-411. https://doi.org/10.1002/em.2860080309

Evans HJ. 1962. Chromosome aberrations induced by ionizing radiations. Int Rev Cytol. 13:221-321. https://doi.org/10.1016/S0074-7696(08)60285-5

Fernandes A. 1996. O táxon *Aeschynomene* no Brasil. Fortaleza: Edições UFC, Brasil, 130 pp.

Fontdevila A. 1992. Genetic instability and rapid speciation: are they coupled? Genetica 86(1-3):247-258. https://doi.org/10.1007/BF00133723

Fontdevila A. 2005. Hybrid genome evolution by transposition. Cytogenet Genome Res. 110:49-55. https://doi.org/10.1159/000084937

Gaulden ME. 1987. Hypothesis: some mutagens directly alter specific chromosomal proteins (DNA topoisomerase II and peripheral proteins) to produce chromosome stickiness, which causes chromosome

aberrations. Mutagenesis 2:357-365. https://doi.org/10.1093/mutage/2.5.357

Golubovskaya IN. 1989. Meiosis in maize: mei-genes and conception of genetic control of meiosis. Adv Genet. 26:149-192. https://doi.org/10.1016/S0065-2660(08)60225-4

Grant WF. 1978. Chromosome aberrations in plants as a monitoring system. Environ Health Perspect. 27:37-43. https://doi.org/10.1289/ehp.782737

Hiraoka T. 1958. Somatic syndesis in *Daphne odora*. I. The chromosome behaviour in mitosis. Proc Jap Acad. 34:700-705.

Huziwara Y. 1962. Karyotype analysis in some genera of Compositae. VIII. Further studies on the chromosomes of *Aster*. Am J Bot. 49:116-119. https://doi.org/10.1002/j.1537-2197.1962.tb14916.x

Kaur D, Singhal VK. 2019. Meiotic abnormalities affect genetic constitution and pollen viability in dicots from Indian cold deserts. BMC Plant Biol. 19:10. https://doi.org/10.1186/s12870-018-1596-7

Kiihl PRP, Pereira ARA, Godoy SMD, Stenzel NMC, Risso-Pascotto C. 2011. Chromosome stickiness during meiotic behavior analysis of *Passiflora serrato-digitata* L. (Passifloraceae). Cienc Rural 41:1018-1023. http://www.redalyc.org/articulo.oa?id=33119153028

Klášterská I, Natarajan AT. 1975. Stickiness in *Rosa* meiosis induced by hybridisation. Caryologia 28:81-88. https://doi.org/10.1080/00087114.1975.10796599

Klášterská I, Natarajan AT, Ramel C. 1976. An interpretation of the origin of subchromatid aberrations and chromosome stickiness as a category of chromatid aberrations. Hereditas 83(2):153-162. https://doi.org/10.1111/j.1601-5223.1976.tb01581.x

Lavin M, Pennington RT, Klitgaard BB, Sprent JI, de Lima HC, Gasson PE. 2001. The dalbergioid legumes (Fabaceae): delimitation of a pantropical monophyletic clade. Am J Bot. 88(3):503-533. https://doi.org/10.2307/2657116

Levan A, Fredga K, Sandberg AA. 1964. Nomenclature for centromeric position on chromosomes. Hereditas 52:201-219. http://dx.doi.org/10.1111/j.1601-5223.1964.tb01953.x

Loidl J, Greilhuber J. 1983. Structural changes of Ag-stained nucleolus organizing regions and nucleoli during meiosis in *Allium flavum*. Can J Genet Cytol. 25(5):524-529. https://doi.org/10.1139/g83-079

McGill M, Pathak S, Hsu TC. 1974. Effects of ethidium bromide on mitosis and chromosomes: A possible material basis for chromosome stickiness. Chromosoma 47:157-166. https://doi.org/10.1007/BF00331803

McVaugh R. 1987. Flora Novo-Galiciana (Leguminosae) V. University of Michigan Press. Ann Arbor, EUA. 786 pp.

Mehra RC, Rai KS. 1970. Cytogenetic studies of meiotic abnormalities in *Collinsia tinctoria*. I. Chromosomal stickiness. Can J Genet Cytol. 12:560-569. https://doi.org/10.1139/g70-075

Mendes-Bonato AB, Pagliarini MS, Do Valle CB, Penteado MIDO. 2001. A severe case of chromosome stickiness in pollen mother cells of *Brachiaria brizantha* (Hochst.) Stapf (Gramineae). Cytologia 66(3):287-291. http://dx.doi.org/10.1508/cytologia.66.287

Metcalfe CJ, Bulazel KV, Ferreri GC, Schroeder-Reiter E, Wanner G, Rens W, Obergfell C, Eldridge MDB, O'Neill RJ. 2007. Genomic instability within centromeres of interspecific marsupial hybrids. Genetics 177(4):2507-2515. https://doi.org/10.1534/genetics.107.082313

Mitra J, Steward FC. 1961. Growth induction in cultures of *Haplopappus gracilis*. II. The behaviour of the nucleus. Amer J Bot. 48(5):358-368. https://doi.org/10.2307/2439327

Moav R. 1961. Genetic instability in *Nicotiana* hybrids. II. Studies of the Ws (pbg) locus of *N. plumbaginifolia* in *N. tabacum* nuclei. Genetics 46(9):1069-1087. https://doi.org/10.1093/genetics/46.9.1069

Moav J, Moav R, Zohary D. 1968. Spontaneous morphological alterations of chromosomes in *Nicotiana* hybrids. Genetics 59(1):57-63. https://doi.org/10.1093/genetics/59.1.57

Olvera-Luna AR, Gama-López S, Delgado-Salinas A. 2012. Flora del Valle de Tehuacán-Cuicatlán: Fabaceae tribu Aeschynomeneae. Universidad Nacional Autónoma de México, Instituto de Biología.

Pathak S, McGill M, Hsu TC. 1975. Actinomycin D effects on mitosis and chromosomes: sticky chromatids and localized lesions. Chromosoma 50:79-88. https://doi.org/10.1007/bf00284964

Pessim C, Pagliarini MS, Silva N, Jank L. 2015. Chromosome stickiness impairs meiosis and influences reproductive success in *Panicum maximum* (Poaceae) hybrid plants. Genet Mol Res. 14(2):4195-4202. https://doi.org/10.4238/2015.April.28.2

Pich U, Fuchs J, Schubert I. 1996. How do Alliaceae stabilize their chromosome ends in the absence of TTTAGGG sequences? Chromosome Res. 4(3):207-213. https://doi.org/10.1007/BF02254961

Puizina J, Siroky J, Mokros P, Schweizer D, Riha K. 2004. Mre11 deficiency in *Arabidopsis* is associated with chromosomal instability in somatic cells and Spo11-dependent genome fragmentation during meiosis. Plant Cell 16:1968-1978. https://doi.org/10.1105/tpc.104.022749

Rao PN, Ranganadham P, Nirmala A. 1990. Behaviour of a sticky desynaptic mutant in pearl millet. Genetica 81:221-227. https://doi.org/10.1007/BF00360869

Reynolds ST. 1990. Aeschynomeneae (Benth.) Hutch. (Leguminosae) in Australia. Austrobaileya 3(2):177-202. https://www.jstor.org/stable/41738754

Rodríguez G. 1990. El género *Aeschynomeme* L. (Leguminosae: Papilionoideae) en Venezuela. Sinopsis. Acta Bot Venez. 16(1):117-136. https://www.jstor.org/stable/41740492

Rudd VE. 1955. The American species of *Aeschynomene*. Contr US Natl Herb. 32:1-172.

Sato S. 1981. Cytological studies on the satellited chromosomes of *Allium cepa*. Caryologia 34(4):431-440. https://doi.org/10.1080/00087114.1981.10796911

Schubert I. 1984. Mobile nucleolus organizing regions (NORs) in *Allium* (Liliaceae s. lat)? Inferences from the specifity of silver staining. Plant Syst Evol. 144(3-4):291-305. https://doi.org/10.1007/BF00984139

Schubert I, Ohle H, Hanelt P. 1983. Phylogenetic conclusions from Giemsa banding and NOR staining in Top Onions (Liliaceae). Plant Syst Evol. 143(4):245-256. https://doi.org/10.1007/BF00986607

Schubert I, Wobus U. 1985. *In situ* hybridization confirms jumping nucleolus organizing regions in *Allium*. Chromosoma 92(2):143-148. https://doi.org/10.1007/BF00328466

Sheidai M, Noormohamadi Z, Mirabdolbaghi-Kashani N, Ahmadi MR. 2003. Cytogenetic study of some rapeseed (*Brassica napus* L.) cultivars and their hybrids. Caryologia 56(4):387-397. https://doi.org/10.1080/00087114.2003.10589349

Solís Neffa VG, Fernández A. 2002. Karyotypic studies in *Turnera sidoides* complex (Turneraceae, Leiocarpae). Am. J Bot. 89(4):551-558. https://doi.org/10.3732/ajb.89.4.551

Sosnikhina SP. 1973. Genetic control of the behaviour of chromosomes in meiosis in inbred lines of diploid rye (*Secale cereale* L.) 2. Abnormalities on the stages of Anaphase I and II tetrads. Genetika 9:21-26.

Souza MC, Vianna LF, Kawakita K, Miotto STS. 2012. O genero *Aeschynomene* L. (Leguminosae, Faboideae, Dalbergieae) na planicie de inundacao do alto rio Parana, Brasil. Braz. J. Biol. 10:198-210.

Tapia-Pastrana F, Delgado-Salinas A. 2020. First cytogenetic register of an allopolyploid lineage of the genus *Aeschynomene* (Leguminosae, Papilionoideae) native to Mexico. Caryologia 73(4):17-26. https://doi.org/10.13128/caryologia-949

Tapia-Pastrana F, Delgado-Salinas A, Caballero J. 2020. Patterns of chromosomal variation in Mexican species of *Aeschynomene* (Fabaceae, Papilionoideae) and their evolutionary and taxonomic implications. Comp Cytogenet. 14:157-182. https://doi.org/10.3897/CompCytogen.v14i1.47264

Tapia-Pastrana F, Mercado-Ruaro P. 2001. A combination of the "squash" and "splash" techniques to obtain the karyotype and asses meiotic behavior of *Prosopis laevigata* L. (Fabaceae: Mimosoideae). Cytologia 66:11-17. https://doi.org/10.1508/cytologia.66.11

Therman E. 1951. Somatic and secondary pairing in *Ornithogalum*. Heredity 5:253-269.

Wagenaar EB. 1969. End-to-end chromosome attachments in mitotic interphase and their possible significance to meiotic chromosome pairing. Chromosoma 26:410-426. https://doi.org/10.1007/BF00326353

WFO (The World Flora Online). *Aeschynomene villosa* var. *villosa*. Published on the internet http://www.worldfloraonline.org/taxon/wfo-0000179554. [accessed on: 21 Feb 2025].

Wojciechowski MF, Lavin M, Sanderson MJ. 2004. A phylogeny of legumes (Leguminosae) based on analysis of the plastid *matK* gene resolves many well-supported subclades within the family. Am J Bot. 91(11):1846-1862. https://doi.org/10.3732/ajb.91.11.1846

OPEN ACCESS POLICY

Caryologia provides immediate open access to its content. Our publisher, Firenze University Press at the University of Florence, complies with the Budapest Open Access Initiative definition of Open Access: By "open access" , we mean the free availability on the public internet, the permission for all users to read, download, copy, distribute, print, search, or link to the full text of the articles, crawl them for indexing, pass them as data to software, or use them for any other lawful purpose, without financial, legal, or technical barriers other than those inseparable from gaining access to the internet itself. The only constraint on reproduction and distribution, and the only role for copyright in this domain is to guarantee the original authors with control over the integrity of their work and the right to be properly acknowledged and cited. We support a greater global exchange of knowledge by making the research published in our journal open to the public and reusable under the terms of a Creative Commons Attribution 4.0 International Public License (CC-BY-4.0). Furthermore, we encourage authors to post their pre-publication manuscript in institutional repositories or on their websites prior to and during the submission process and to post the Publisher's final formatted PDF version after publication without embargo. These practices benefit authors with productive exchanges as well as earlier and greater citation of published work.

PUBLICATION FREQUENCY

Papers will be published online as soon as they are accepted, and tagged with a DOI code. The final full bibliographic record for each article (initial-final page) will be released with the hard copies of *Caryologia*. Manuscripts are accepted at any time through the online submission system.

COPYRIGHT NOTICE

Authors who publish with *Caryologia* agree to the following terms:

- Authors retain the copyright and grant the journal right of first publication with the work simultaneously licensed under a Creative Commons Attribution 4.0 International Public License (CC-BY-4.0) that allows others to share the work with an acknowledgment of the work's authorship and initial publication in Caryologia.
- Authors are able to enter into separate, additional contractual arrangements for the non-exclusive distribution of the journal's published version of the work (e.g., post it to an institutional repository or publish it in a book), with an acknowledgment of its initial publication in this journal.
- Authors are permitted and encouraged to post their work online (e.g., in institutional repositories or on their website) prior to and during the submission process, as it can lead to productive exchanges, as well as earlier and greater citation of published work (See The Effect of Open Access).

PUBLICATION FEES

Open access publishing is not without costs. *Caryologia* therefore levies an article-processing charge of € 150.00 for each article accepted for publication, plus VAT or local taxes where applicable.

We routinely waive charges for authors from low-income countries. For other countries, article-processing charge waivers or discounts are granted on a case-by-case basis to authors with insufficient funds. Authors can request a waiver or discount during the submission process.

PUBLICATION ETHICS

Responsibilities of *Caryologia*'s editors, reviewers, and authors concerning publication ethics and publication malpractice are described in *Caryologia*'s Guidelines on Publication Ethics.

CORRECTIONS AND RETRACTIONS

In accordance with the generally accepted standards of scholarly publishing, *Caryologia* does not alter articles after publication: "Articles that have been published should remain extant, exact and unaltered to the maximum extent possible".

In cases of serious errors or (suspected) misconduct *Caryologia* publishes corrections and retractions (expressions of concern).

Corrections

In cases of serious errors that affect or significantly impair the reader's understanding or evaluation of the article, *Caryologia* publishes a correction note that is linked to the published article. The published article will be left unchanged.

Retractions

In accordance with the "Retraction Guidelines" by the Committee on Publication Ethics (COPE) *Caryologia* will retract a published article if:

- there is clear evidence that the findings are unreliable, either as a result of misconduct (e.g. data fabrication) or honest error (e.g. miscalculation)
- the findings have previously been published elsewhere without proper crossreferencing, permission or justification (i.e. cases of redundant publication)
- it turns out to be an act of plagiarism
- it reports unethical research.

An article is retracted by publishing a retraction notice that is linked to or replaces the retracted article. *Caryologia* will make any effort to clearly identify a retracted article as such.

If an investigation is underway that might result in the retraction of an article *Caryologia* may choose to alert readers by publishing an expression of concern.

COMPLYNG WITH ETHICS OF EXPERIMENTATION

Please ensure that all research reported in submitted papers has been conducted in an ethical and responsible manner, and is in full compliance with all relevant codes of experimentation and legislation. All papers which report in vivo experiments or clinical trials on humans or animals must include a written statement in the Methods section. This should explain that all work was conducted with the formal approval of the local human subject or animal care committees (institutional and national), and that clinical trials have been registered as legislation requires. Authors who do not have formal ethics review committees should include a statement that their study follows the principles of the Declaration of Helsinki

ARCHIVING

Caryologia and Firenze University Press are experimenting a National legal deposition and long-term digital preservation service.

ARTICLE PROCESSING CHARGES

All articles published in *Caryologia* are open access and freely available online, immediately upon publication. This is made possible by an article-processing charge (APC) that covers the range of publishing services we provide. This includes provision of online tools for editors and authors, article production and hosting, liaison with abstracting and indexing services, and customer services. The APC, payable when your manuscript is editorially accepted and before publication, is charged to either you, or your funder, institution or employer.

Open access publishing is not without costs. *Caryologia* therefore levies an article-processing charge of € 150.00 for each article accepted for publication, plus VAT or local taxes where applicable.

FREQUENTLY-ASKED QUESTIONS (FAQ)

Who is responsible for making or arranging the payment?

As the corresponding author of the manuscript you are responsible for making or arranging the payment (for instance, via your institution) upon editorial acceptance of the manuscript.

At which stage is the amount I will need to pay fixed?

The APC payable for an article is agreed as part of the manuscript submission process. The agreed charge will not change, regardless of any change to the journal's APC.

When and how do I pay?

Upon editorial acceptance of an article, the corresponding author (you) will be notified that payment is due.

We advise prompt payment as we are unable to publish accepted articles until payment has been received. Payment can be made by Invoice. Payment is due within 30 days of the manuscript receiving editorial acceptance. Receipts are available on request.

No taxes are included in this charge. If you are resident in any European Union country you have to add Value-Added Tax (VAT) at the rate applicable in the respective country. Institutions that are not based in the EU and are paying your fee on your behalf can have the VAT charge recorded under the EU reverse charge method, this means VAT does not need to be added to the invoice. Such institutions are required to supply us with their VAT registration number. If you are resident in Japan you have to add Japanese Consumption Tax (JCT) at the rate set by the Japanese government.

Can charges be waived if I lack funds?

We consider individual waiver requests for articles in Caryologia on a case-by-case basis and they may be granted in cases of lack of funds. To apply for a waiver please request one during the submission process. A decision on the waiver will normally be made within two working days. Requests made during the review process or after acceptance will not be considered.

I am from a low-income country, do I have to pay an APC?

We will provide a waiver or discount if you are based in a country which is classified by the World Bank as a low-income or a lower-middle-income economy with a gross domestic product (GDP) of less than $200bn. Please request this waiver of discount during submission.

What funding sources are available?

Many funding agencies allow the use of grants to cover APCs. An increasing number of funders and agencies strongly encourage open access publication. For more detailed information and to learn about our support service for authors.

APC waivers for substantial critiques of articles published in OA journals

Where authors are submitting a manuscript that represents a substantial critique of an article previously published in the same fully open access journal, they may apply for a waiver of the article processing charge (APC).

In order to apply for an APC waiver on these grounds, please contact the journal editorial team at the point of submission. Requests will not be considered until a manuscript has been submitted, and will be awarded at the discretion of the editor. Contact details for the journal editorial offices may be found on the journal website.

What is your APC refund policy?

Firenze University Press will refund an article processing charge (APC) if an error on our part has resulted in a failure to publish an article under the open access terms selected by the authors. This may include the failure to make an article openly available on the journal platform, or publication of an article under a different Creative Commons licence from that selected by the author(s). A refund will only be offered if these errors have not been corrected within 30 days of publication.

2025
Vol. 78 – n. 3

Caryologia

International Journal of Cytology, Cytosystematics and Cytogenetics

Table of contents